Copyright 2014 Nidhi Khanna

MOLECULAR MECHANISMS OF MAMMALIAN CELL SURVIVAL AND DIFFERENTIATION

BY

NIDHI KHANNA

DISSERTATION

Submitted in partial fulfillment of the requirements
for the degree of Doctor of Philosophy in Cell and Developmental Biology
in the Graduate College of the
University of Illinois at Urbana-Champaign, 2014

Urbana, Illinois

Doctoral Committee:

Professor Lisa Stubbs, Chair
Professor Jie Chen, Director of Research
Professor Benita S Katzenellenbogen
Associate Professor Stephanie Ceman
Associate Professor K V Prasanth

ABSTRACT

Cellular and developmental processes are regulated by extracellular and intracellular signals that are mediated by networks of signaling pathways. In recent years, microRNAs have also emerged as a class of critical modulators of the same processes. For my thesis studies, I focused on regulatory mechanisms underlying mammalian cell survival and differentiation. In particular, I investigated the regulation of mammalian target of rapamycin (mTOR), an evolutionarily conserved Ser/Thr kinase that integrates signals from nutrient availability, growth factors, differentiation inducers, and various types of stress, to control a wide range of biological processes. Separately, I also discovered a novel microRNA regulator of myogenic differentiation, microRNA-146b.

Emerging evidence implicates the deregulation of mTOR signaling in a variety of diseases including cancer and diabetes, underscoring the importance to fully understand the regulation of mTOR signaling. mTOR forms two distinct complexes known as mTORC1 and mTORC2. mTORC2 controls a wide range of cellular functions, but the regulation of its signaling remains incompletely understood. In Chapter 2, I identified XPLN, a RhoGEF, as an endogenous inhibitor of mTORC2 kinase activity towards Akt. Furthermore, I showed that the GEF activity of XPLN is dispensable for its regulation of mTORC2 and Akt, whereas an N-terminal 125-amino acid fragment of XPLN is both necessary and sufficient for the inhibition of mTORC2. XPLN negatively regulates myoblast differentiation and cell survival by suppressing mTORC2 and Akt, and could likely be an important player in many other aspects of biology and diseases involving mTORC2 and Akt.

Next, I set out to search for a mechanism by which XPLN could be regulated in cells in order to allow Akt activation following growth factor stimulation. In Chapter 3, I investigated the subcellular localization of XPLN, and found it to be localized throughout the cell but concentrated in the nucleus. I subsequently manipulated the location by tagging various localization signals to XPLN and examined the functional consequence. Furthermore, I studied the function and localization of alternative splice isoforms of XPLN.

Given the well-known hyperactivation of Akt in many human tumors, I probed a potential role of XPLN in cancer by analyzing its protein levels in various cancer cell lines, as described in Appendix A. Knockdown and overexpressed XPLN were also performed in cancer cells to probe the effects on Akt phosphorylation. Finally, as described in Appendix B, I am in the process of generating XPLN knockout mice using the TALEN technology, in order to facilitate future in vivo studies of XPLN.

In Chapter 4, I identified and characterized microRNA-146b (miR-146b) as a novel positive regulator of skeletal myogenesis. Inhibition of miR-146b led to reduced myoblast differentiation, whereas overexpression of miR-146b enhanced differentiation. In addition, miR-146b directly targets Smad4, Hmga2, and Notch1 in muscle cells. The expression of miR-146b and its target genes was inversely correlated during myoblast differentiation and muscle regeneration, suggesting that these genes most likely mediate the myogenic function of miR-146b.

In conclusion, my studies have uncovered novel regulators and mechanisms of mammalian cell survival and myogenic differentiation, and laid the foundation for future investigations.

To my loving husband, Nimish Khanna, and our parents

ACKNOWLEDGEMENTS

First and foremost, I would like to thank my thesis advisor, Dr. Jie Chen, for her constant support and guidance throughout the graduate school. I thank her for believing in me and allowing me the freedom to try my crazy scientific ideas.

I am indebted to my committee members, Dr. Lisa Stubbs, Dr. Stephanie Ceman, Dr. K. V. Prasanth, and Dr. Benita Katzenellenbogen for their continued support and commitment. I thank them all for providing me critique on experiments, results, scientific writing, and presentations. I would specially like to acknowledge Dr. Prasanth who always raised tough questions that challenged me to think deeper about science.

Next, I would like to thank Dr. Yimin Fang (Julia) who I never had a chance to meet but was instrumental in carrying out the yeast two-hybrid screen and finding XPLN as a positive hit. I am grateful to Dr. MeeSup Yoon who trained me on all the bench techniques during my initial years in the lab. I would also like to thank Dr. Yejing Ge for teaching me in vivo mouse work, specially the muscle regeneration experiments. I am thankful to all the current Chen lab members; Rachel Waldemer, Christina Rosenberg, Edwin Arauz, Min Zeng, Nilmani Singh, and Kook Son for making the lab a fun and enjoyable place to work.

Lastly, I am extremely grateful to my friends and family, especially my husband, Nimish Khanna, who has been a pillar of strength in my life. I can't thank him enough for his love, support, and patience towards me. I am grateful to him for holding my hand and cheering me on through some of the hard days of my graduate life. Lastly, I am lucky to have a very supporting family who prayed for me when the times were tough.

TABLE OF CONTENTS

CHAPTER 1. INTRODUCTION

1.1. Mammalian (Mechanistic) Target of Rapamycin (mTOR)

mTOR is an evolutionarily conserved Ser/Thr kinase that integrates signals from nutrient availability, growth factors, differentiation inducers, and various types of stress, to control a wide range of cellular and developmental processes (Laplante and Sabatini, 2009b). Emerging evidence indicates the deregulation of mTOR signaling in a variety of diseases including cancer and diabetes (Zoncu et al., 2011), underscoring the importance to fully understand the regulation of mTOR signaling.

mTOR was first identified in the budding yeast *Saccharomyces cerevisiae* as a specific target of Rapamycin (Heitman et al., 1991). Rapamycin is a bacterial macrolide that has demonstrated enormous clinical value as a three-time FDA approved drug: an immunosuppressant (Abraham and Wiederrecht, 1996), an anti-restenosis drug in angioplastic stenting (Serruys et al., 2002), and an anti-cancer drug (Hidalgo and Rowinsky, 2000; Vogt, 2001). Rapamycin forms a complex with the ubiquitous cellular protein FKBP12, which then binds to the FRB (FKBP12-rapamycin binding) domain and inhibits TOR functions. Four years after the discovery of yeast TOR, cloning of mTOR was reported independently by two groups at the same time and named as FRAP (FK506-binding protein 12 (FKBP12), rapamycin-associated protein) (Brown et al., 1994), RAFT1 (rapamycin and FKBP12 target-1) (Sabatini et al., 1994), in addition to mTOR (Sabers et al., 1995).

As shown in Fig. 1.1, mTOR nucleates two distinct multi-protein complexes known as mTOR Complex 1 (mTORC1) and mTOR Complex 2 (mTORC2) (Foster and

Fingar, 2010). mTORC1 consists of the defining subunit rapamycin-sensitive adaptor protein of mTOR (raptor). Besides raptor and mTOR, mTORC1 also includes negative regulators 40 kDa Prorich Akt substrate (PRAS40) and DEP domain-containing mTOR-interacting protein (Deptor), as well as a positive regulator mammalian lethal with SEC13 protein 8 (mLST8), also known as G protein β-subunit-like protein (GβL) (Kim et al., 2003) in addition to mTOR. mTORC1 regulates cell growth and proliferation by promoting biosynthesis of proteins, lipids, and organelles while inhibiting autophagy (Laplante and Sabatini, 2009a). The best characterized substrates for the mTORC1 kinase are S6 Kinase 1 (S6K1) and eIF-4E-Binding Protein-1 (4E-BP1), both key regulators of protein synthesis (Ma and Blenis, 2009).

The TSC1/TSC2 complex has emerged as a critical regulator of mTORC1 signaling in cell growth by serving as a hub for receiving multiple upstream signals (Marygold and Leevers, 2002; McManus and Alessi, 2002), including mitogenic stimulation, cellular energy deprivation, hypoxia, inflammatory signals, and oncogenic Wnt signaling (Erbay et al., 2005; Guertin and Sabatini, 2007; Hay and Sonenberg, 2004; Inoki et al., 2006; Lee et al., 2007; Wullschleger et al., 2006). The TSC1/2 complex inhibits mTORC1 by inactivating the small GTPase Rheb through a GTPase-activating protein (GAP) activity in TSC2.

mTORC2 is defined by the subunits rapamycin-insensitive companion of mTOR (rictor), positive regulators protein observed with rictor (Protor), and mammalian stress-activated map kinase-interacting protein 1 (mSIN1). It also shares mTOR, Deptor and mLST8 with mTORC1 (Foster and Fingar, 2010). mTORC2 phosphorylates the hydrophobic motif site Ser473 on Akt that is necessary for its activation (Sarbassov et al.,

2005), as well as the turn motif controlling the folding and stability of Akt (Facchinetti et al., 2008; Ikenoue et al., 2008). Thus, mTORC2 is involved in a variety of processes that are regulated by Akt, including cell survival, glucose metabolism, and cellular differentiation (Ge and Chen, 2012; Manning and Cantley, 2007). In addition, mTORC2 regulates cytoskeleton organization by promoting phosphorylation of protein Kinase C (PKCα) (Facchinetti et al., 2008; Ikenoue et al., 2008; Jacinto et al., 2004; Sarbassov et al., 2004). More recently, serum/glucocorticoid regulated kinase 1 (SGK1) has also been identified as a substrate of mTORC2 (Hong et al., 2008).

In contrast to mTORC1, for which mechanisms of activation by upstream signals have been extensively studied, relatively little is known about the regulation of mTORC2 signaling. PI3K activity and TSC1/2 have been reported to mediate mitogenic stimulation of mTORC2 kinase activity (Huang et al., 2008). Growth factor receptors activate mTORC2 near the plasma membrane, where mTORC2 may be recruited through binding of mSIN1. While PRAS40 and FKBP38 both specifically inhibit mTORC1, DEPTOR interacts with mTOR to negatively regulate both mTORC1 and mTORC2 (Foster and Fingar, 2010; Laplante and Sabatini, 2009a).

1.2. Akt/Protein Kinase B (PKB)

Akt/PKB is a member of the AGC kinase family that includes S6K, SGK, and PKC. Akt is a serine/threonine kinase that was originally implicated in cancer development, cell proliferation and inhibition of apoptosis (Datta et al., 1999). Mammals have three known isoforms - Akt1, Akt2, and Akt3, all having the same general structure consisting of an N-terminal PH domain, known to target Akt to the plasma membrane,

and a C-terminal kinase domain. Akt1 and Akt2 are widely distributed in all the tissues whereas Akt3 is predominantly restricted to the nervous system and testis. Knockdown and knockout studies have shown that different isoforms of Akt are involved in distinct biological processes (Gonzalez and McGraw, 2009). Akt1 is majorly implicated in cell growth and lifespan (Chen et al., 2001), while Akt2 is involved in glucose homeostasis by regulating glucose utilization and hepatic glucose output (Cho et al., 2001). Akt3 has a significant role in neural development (Tschopp et al., 2005).

Akt plays a central role in controlling cell growth, proliferation, survival, and differentiation by phosphorylating a diverse number of protein substrates. Most of the substrates of Akt contain a minimal consensus sequence RXRXXS/T (Scheid and Woodgett, 2001). Akt substrates implicated in metabolism, cell growth, and proliferation are GSK3, mTOR, and TSC2. Glycogen synthase kinase 3 (GSK3) was identified as the first physiological target of Akt (Cross et al., 1995). Akt phosphorylates and inactivates GSK3 preventing it from phosphorylating glycogen synthase. Therefore, inactivation of GSK3 by Akt results in dephosphorylation of glycogen synthase and hence the activation of glycogen synthesis (Frame and Cohen, 2001). Akt has also been well characterized as a major pro-survival molecule, through regulation of apoptosis by phosphorylation of BAD, ASK1, and FoxO proteins (Lawlor and Alessi, 2001).

Akt activation is a highly regulated multistep process that involves both membrane translocation and phosphorylation. Upon activation by membrane-bound receptors, such as receptor tyrosine kinases (RTKs) PI3K generates PI-3,4-P_2 and PI-3,4,5-P_3 at the plasma membrane. Both phospholipids bind with high affinity to the PH domain, mediating membrane translocation of Akt. Once situated at the membrane, Akt

is phosphorylated at two sites. First is threonine (Thr) 308 in Akt1 (309 in Akt2 and 305 in Akt3) in the activation loop or T-loop, by PH domain-containing AGC kinase, PDK1. Second is serine (Ser) 473 (474 in Akt2 and 472 in Akt3) in the hydrophobic motif of the C-terminal tail by mTORC2 (Sarbassov et al., 2005). Whereas T-loop phosphorylation is absolutely required for Akt activation, the C-terminal phosphorylation potentiates Akt activity by promoting a conformational change in the T-loop (Yang et al., 2006). Although mTORC2 is the major kinase for Ser 473 phosphorylation, other candidates include the integrin-linked kinase (ILK) (Persad et al., 2001), mitogen-activated protein kinase-activated kinase 2 (MAPKAPK2), Ataxia telangiectasia mutated (ATM) kinase and Akt itself. These kinases have been proposed to phosphorylate in various cell contexts (Liao and Hung, 2010). Very recently, a direct link between cell cycle and Akt activation was revealed through identification of cyclin-dependent-kinase2 (cdk2)/cyclin A2 as a physiological kinase for Akt at amino acid residues S477 and T479 in the extreme C terminus of Akt (Liu et al., 2014). Similar to S473 regulation, it was shown that S477/T479 phosphorylation can be mediated by cdk2, DNAPK, or mTORC2 depending on the particular cell context.

There are a couple of known negative regulators of Akt signaling. The PI3K/Akt axis is directly antagonized by the 3′-lipid phosphatase activity of the phosphatase PTEN, which removes the 3′-phosphate of PI3K products, leading to abrogation of PI3K signaling (Di Cristofano and Pandolfi, 2000). Another negative regulator is a Ser/Thr phosphatase called PHLLP (PH domain leucine-rich repeat protein phosphatase). PHLLP removes the hydrophobic motif phosphorylation (Ser473 phosphate of Akt1) to dampen Akt signaling (Gao et al., 2005). In addition, several other serine-threonine

phosphatases, including protein phosphatase 2A, are proposed to be involved in the inactivation of Akt.

Akt is one of the most frequently activated kinases in cancer (Bellacosa et al., 2005; Hay, 2005; Khan et al., 2013; Manning and Cantley, 2007; Morgensztern and McLeod, 2005; Zoncu et al., 2011). Over-expression and amplification of Akt2 was first reported in 1992 and is now frequently seen in prostate and ovarian carcinomas (Altomare and Testa, 2005). Akt2 overexpression is linked to the malignant phenotype leading to generation of hyper responsive cells that are overly sensitive to normal growth factors. Unlike Akt2, Akt1 and Akt3 are not commonly overexpressed in cancer. Instead, mutations and genomic deletions of the upstream regulators of Akt lead to hyperactivated Akt signaling and resistance to apoptosis.

Various mechanisms contribute to Akt hyperactivation in cancer. Most commonly occurring germ line modifications are activating mutations in or overexpression of PI3K, inactivating mutations in or deletion of PTEN, and amplification or overexpression of receptor tyrosine kinases such as EGFR and Her2 (Yuan and Cantley, 2008).

1.3. Skeletal Myogenesis

Skeletal myogenesis occurs both during embryonic development and adulthood. During embryonic development, mesodermal cells undergo myogenic commitment forming proliferating myoblasts, which differentiate terminally and fuse to give rise to nascent myofibers, characterized as the first stage of skeletal myogenesis. These nascent myofibers continue to fuse to form mature myofibers during the next stage (Parker et al., 2003a). Adult skeletal muscle generates force in a controlled and directed manner

through contraction of these highly specialized multinucleated myofibers (Wagers and Conboy, 2005). Its life-long action relies on maintenance and regeneration of myofibers. Muscle repair is carried out by a population of stem cells called satellite cells present between plasma membrane and surrounding basal lamina of mature muscle fibers (Wagers and Conboy, 2005). Following injury, mitotically quiescent satellite cells re-enter cell cycle, divide and ultimately fuse with existing myofibers or with each other to promote repair and regeneration (Sabourin and Rudnicki, 2000).

Embryonic myogenesis is believed to share regulatory mechanisms with adult muscle regeneration, especially at myoblast differentiation stages. Muscle progenitor cells in the somites express Pax3 allowing proliferation while simultaneously preventing precocious differentiation. To initiate myogenesis, these mesodermal cells migrate to limb buds and initiate Pax7 expression. Paired-domain transcription factors Pax3 and Pax7 act upstream of the primary myogenic basic helix–loop–helix (bHLH) transcription factors Myf5 and MyoD in allowing myogenic specification. Following downregulation of Pax3/7, these cells proliferate as myoblasts and then differentiate after activation of Myogenin, another myogenic regulatory gene of the MyoD family. Myogenin expression is followed by p21 induction marking cell cycle withdrawal and phenotypic differentiation as marked by MHC expression. These myoblasts then undergo initial cell fusion to form nascent myofibers followed by second-stage fusion to form mature myofibers (Parker et al., 2003b).

The C2C12 murine myoblast cell line serves as a commonly used model that recapitulates myoblast differentiation in vitro, and provides a powerful system. When kept subconfluent, these cells proliferate continuously in the presence of growth factors.

Upon growth factor deprivation, they exit cell cycle and fuse to form multi-nucleated myotubes expressing muscle-specific genes (Yaffe and Saxel, 1977).

1.4. mTOR Signaling in Myogenesis

In addition to regulating various aspects of skeletal muscle physiology including metabolic homeostasis, muscle hypertrophy and atrophy (Glass, 2003), mTOR is a master regulator of myogenesis, and it regulates distinct stages of myogenesis by assembling different pathways (Ge and Chen, 2012). As shown in Fig. 1.2, at the initiation stage, mTOR controls the transcription of IGF-II through a muscle-specific enhancer in a kinase-independent manner (Erbay and Chen, 2001; Erbay et al., 2003). On the other hand, the catalytic activity of mTOR is required for a second-stage fusion that results in formation of mature myotubes (Park and Chen, 2005).

The insulin-like growth factors (IGF-I and IGF-II) are critically involved in skeletal muscle development as well as adult muscle regeneration (Barton-Davis et al., 1998; Florini et al., 1991a; Musaro et al., 2001). In various myoblast cultures the autocrine/paracrine actions of IGFs, induced in response to growth factor deprivation, are instrumental in the initiation of differentiation (Florini et al., 1991b; Musaro and Rosenthal, 1999; Tollefsen et al., 1989a; Tollefsen et al., 1989b). Pharmacological and genetic evidence has indicated the PI3K/Akt pathway as a major mediator of myogenic signaling downstream of IGFs (Jiang et al., 1999; Jiang et al., 1998; Kaliman et al., 1998; Kaliman et al., 1996).

FoxO1 (Forkhead box protein O1) is the major downstream target of Akt signaling known to suppress myogenic differentiation (Hribal et al., 2003). The FoxO

proteins are key regulators of a wide range of cellular functions, such as proliferation, survival, differentiation, and metabolism (Accili and Arden, 2004; Barthel et al., 2005). Many signaling pathways converge on FoxO, but inactivation by Akt phosphorylation appears to be a prevalent mechanism in a variety of cellular contexts (Tran et al., 2003).

1.5. MicroRNAs

MicroRNAs are a class of small non-coding RNAs that have emerged as important regulators of gene expression (Bartel, 2009).There are >3000 miRNAs in humans (miRBase.org) and they are predicted to target ~30-60% genes in the human genome. They are important in regulating cellular and developmental processes as diverse as embryonic development, cell proliferation, cell growth, tissue differentiation, and apoptosis (Felekkis et al.; Stefani and Slack, 2008).

Mature microRNAs are derived from longer transcripts (named pri-miRNA) transcribed by RNA Polymerase II (Lee and Dutta, 2009), either as independent transcriptional units or as parts of introns of protein coding genes. These pri-miRNAs are processed by nuclear RNaseIII-type endonuclease Drosha along with DGCR8 (Gregory et al., 2004; Han et al., 2006), also called microprocessor complex, to generate ~70 nucleotide pre-miRNAs containing a stem-loop structure. A subset of miRNA called miRtrons bypass the Drosha processing through an alternative pathway, where they are produced during gene splicing (Ruby et al., 2007). These pre-miRNAs are then exported to the cytoplasm by Exportin-5 in a Ran-GTP dependent manner (Yi et al., 2003) where they are further processed by Dicer, another RNaseIII-type endonuclease, in complex with TRBP, to yield ~22 nucleotide mature miRNA duplexes (Hutvagner et al., 2001).

Adequate levels of both components of Microprocessor (Drosha and DGCR8) are ensured by a positive–negative feedback loop. DGCR8 stabilizes Drosha and Drosha downregulates the DGCR8 mRNA by targeting two hairpin structures in the 5′UTR and coding sequence of DGCR8 that resemble those found in pri-miRs (Han et al., 2009).

One strand of these duplexes is then selected for incorporation into RNA induced Silencing Complexes (RISC) composed of proteins of Argonaute family and other accessory factors along with the target mRNA (Filipowicz et al., 2008). The target mRNA is subsequently translationally repressed and often decayed as well (Filipowicz et al., 2008; Wu et al., 2006).

MicroRNAs bind to their target mRNAs through partial complementarity. Rigorous bioinformatic analysis of miRNA-regulated genes showed that pairing of miRNA nucleotides 2–8, called the seed region, to the 3′ untranslated region (UTR) of the target mRNA is often important. Other factors that play an important role in predicting targets are evolutionary conservation of the MRE (miRNA recognition element), free energy of the miRNA-mRNA heteroduplex, and mRNA sequence features outside the target site (Thomas et al., 2010).

1.6. MicroRNAs in Skeletal Myogenesis

Every aspect of skeletal myogenesis has been shown to be regulated by miRNA (Ge and Chen, 2011), with more myogenic miRNAs discovered continuously. The strongest evidence for the essential role of miRNAs in skeletal myogenesis came from the analysis of skeletal muscle-specific Dicer knockout mice, which have severely

reduced muscle mass along with abnormal myofiber morphology leading to death within minutes of birth (O'Rourke et al., 2007).

Overexpression and knockdown experiments in myoblasts first revealed the myogenic roles of the highly conserved miR-1, miR-206 and miR-133 (Chen et al., 2006; Kim et al., 2006). Later, more miRNAs were recognized to regulate most known steps of skeletal myogenesis by targeting crucial regulators that regulate the process (Ge and Chen, 2011). Chapter 4 of my thesis will describe the identification and characterization of a novel miRNA, miR-146b, in regulating skeletal myogenesis.

1.7. Figures

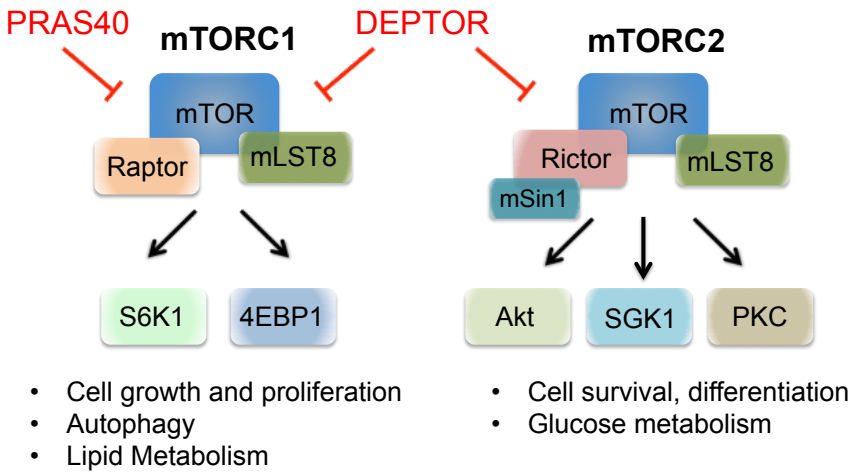

Fig. 1.1. mTOR complexes. Two biochemically distinct mTOR complexes that have distinct and shared regulators, and substrates that mediate specific functions.

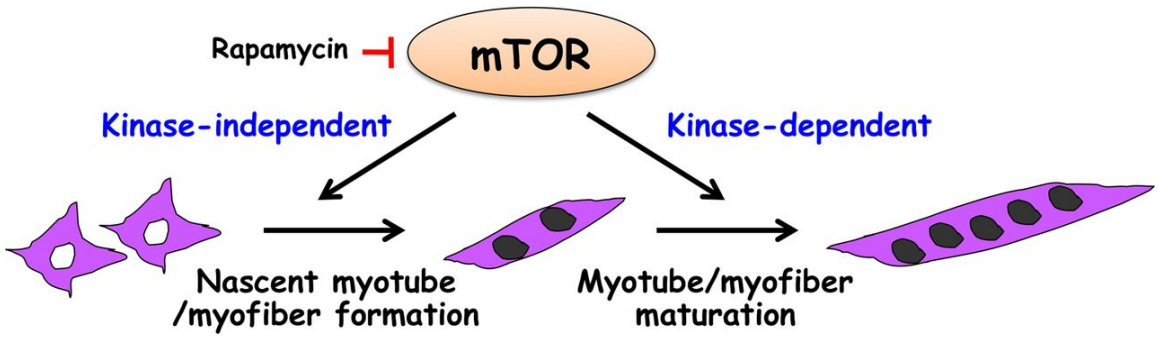

Fig. 1.2. Rapamycin-sensitive mTOR signaling controls distinct stages of skeletal myogenesis. Formation of nascent myotubes is regulated by mTOR in a kinase-independent manner, whereas maturation of myotubes/myofibers requires mTOR kinase activity. Borrowed from (Ge and Chen, 2012).

1.8. References

Abraham, R.T., and Wiederrecht, G.J. (1996). Immunopharmacology of rapamycin. Annu Rev Immunol *14*, 483-510.

Accili, D., and Arden, K.C. (2004). FoxOs at the crossroads of cellular metabolism, differentiation, and transformation. Cell *117*, 421-426.

Altomare, D.A., and Testa, J.R. (2005). Perturbations of the AKT signaling pathway in human cancer. Oncogene *24*, 7455-7464.

Bartel, D.P. (2009). MicroRNAs: target recognition and regulatory functions. Cell *136*, 215-233.

Barthel, A., Schmoll, D., and Unterman, T.G. (2005). FoxO proteins in insulin action and metabolism. Trends Endocrinol Metab *16*, 183-189.

Barton-Davis, E.R., Shoturma, D.I., Musaro, A., Rosenthal, N., and Sweeney, H.L. (1998). Viral mediated expression of insulin-like growth factor I blocks the aging-related loss of skeletal muscle function. Proc Natl Acad Sci U S A *95*, 15603-15607.

Bellacosa, A., Kumar, C.C., Di Cristofano, A., and Testa, J.R. (2005). Activation of AKT kinases in cancer: implications for therapeutic targeting. Advances in cancer research *94*, 29-86.

Brown, E.J., Albers, M.W., Shin, T.B., Ichikawa, K., Keith, C.T., Lane, W.S., and Schreiber, S.L. (1994). A mammalian protein targeted by G1-arresting rapamycin-receptor complex. Nature *369*, 756-758.

Chen, J.F., Mandel, E.M., Thomson, J.M., Wu, Q., Callis, T.E., Hammond, S.M., Conlon, F.L., and Wang, D.Z. (2006). The role of microRNA-1 and microRNA-133 in skeletal muscle proliferation and differentiation. Nat Genet *38*, 228-233.

Chen, W.S., Xu, P.Z., Gottlob, K., Chen, M.L., Sokol, K., Shiyanova, T., Roninson, I., Weng, W., Suzuki, R., Tobe, K., *et al*. (2001). Growth retardation and increased apoptosis in mice with homozygous disruption of the Akt1 gene. Genes Dev *15*, 2203-2208.

Cho, H., Mu, J., Kim, J.K., Thorvaldsen, J.L., Chu, Q., Crenshaw, E.B., 3rd, Kaestner, K.H., Bartolomei, M.S., Shulman, G.I., and Birnbaum, M.J. (2001). Insulin resistance and a diabetes mellitus-like syndrome in mice lacking the protein kinase Akt2 (PKB beta). Science *292*, 1728-1731.

Cross, D.A., Alessi, D.R., Cohen, P., Andjelkovich, M., and Hemmings, B.A. (1995). Inhibition of glycogen synthase kinase-3 by insulin mediated by protein kinase B. Nature *378*, 785-789.

Datta, S.R., Brunet, A., and Greenberg, M.E. (1999). Cellular survival: a play in three Akts. Genes & development *13*, 2905-2927.

Di Cristofano, A., and Pandolfi, P.P. (2000). The multiple roles of PTEN in tumor suppression. Cell *100*, 387-390.

Erbay, E., and Chen, J. (2001). The mammalian target of rapamycin regulates C2C12 myogenesis via a kinase-independent mechanism. J Biol Chem *276*, 36079-36082. Epub 32001 Aug 36010.

Erbay, E., Kim, J.E., and Chen, J. (2005). Amino acid-sensing mTOR signaling. In Nutrient and Cell Signaling, J. Zempleni, and K. Dakshinamurti, eds. (CRC Press), pp. 353-380.

Erbay, E., Park, I.H., Nuzzi, P.D., Schoenherr, C.J., and Chen, J. (2003). IGF-II transcription in skeletal myogenesis is controlled by mTOR and nutrients. J Cell Biol *163*, 931-936.

Facchinetti, V., Ouyang, W., Wei, H., Soto, N., Lazorchak, A., Gould, C., Lowry, C., Newton, A.C., Mao, Y., Miao, R.Q., *et al*. (2008). The mammalian target of rapamycin complex 2 controls folding and stability of Akt and protein kinase C. The EMBO Journal *27*, 1932-1943.

Felekkis, K., Touvana, E., Stefanou, C., and Deltas, C. microRNAs: a newly described class of encoded molecules that play a role in health and disease. Hippokratia *14*, 236-240.

Filipowicz, W., Bhattacharyya, S.N., and Sonenberg, N. (2008). Mechanisms of post-transcriptional regulation by microRNAs: are the answers in sight? Nat Rev Genet *9*, 102-114.

Florini, J.R., Ewton, D.Z., and Magri, K.A. (1991a). Hormones, growth factors, and myogenic differentiation. Annu Rev Physiol *53*, 201-216.

Florini, J.R., Magri, K.A., Ewton, D.Z., James, P.L., Grindstaff, K., and Rotwein, P.S. (1991b). "Spontaneous" differentiation of skeletal myoblasts is dependent upon autocrine secretion of insulin-like growth factor-II. J Biol Chem *266*, 15917-15923.

Foster, K.G., and Fingar, D.C. (2010). Mammalian target of rapamycin (mTOR): conducting the cellular signaling symphony. J Biol Chem *285*, 14071-14077. doi: 14010.11074/jbc.R14109.094003. Epub 092010 Mar 094015.

Frame, S., and Cohen, P. (2001). GSK3 takes centre stage more than 20 years after its discovery. Biochem J *359*, 1-16.

Gao, T., Furnari, F., and Newton, A.C. (2005). PHLPP: a phosphatase that directly dephosphorylates Akt, promotes apoptosis, and suppresses tumor growth. Molecular cell *18*, 13-24.

Ge, Y., and Chen, J. (2011). MicroRNAs in skeletal myogenesis. Cell Cycle *10*, 441-448. Epub 2011 Feb 2011.

Ge, Y., and Chen, J. (2012). Mammalian target of rapamycin (mTOR) signaling network in skeletal myogenesis. J Biol Chem *31*, 31.

Glass, D.J. (2003). Signalling pathways that mediate skeletal muscle hypertrophy and atrophy. Nat Cell Biol *5*, 87-90.

Gonzalez, E., and McGraw, T.E. (2009). The Akt kinases: isoform specificity in metabolism and cancer. Cell cycle (Georgetown, Tex) *8*, 2502-2508.

Gregory, R.I., Yan, K.P., Amuthan, G., Chendrimada, T., Doratotaj, B., Cooch, N., and Shiekhattar, R. (2004). The Microprocessor complex mediates the genesis of microRNAs. Nature *432*, 235-240. Epub 2004 Nov 2007.

Guertin, D.A., and Sabatini, D.M. (2007). Defining the role of mTOR in cancer. Cancer Cell *12*, 9-22.

Han, J., Lee, Y., Yeom, K.H., Nam, J.W., Heo, I., Rhee, J.K., Sohn, S.Y., Cho, Y., Zhang, B.T., and Kim, V.N. (2006). Molecular basis for the recognition of primary microRNAs by the Drosha-DGCR8 complex. Cell *125*, 887-901.

Han, J., Pedersen, J.S., Kwon, S.C., Belair, C.D., Kim, Y.K., Yeom, K.H., Yang, W.Y., Haussler, D., Blelloch, R., and Kim, V.N. (2009). Posttranscriptional crossregulation between Drosha and DGCR8. Cell *136*, 75-84.

Hay, N. (2005). The Akt-mTOR tango and its relevance to cancer. Cancer cell *8*, 179-183.

Hay, N., and Sonenberg, N. (2004). Upstream and downstream of mTOR. Genes Dev *18*, 1926-1945.

Heitman, J., Movva, N.R., and Hall, M.N. (1991). Targets for cell cycle arrest by the immunosuppressant rapamycin in yeast. Science *253*, 905-909.

Hidalgo, M., and Rowinsky, E.K. (2000). The rapamycin-sensitive signal transduction pathway as a target for cancer therapy. Oncogene *19*, 6680-6686.

Hong, F., Larrea, M.D., Doughty, C., Kwiatkowski, D.J., Squillace, R., and Slingerland, J.M. (2008). mTOR-raptor binds and activates SGK1 to regulate p27 phosphorylation. Mol Cell *30*, 701-711. doi: 710.1016/j.molcel.2008.1004.1027.

Hribal, M.L., Nakae, J., Kitamura, T., Shutter, J.R., and Accili, D. (2003). Regulation of insulin-like growth factor-dependent myoblast differentiation by Foxo forkhead transcription factors. J Cell Biol *162*, 535-541.

Huang, J., Dibble, C.C., Matsuzaki, M., and Manning, B.D. (2008). The TSC1-TSC2 complex is required for proper activation of mTOR complex 2. Mol Cell Biol *28*, 4104-4115.

Hutvagner, G., McLachlan, J., Pasquinelli, A.E., Balint, E., Tuschl, T., and Zamore, P.D. (2001). A cellular function for the RNA-interference enzyme Dicer in the maturation of the let-7 small temporal RNA. Science *293*, 834-838. Epub 2001 Jul 2012.

Ikenoue, T., Inoki, K., Yang, Q., Zhou, X., and Guan, K.-L. (2008). Essential function of TORC2 in PKC and Akt turn motif phosphorylation, maturation and signalling. The EMBO Journal *27*, 1919-1931.

Inoki, K., Ouyang, H., Zhu, T., Lindvall, C., Wang, Y., Zhang, X., Yang, Q., Bennett, C., Harada, Y., Stankunas, K., *et al*. (2006). TSC2 Integrates Wnt and Energy Signals via a Coordinated Phosphorylation by AMPK and GSK3 to Regulate Cell Growth. Cell *126*, 955-968.

Jacinto, E., Loewith, R., Schmidt, A., Lin, S., Ruegg, M.A., Hall, A., and Hall, M.N. (2004). Mammalian TOR complex 2 controls the actin cytoskeleton and is rapamycin insensitive. Nature cell biology *6*, 1122-1128.

Jiang, B.H., Aoki, M., Zheng, J.Z., Li, J., and Vogt, P.K. (1999). Myogenic signaling of phosphatidylinositol 3-kinase requires the serine-threonine kinase Akt/protein kinase B. Proc Natl Acad Sci U S A *96*, 2077-2081.

Jiang, B.H., Zheng, J.Z., and Vogt, P.K. (1998). An essential role of phosphatidylinositol 3-kinase in myogenic differentiation. Proc Natl Acad Sci U S A *95*, 14179-14183.

Kaliman, P., Canicio, J., Shepherd, P.R., Beeton, C.A., Testar, X., Palacin, M., and Zorzano, A. (1998). Insulin-like growth factors require phosphatidylinositol 3-kinase to signal myogenesis: dominant negative p85 expression blocks differentiation of L6E9 muscle cells. Mol Endocrinol *12*, 66-77.

Kaliman, P., Vinals, F., Testar, X., Palacin, M., and Zorzano, A. (1996). Phosphatidylinositol 3-kinase inhibitors block differentiation of skeletal muscle cells. J Biol Chem *271*, 19146-19151.

Khan, K.H., Yap, T.A., Yan, L., and Cunningham, D. (2013). Targeting the PI3K-AKT-mTOR signaling network in cancer. Chinese journal of cancer *32*, 253-265.

Kim, D.H., Sarbassov dos, D., Ali, S.M., Latek, R.R., Guntur, K.V., Erdjument-Bromage, H., Tempst, P., and Sabatini, D.M. (2003). GbetaL, a Positive Regulator of the Rapamycin-Sensitive Pathway Required for the Nutrient-Sensitive Interaction between Raptor and mTOR. Mol Cell *11*, 895-904.

Kim, H.K., Lee, Y.S., Sivaprasad, U., Malhotra, A., and Dutta, A. (2006). Muscle-specific microRNA miR-206 promotes muscle differentiation. J Cell Biol *174*, 677-687.

Laplante, M., and Sabatini, D.M. (2009a). mTOR signaling at a glance. Journal of Cell Science *122*, 3589-3594.

Laplante, M., and Sabatini, D.M. (2009b). mTOR signaling at a glance. J Cell Sci *122*, 3589-3594.

Lee, D.F., Kuo, H.P., Chen, C.T., Hsu, J.M., Chou, C.K., Wei, Y., Sun, H.L., Li, L.Y., Ping, B., Huang, W.C., *et al*. (2007). IKKbeta Suppression of TSC1 Links Inflammation and Tumor Angiogenesis via the mTOR Pathway. Cell *130*, 440-455.

Lee, Y.S., and Dutta, A. (2009). MicroRNAs in cancer. Annu Rev Pathol *4*, 199-227.

Liao, Y., and Hung, M.C. (2010). Physiological regulation of Akt activity and stability. Am J Transl Res *2*, 19-42.

Liu, P., Begley, M., Michowski, W., Inuzuka, H., Ginzberg, M., Gao, D., Tsou, P., Gan, W., Papa, A., Kim, B.M., *et al*. (2014). Cell-cycle-regulated activation of Akt kinase by phosphorylation at its carboxyl terminus. Nature *508*, 541-545.

Ma, X.M., and Blenis, J. (2009). Molecular mechanisms of mTOR-mediated translational control. Nature Reviews Molecular Cell Biology *10*, 307-318.

Manning, B.D., and Cantley, L.C. (2007). AKT/PKB signaling: navigating downstream. Cell *129*, 1261-1274.

Marygold, S.J., and Leevers, S.J. (2002). Growth Signaling: TSC Takes Its Place. Curr Biol *12*, R785-787.

McManus, E.J., and Alessi, D.R. (2002). TSC1-TSC2: a complex tale of PKB-mediated S6K regulation. Nat Cell Biol *4*, E214-216.

Morgensztern, D., and McLeod, H.L. (2005). PI3K/Akt/mTOR pathway as a target for cancer therapy. Anti-cancer drugs *16*, 797-803.

Musaro, A., McCullagh, K., Paul, A., Houghton, L., Dobrowolny, G., Molinaro, M., Barton, E.R., Sweeney, H.L., and Rosenthal, N. (2001). Localized Igf-1 transgene expression sustains hypertrophy and regeneration in senescent skeletal muscle. Nat Genet *27*, 195-200.

Musaro, A., and Rosenthal, N. (1999). Maturation of the myogenic program is induced by postmitotic expression of insulin-like growth factor I. Mol Cell Biol *19*, 3115-3124.

O'Rourke, J.R., Georges, S.A., Seay, H.R., Tapscott, S.J., McManus, M.T., Goldhamer, D.J., Swanson, M.S., and Harfe, B.D. (2007). Essential role for Dicer during skeletal muscle development. Dev Biol *311*, 359-368.

Park, I.H., and Chen, J. (2005). Mammalian Target of Rapamycin (mTOR) Signaling Is Required for a Late-stage Fusion Process during Skeletal Myotube Maturation. J Biol Chem *280*, 32009-32017.

Parker, M.H., Seale, P., and Rudnicki, M.A. (2003a). Looking back to the embryo: defining transcriptional networks in adult myogenesis. Nat Rev Genet *4*, 497-507.

Parker, M.H., Seale, P., and Rudnicki, M.A. (2003b). Looking back to the embryo: defining transcriptional networks in adult myogenesis. Nat Rev Genet *4*, 497-507.
Persad, S., Attwell, S., Gray, V., Mawji, N., Deng, J.T., Leung, D., Yan, J., Sanghera, J., Walsh, M.P., and Dedhar, S. (2001). Regulation of protein kinase B/Akt-serine 473 phosphorylation by integrin-linked kinase: critical roles for kinase activity and amino acids arginine 211 and serine 343. J Biol Chem *276*, 27462-27469.
Ruby, J.G., Jan, C.H., and Bartel, D.P. (2007). Intronic microRNA precursors that bypass Drosha processing. Nature *448*, 83-86. Epub 2007 Jun 2024.
Sabatini, D.M., Erdjument-Bromage, H., Lui, M., Tempst, P., and Snyder, S.H. (1994). RAFT1: a mammalian protein that binds to FKBP12 in a rapamycin- dependent fashion and is homologous to yeast TORs. Cell *78*, 35-43.
Sabers, C.J., Martin, M.M., Brunn, G.J., Williams, J.M., Dumont, F.J., Wiederrecht, G., and Abraham, R.T. (1995). Isolation of a protein target of the FKBP12-rapamycin complex in mammalian cells. J Biol Chem *270*, 815-822.
Sabourin, L.A., and Rudnicki, M.A. (2000). The molecular regulation of myogenesis. Clin Genet *57*, 16-25.
Sarbassov, D., D., Ali, S.M., Kim, D.H., Guertin, D.A., Latek, R.R., Erdjument-Bromage, H., Tempst, P., and Sabatini, D.M. (2004). Rictor, a novel binding partner of mTOR, defines a rapamycin-insensitive and raptor-independent pathway that regulates the cytoskeleton. Curr Biol *14*, 1296-1302.
Sarbassov, D.D., Guertin, D.A., Ali, S.M., and Sabatini, D.M. (2005). Phosphorylation and regulation of Akt/PKB by the rictor-mTOR complex. Science *307*, 1098-1101.
Serruys, P.W., Regar, E., and Carter, A.J. (2002). Rapamycin eluting stent: the onset of a new era in interventional cardiology. Heart *87*, 305-307.
Stefani, G., and Slack, F.J. (2008). Small non-coding RNAs in animal development. Nat Rev Mol Cell Biol *9*, 219-230.
Thomas, M., Lieberman, J., and Lal, A. (2010). Desperately seeking microRNA targets. Nature structural & molecular biology *17*, 1169-1174.
Tollefsen, S.E., Lajara, R., McCusker, R.H., Clemmons, D.R., and Rotwein, P. (1989a). Insulin-like growth factors (IGF) in muscle development. Expression of IGF-I, the IGF-I receptor, and an IGF binding protein during myoblast differentiation. J Biol Chem *264*, 13810-13817.
Tollefsen, S.E., Sadow, J.L., and Rotwein, P. (1989b). Coordinate expression of insulin-like growth factor II and its receptor during muscle differentiation. Proc Natl Acad Sci U S A *86*, 1543-1547.
Tran, H., Brunet, A., Griffith, E.C., and Greenberg, M.E. (2003). The many forks in FOXO's road. Sci STKE *2003*, RE5.
Tschopp, O., Yang, Z.Z., Brodbeck, D., Dummler, B.A., Hemmings-Mieszczak, M., Watanabe, T., Michaelis, T., Frahm, J., and Hemmings, B.A. (2005). Essential role of protein kinase B gamma (PKB gamma/Akt3) in postnatal brain development but not in glucose homeostasis. Development *132*, 2943-2954.
Vogt, P.K. (2001). PI 3-kinase, mTOR, protein synthesis and cancer. Trends Mol Med *7*, 482-484.

Wagers, A.J., and Conboy, I.M. (2005). Cellular and molecular signatures of muscle regeneration: current concepts and controversies in adult myogenesis. Cell *122*, 659-667.

Wu, L., Fan, J., and Belasco, J.G. (2006). MicroRNAs direct rapid deadenylation of mRNA. Proc Natl Acad Sci U S A *103*, 4034-4039.

Wullschleger, S., Loewith, R., and Hall, M.N. (2006). TOR signaling in growth and metabolism. Cell *124*, 471-484.

Yaffe, D., and Saxel, O. (1977). Serial passaging and differentiation of myogenic cells isolated from dystrophic mouse muscle. Nature *270*, 725-727.

Yang, Q., Inoki, K., Ikenoue, T., and Guan, K.L. (2006). Identification of Sin1 as an essential TORC2 component required for complex formation and kinase activity. Genes Dev *20*, 2820-2832.

Yi, R., Qin, Y., Macara, I.G., and Cullen, B.R. (2003). Exportin-5 mediates the nuclear export of pre-microRNAs and short hairpin RNAs. Genes Dev *17*, 3011-3016.

Yuan, T.L., and Cantley, L.C. (2008). PI3K pathway alterations in cancer: variations on a theme. Oncogene *27*, 5497-5510.

Zoncu, R., Efeyan, A., and Sabatini, D.M. (2011). mTOR: from growth signal integration to cancer, diabetes and ageing. Nat Rev Mol Cell Biol *12*, 21-35. doi: 10.1038/nrm3025. Epub 2010 Dec 1015.

CHAPTER 2. XPLN IS AN ENDOGENOUS INHIBITOR OF mTORC2 [1]

2.1. Introduction

Mammalian Target of Rapamycin (mTOR) is an evolutionarily conserved Ser/Thr kinase that integrates signals from nutrient availability, growth factors, differentiation inducers, and various types of stress, to control a wide range of cellular and developmental processes (Foster and Fingar, 2010; Zoncu et al., 2011). mTOR nucleates two distinct multi-protein complexes known as mTOR Complex 1 (mTORC1) and mTOR Complex 2 (mTORC2), characterized by the presence of raptor and rictor, respectively. Emerging evidence implicates the deregulation of mTOR signaling in a variety of diseases including cancer and diabetes (Zoncu et al., 2011), underscoring the importance to fully understand the regulation of mTOR signaling.

mTORC1 regulates cell growth and proliferation by promoting biosynthesis of proteins, lipids, and organelles while inhibiting autophagy (Foster and Fingar, 2010; Zoncu et al., 2011). The best characterized substrates for the mTORC1 kinase are S6 Kinase 1 (S6K1) and eIF-4E-Binding Protein-1 (4E-BP1), both key regulators of protein synthesis (Ma and Blenis, 2009). mTORC2 phosphorylates the hydrophobic motif site Ser473 on Akt that is necessary for its activation (Sarbassov et al., 2005), as well as the turn motif controlling the folding and stability of Akt (Facchinetti et al., 2008; Ikenoue et al., 2008). The ribosome plays a direct role in activating mTORC2 (Zinzalla et al., 2011),

[1] All the data in this chapter except Fig. 2.11 appeared in PNAS as :
Khanna N., et al, 2013. XPLN is endogenous inhibitor of mTORC2. Proc Natl Acad Sci U S A. 2013 Oct 1;110(40):15979-84. It is available from http://www.pnas.org/content/110/40/15979.long and using doi: 10.1073/pnas.1310434110.

and association with the ribosome also allows mTORC2 to phosphorylate and stabilize Akt co-translationally (Oh et al., 2010). Thus, mTORC2 is involved in a variety of processes that are regulated by Akt, including cell survival, glucose metabolism, and cellular differentiation (Ge and Chen, 2012; Manning and Cantley, 2007; Oh and Jacinto, 2011). In addition, mTORC2 regulates cytoskeleton organization by promoting phosphorylation of protein Kinase C (PKCα) (Facchinetti et al., 2008; Ikenoue et al., 2008; Jacinto et al., 2004; Sarbassov et al., 2004), and serum/glucocorticoid regulated kinase 1 (SGK1) has also been identified as a substrate of mTORC2 (Garcia-Martinez and Alessi, 2008). Compared to mTORC1, for which mechanisms of activation by upstream signals have been extensively studied, less is known about the regulation of mTORC2 signaling. Several endogenous inhibitors of mTOR have been reported. While PRAS40 and FKBP38 are specific inhibitors of mTORC1, DEPTOR interacts with and inhibits both mTORC1 and mTORC2 (Foster and Fingar, 2010; Zoncu et al., 2011). Recently, the glucocorticoidinduced leucine zipper protein (GILZ) was reported to inhibit mTORC2 when overexpressed in BCR-ABL-expressing chronic myeloid leukemia (CML) cells (Joha et al., 2012).

XPLN (eXchange factor found in platelets, leukemic, and neuronal tissues) is a RhoGEF (guanine exchange factor) selectively activating RhoA and RhoB *in vitro* (Arthur et al., 2002). Like most RhoGEFs, XPLN contains a Dbl homology (DH) domain followed by a pleckstrin homology (PH) domain. This protein is expressed in several human tissues, with the highest levels found in the skeletal muscle and brain (Arthur et al., 2002). As expected for a protein with RhoGEF activity *in vitro*, overexpression of recombinant XPLN stimulates Rho-kinase dependent assembly of stress fibers and focal

adhesion, and has cell transforming activity (Arthur et al., 2002). However, a biological function for the endogenous XPLN has not been reported.

Here we identify XPLN as an mTORC2-interacting protein. We find that XPLN inhibits mTORC2 kinase activity *in vitro* and activation of Akt in cells. Interestingly, this function of XPLN is independent of its GEF activity and is most likely mediated by a physical interaction between its N-terminus and mTORC2. Furthermore, we show that XPLN negatively regulates cell survival and myoblast differentiation through inhibiting mTORC2 and Akt. These findings reveal XPLN as a novel regulator of mTORC2 signaling to Akt via a non-canonical mechanism.

2.2. Materials and Methods

2.2.1. Antibodies and other reagents. Rabbit polyclonal antibody against XPLN was generated by Proteintech Group Inc. using peptide REPQGETKLEQMDQSDSE as the antigen, and affinity purified. Anti-MHC (MF20) and anti-myogenin (F5D) were from the Developmental Studies Hybridoma Bank developed under the auspices of the NICHD, National Institutes of Health, and maintained by The University of Iowa, Department of Biological Sciences. Anti-tubulin antibody was from Abcam, anti-Myc clone 9E10 from Covance, anti-Flag M2 from Sigma, anti-GST (B-14) from Santa Cruz, anti-pS657-PKC from upstate technology, anti-raptor and anti-rictor from Bethyl Laboratories. All other primary antibodies were from Cell Signaling Technology. All secondary antibodies were from Jackson ImmunoResearch Laboratories, Inc. Akt inhibitor (Akti-1/2) was from Calbiochem. Glutathione Sepharose was from GE

Healthcare. Protein G-agarose and His-Akt were from Millipore. All other reagents were from Sigma-Aldrich.

2.2.2. Plasmids. pCMV6-myristoylated-HA-Akt (c.a.-Akt) was previously described (Erbay et al., 2003). pCMV-Myc-XPLN (human) and pGEX-4T-1-XPLN were generous gifts from Dr. Krister Wennerberg (University of Helsinki) (Arthur et al., 2002). Various fragments and mutants of XPLN cDNA were generated by PCR or site-directed mutagenesis (Mutagenesis Kit, Stratagene).

2.2.3. Cell culture. HEK 293 and HeLa cells were maintained in DME containing 10% fetal bovine serum (FBS) at 37 °C with 5% CO_2. All transient transfections in HEK293 cells were performed with PolyFect (Qiagen) following manufacturer's protocols at 60-70% cell confluence. C2C12 myoblasts were maintained in DME containing 1 g/L glucose and 10% FBS at 37°C with 7.5% CO_2. Transfection of C2C12 was performed using TransIT-LT1 (Mirus) following the manufacturer's recommendations, followed by selection in 1.0 mg/ml G418 for 2-3 days. Primary myoblasts were isolated from 2- to 5-day-old FVB neonates as described previously (Ge et al., 2011a), and maintained at low density on 1% gelatin-coated tissue culture plates. All animal experiments in this study followed protocols approved by the Animal Care and Use Committee at the University of Illinois at Urbana-Champaign. Lentiviral infection of C2C12 and primary myoblasts was performed as previously described (Yoon and Chen, 2008), with 3 mg/mL puromycin selection in C2C12 for 2 days and no drug selection for primary myoblasts.

Myogenic differentiation of C2C12 cells and primary myoblasts were induced at 100% and 50-70% confluence, respectively, by switching to DME containing 2% horse serum as previously described (Yoon and Chen, 2008). Differentiated cells in 12-well

plates were fixed, and stained for MHC and DAPI as previously described (Yoon and Chen, 2008). The stained cells were examined with a Leica DMI 4000B fluorescence microscope, and the fluorescent images were captured using a RETIGA EXi camera and analyzed with Q-capture Pro51 software (Q-Imaging™). The fusion index was calculated as the percentage of nuclei in myocytes with ≥2 nuclei. Each data point was generated from scoring 5 randomly chosen microscopic fields.

2.2.4. Lentivirus-mediated RNAi. Lentivirus packaging and infection were performed as previously described (Ge et al., 2011b). All shRNAs were from the MISSION® TRC library (Sigma-Aldrich). The shRNAs for mouse mTOR, Raptor, rictor, and negative control (scramble hairpin) have been reported (Ge et al., 2011b). XPLN shRNAs were from the MISSION® TRC library (Sigma-Aldrich). The clone IDs are: mouse XPLN #1, NM_027871.1-458s1c1; human XPLN #1, NM_019555.1-226s1c1; mouse and human XPLN #2, NM_019555.1-578s1c1.

2.2.5. Western blotting, immunoprecipitation. Cells were lysed in ice-cold lysis buffer (40 mM HEPES, pH7.2, 120 mM NaCl, 10 mM pyrophosphate, 50 mM NaF, 10 mM b-glycerophosphate, 2 mM EDTA, 1x Sigma protease inhibitor cocktail, and 0.3% CHAPS). The supernatant after microcentrifugation at 13,000 rpm for 10 min was collected and subjected to immunoprecipitation at 4ºC with various antibodies in the lysis buffer, followed by incubation with Protein G-agarose. The beads were washed with lysis buffer, and then boiled in SDS sample buffer. Proteins were resolved on SDS-PAGE and transferred onto PVDF membrane (Millipore), followed by incubation with various antibodies according to the manufacturers' recommendations. Detection of horseradish peroxidase-conjugated secondary antibodies was performed with Western Lightning™

Chemiluminescence Reagent Plus (Perkin Elmer, Inc.). Quantification of Western band intensities was performed by densitometry of X-ray film images using the software Image J.

2.2.6. Purification of GST-fusion proteins, GST pulldown assays. GST and GST-XPLN were expressed in *E. coli* and purified using glutathione Sepharose beads (GE Healthcare) following the manufacturer's recommendations. Purified proteins (20 μg each) were pre-incubated with cell lysates for 60 min before incubation with glutathione Sepharose for 90 min, followed by washing with lysis buffer.

2.2.7. In-vitro mTOR kinase assays. mTORC1 and mTORC2 were immunoprecipitated using anti-raptor and anti-rictor antibodies, respectively. The kinase assays were performed following procedures described by Ikenoue et al. (Ikenoue et al., 2009). mTORC1 kinase assays were carried out at 30ºC for 30 min in 25mM HEPES (pH 7.4), 50 mM KCl, 10 mM $MgCl_2$ and 250 μM ATP, with 100 ng GST-S6K1 4EBP1 as the substrate. mTORC2 kinase assays were carried out at 37ºC for 30 min in 25mM HEPES (pH 7.4), 100 mM potassium acetate, 1 mM $MgCl_2$ and 500 μM ATP, with 250 ng His-Akt as the substrate. Where applicable, purified GST proteins (1 μg each) were added to the immunocomplexes 15 30 min before initiation of the kinase assay by the addition of ATP. Reactions were stopped by the addition of SDS sample buffer and boiling.

2.2.8. RhoA activity assay. GTP-bound RhoA was measured following the method described by Ren and Schwartz (Ren and Schwartz, 2000). The amount of GTP-bound RhoA was measured using the method described by Ren and Schwartz (Ren and Schwartz, 2000). Briefly, cells were lysed in 50 mM Tris, pH 7.4, 10 mM $MgCl_2$, 500

mM NaCl, 1% Triton X-100, 0.1% SDS, 0.5% deoxycholate, and 1x Protease Inhibitor Cocktail. Cleared lysates were incubated with glutathione-Sepharose beads containing 30 μg of GST-RBD (GST fusion to the Rho-binding domain of Rhotekin protein), and the beads were washed in 50 mM Tris, pH 7.4, 10 mM $MgCl_2$, 150 mM NaCl, 1% Triton X-100, and 1x Protease Inhibitor Cocktail. Bound proteins and lysates were analyzed by Western blotting with anti-RhoA antibody.

2.2.9. Statistical analysis. All data are presented as mean ± SD, or representative blots, of at least 3 sets of independent experiments. Whenever necessary, statistical significance of the data was analyzed by performing one-sample or paired *t* tests.

2.3. Results

2.3.1. XPLN interacts with mTORC2. To explore novel interacting partners of mTOR, we carried out yeast two-hybrid screens using the C-terminal 1188 amino acids of mTOR (a.a. 1362-2549) as bait against a HeLa cell cDNA prey library. XPLN cDNA emerged as a positive hit and was confirmed in secondary assays in yeast. The interaction between full-length mTOR and XPLN was then examined in mammalian cells. As shown in Fig. 2.1A, Flag-mTOR stably expressed in HEK293 cells co-immunoprecipitated with transiently expressed Myc-XPLN, and *vice versa*. In addition, bacterially purified GST-XPLN associated with endogenous mTOR in pull-down assays performed with both HEK293 (Fig. 2.1B) and mouse C2C12 cell lysates (Fig. 2.1C). Furthermore, GST-XPLN associated with endogenous rictor, and not raptor (Fig. 2.1B & C), suggesting that the interaction may be specific for mTORC2. Indeed, both mSin1 and mLST8, the other components of mTORC2 (Oh and Jacinto, 2011), were found to associate with GST-

XPLN (Fig. 2.1B), and immunoprecipitation of endogenous rictor and mSin1 brought down Myc-XPLN stably expressed in HEK293 cells (Fig. 2.1D).

The interaction between XPLN and mTOR complexes was further investigated in cells with lentivirus-delivered shRNA-mediated knockdown of mTOR, raptor, and rictor. Depletion of rictor significantly impaired the interaction between mTOR and XPLN, whereas removal of mTOR had no effect on rictor-XPLN interaction (Fig. 2.1E). On the other hand, raptor depletion slightly increased XPLN interaction with mTOR and rictor (Fig. 2.1E). Hence, the XPLN-mTOR interaction appears to be mediated by rictor, although we cannot rule out a possible involvement of mSin1, the presence of which is necessary for rictor association with mTOR (Oh and Jacinto, 2011). Our original two-hybrid result could be explained by the presence of orthologs of mTORC2 components in yeast (Avo3 and Avo1) (Frias et al., 2006; Jacinto et al., 2006). Although the Avo3 (yeast rictor)-binding site (Wullschleger et al., 2005) is in a region of TOR2 absent in our two-hybrid bait, the C-terminal 80 kDa of mTOR – included in the bait – binds rictor (Panasyuk et al., 2009) and thus may also bind Avo3.

2.3.2. XPLN negatively regulates Akt phosphorylation and cell survival. XPLN has been reported to stimulate the assembly of focal adhesions and stress fibers in a Rho-kinase dependent manner (Arthur et al., 2002). Since mTORC2 has been implicated in the regulation of actin cytoskeleton (Jacinto et al., 2004; Sarbassov et al., 2004), and in yeast TOR2 activates RHO1 and RHO2 through its GEF ROM2 (Schmidt et al., 1997), a plausible model would be that mTORC2 regulates GEF activity of XPLN towards RhoA proteins. However, knockdown of mTOR or rictor had no effect on RhoA-GTP levels in

HEK293 cells, as assayed by pull-down of active RhoA with GST-RBD (Rho-binding domain of Rhotekin) (Fig. 2.6). RhoB expression was not detected in these cells. Although this lack of mTORC2 effect on RhoA did not completely rule out XPLN being a target of mTORC2 because of the existence of other RhoGEFs, we decided to examine the alternative possibility of XPLN being upstream of mTORC2. We used Akt as a readout because it was the best characterized substrate of mTORC2.

As shown in Fig. 2.2A, Akt phosphorylation on Ser473, the mTORC2 site, was markedly increased upon XPLN knockdown in both HEK293 and C2C12 cells, with two independent shRNAs for each cell line. On the other hand, XPLN knockdown did not affect the mTORC1 substrate S6K1, or the phosphorylation of NDRG1 (substrate of SGK1 – another target of mTORC2) (Fig. 2.2A). The effect of XPLN depletion was observed on both steady-state and serum-stimulated Akt phosphorylation (Fig. 2.2A&B). Phosphorylation of T308 on Akt was not markedly affected by XPLN knockdown (Fig. 2.2B), further confirming that XPLN acted through mTORC2. Several substrates of Akt are known to be differentially dependent on the phosphorylation status of Akt – while FoxO3a phosphorylation requires pS473, phosphorylation of TSC2 and GSK3b can occur in the absence of pS473 (Guertin et al., 2006; Jacinto et al., 2006). Indeed, XPLN knockdown did not affect the levels of pT1462-TSC2 and pS9-GSK3b, both markedly stimulated by serum (Fig. 2.2B). The level of FoxO3a, on the other hand, was drastically reduced upon XPLN knockdown in serum-stimulated cells (Fig. 2.2B), most likely a consequence of enhanced phosphorylation by hyperactive Akt (Plas and Thompson, 2003). Furthermore, overexpression of XPLN resulted in a modest, but nevertheless statistically significant, reduction of serum- and insulin-stimulated pSer473-Akt, with a

similar effect on pT32-FoxO3a but no effect on pT346-NDRG1 (Fig. 2.2C). Taken together, these observations strongly suggest that XPLN is an endogenous inhibitor of Akt phosphorylation by mTORC2.

Since one of the major functions of Akt is to support cell survival, at least partly through regulation of FoxO (Greer and Brunet, 2005; Lawlor and Alessi, 2001), we tested whether XPLN might impact apoptosis. To examine this possibility, HeLa cells were serum-starved to induce apoptosis. As shown in Fig. 2.2D, XPLN knockdown decreased the levels of PARP cleavage as well as cleaved Caspase-3, both markers of apoptosis. Importantly, an Akt1/Akt2 inhibitor (Akti) and the mTOR kinase inhibitor Torin1 reversed the protective effect of XPLN depletion and enhanced apoptosis (Fig. 2.2D), suggesting that XPLN acts through Akt and mTOR. This is further confirmed by the reversal of XPLN knockdown phenotype by the co-knockdown of rictor (Fig. 2.2E). It is noted that XPLN knockdown modestly enhanced pAkt even in rictor knockdown cells (Fig. 2.2E), most likely due to residual rictor protein especially in cells infected by both XPLN and rictor shRNA viruses, which had reduced rictor knockdown efficiency. In conclusion, XPLN negatively regulates cell survival by suppressing mTORC2 and Akt.

2.3.3. XPLN regulation of Akt phosphorylation is independent of its GEF activity and dependent on its N-terminus. Because the only reported function of XPLN thus far is to act as a RhoGEF, we set out to test whether the GEF activity of XPLN was necessary for its regulation of Akt. It has been reported that two point mutations, L321E in the DH domain and W492L in the PH domain, are each sufficient to inactivate the GEF activity of NET1, the closest homologue of XPLN (Alberts and Treisman, 1998).

We constructed analogous mutants of XPLN – L269E and W440L, and found that indeed each mutation abolished the GEF activity of recombinant XPLN when overexpressed in cells (Fig. 2.3A). Strikingly, these XPLN mutants suppressed Akt phosphorylation in cells to the same degree as WT XPLN (Fig. 2.3B). Consistent with a GEF-independent, mTORC2 binding-dependent function of XPLN, both GEF-inactive XPLN mutants interacted with mTORC2 (Fig. 2.3C). These observations suggest that XPLN regulates phosphorylation of Akt in cells independently of its GEF activity.

To further examine the mechanism of XPLN action, we set out to map the region(s) of XPLN interacting with mTORC2. XPLN contains DH and PH domains with N- and C-terminal regions having no known sequence motifs. The DH domain of most GEFs confers the catalytic activity, whereas the PH domain may regulate protein localization by mediating protein-lipid or protein-protein interactions at least in some GEFs (Rossman et al., 2005). As shown in Fig. 2.3D, the N-terminal region of XPLN (amino acids 1-125, designated N125) and the PH domain (amino acids 304-466) interacted with endogenous mTOR and rictor, suggesting that XPLN may have two independent binding sites for mTORC2. Importantly, overexpression of XPLN-N125 suppressed Akt phosphorylation to the same extent as overexpression of full-length XPLN (Fig. 2.3E). On the other hand, overexpression of the PH domain did not affect Akt (Fig. 2.3E) even though it interacted with rictor. Hence, we surmise that XPLN inhibits mTORC2 function via its N-terminus interacting with rictor. A second interaction, between the PH domain and rictor, may serve to strengthen the interaction and enhance the inhibitory function of the N-terminus of the full-length protein.

2.3.4. XPLN inhibits mTORC2 kinase activity towards Akt *in vitro*. Given the physical interaction between XPLN and mTORC2, and the lack of detectable interaction between XPLN and Akt (Fig. 2.7), we reasoned that the simplest model explaining our observations thus far would be the inhibition of mTORC2 activity through XPLN binding. XPLN did not disrupt mTORC2 assembly, as overexpression of XPLN did not affect the amount of mTOR co-immunoprecipitated with rictor (Fig. 2.8). To examine if XPLN had a direct effect on mTORC2 kinase activity, we performed *in vitro* kinase assays with endogenous mTORC2 immunoprecipitated through rictor, using Akt as a substrate. Addition of bacterially purified GST-XPLN, but not GST-Cdc42, to the reaction markedly inhibited phosphorylation of Akt (Fig. 2.4A). At the same time, GST-XPLN had no effect on *in vitro* mTORC1 kinase activity using 4E-BP1 as a substrate (Fig. 2.4B).

Next, we examined XPLN mutants for their capacity to impact mTORC2 kinase activity. As shown in Fig. 2.4C, the GEF-inactive mutant, W440L, inhibited Akt phosphorylation *in vitro* as effectively as the wt XPLN. The N125 fragment was also inhibitory, whereas XPLN with the N-terminal 125 amino acids deleted (DN-XPLN) had no effect on the kinase activity (Fig. 2.4C), indicating that N125 is both necessary and sufficient for XPLN's inhibition of mTORC2. Hence, in line with its regulation of Akt phosphorylation in cells, XPLN directly inhibits mTORC2 by a GEF-independent mechanism through its N-terminus, most likely via physical interaction with the mTORC2 complex.

2.3.5. XPLN negatively regulates myoblast differentiation through mTORC2 and Akt. To further probe the biological relevance of this novel role of XPLN in regulating mTORC2 and Akt, we set out to examine a potential function of XPLN in myoblast differentiation, because XPLN expression has been reported to be the highest in skeletal muscles among human tissues (Arthur et al., 2002) and, additionally, Akt is a well-established regulator of skeletal myogenesis (Jiang et al., 1999; Peng et al., 2003). To that end, C2C12 myoblasts were induced to undergo myogenic differentiation by serum withdrawal. XPLN depletion led to a significant enhancement in myoblast differentiation compared to the control cells, as evidenced by elevated expression of the myogenic markers, myosin heavy chain (MHC) and myogenin (Fig. 2.5A), as well as increased fusion index (Fig. 2.5B). This XPLN knockdown phenotype was recapitulated in mouse primary myoblasts (Fig. 2.5A&B).

To determine the function of XPLN in muscle regeneration, we injected lentiviruses expressing shRNA against XPLN together with $BaCl_2$ into tibialis anterior muscles. Interestingly, XPLN depletion enhanced muscle regeneration (Fig. 2.11), as depicted by the increase in muscle cross-section area (CSA) compared to the control shRNA.

XPLN overexpression decreased the degree of C2C12 differentiation (Fig. 2.5C&D), which corroborated the knockdown phenotype. Interestingly, overexpression of the GEF-inactive mutants, as well as the N-terminal fragment of XPLN, had the same inhibitory effect on differentiation as WT XPLN (Fig. 2.5C&D), indicating that the anti-myogenic function of XPLN is independent of its GEF activity and is conferred by its N-terminus. This function closely correlates with the mode of XPLN action on Akt activity.

Furthermore, knockdown of rictor suppressed the increase in differentiation induced by XPLN knockdown (Fig. 2.5E&F), confirming that XPLN acts through mTORC2. Similar to the observations in HeLa cells (Fig. 2.2E), co-knockdown led to less efficient depletion of rictor protein, which could explain the increased pAkt compared to rictor knockdown alone (Fig. 2.5E). The degree of differentiation correlated with the degree of pAkt (Fig. 2.5E&F). In addition, a constitutively active (c.a.) Akt overcame the inhibition by overexpressed XPLN and restored differentiation (Fig. 2.5G). Conversely, Akti severely impaired differentiation in cells with XPLN knockdown (Fig. 2.5H). In aggregate, our observations strongly suggest that XPLN negatively regulates myoblast differentiation by inhibiting Akt activation, through suppression of mTORC2.

2.4. Discussion

mTORC2 is critically involved in various cellular and developmental processes, but knowledge of its regulation has been scarce. Our studies have identified XPLN as a direct mTORC2 inhibitor in cells and *in vitro*. XPLN inhibits the kinase activity of mTORC2 towards Akt. This function of XPLN does not require its GEF activity and is most likely mediated by its direct interaction with mTORC2, revealing a non-canonical role of XPLN that is Rho-independent. Furthermore, we show that the endogenous XPLN negatively regulates cell survival and skeletal myoblast differentiation through inhibiting mTORC2 and Akt, validating the biological significance of this newly discovered regulatory mechanism. The only other mTORC2-specific inhibitor reported, GILZ, has been shown to inhibit mTORC2/Akt signaling when overexpressed in BCR-ABL-

positive CML cells (Joha et al., 2012), but it is not known whether GILZ is an endogenous inhibitor of mTORC2 in normal physiological contexts.

Several RhoGEF proteins have been reported to have GEF activity-independent functions. For example, the GEF activity of Vav1 is not necessary for its ability to potentiate NF-AT activation in response to T cell receptor signaling (Kuhne et al., 2000). Dbl binds and translocates Ezrin to the plasma membrane in a GEF-independent manner (Vanni et al., 2004). The exact mechanisms by which such non-canonical functions are exerted by these GEFs are not clear, although protein-protein interactions mediated by modular domains outside of the catalytic region appear to be important. Interestingly, XPLN binds and inhibits mTORC2 via an N-terminal region that lacks sequence homology to any known modular domain. A second binding site is found in the PH domain of XPLN, but this domain is not sufficient to elicit an effect on mTORC2. It is possible that this additional interaction serves to increase the overall affinity between XPLN and mTORC2, in which case overexpression of the N-terminus resulting in a high local concentration would be sufficient to exert an inhibitory effect without the need for the PH domain, as we have observed.

Interestingly, the action of XPLN is not only specific for mTORC2 but may even be selective toward Akt. Another substrate of mTORC2, SGK1, is not regulated by XPLN in cells. This contrasts the observation with DEPTOR, which inhibits the phosphorylation of all mTORC1 and mTORC2 substrates tested (Peterson et al., 2009). Overexpression of GILZ also inhibits all mTORC2 substrates in CML cells (Joha et al., 2012). It is possible that endogenous XPLN is localized in the cell where Akt, but not SGK1, is regulated. However, the lack of effect on SGK1 by XPLN overexpression

(Fig. 2.2C), which would presumably override any requirement for subcellular localization, seems to argue against that possibility. An alternative mechanism is that XPLN binding to mTORC2 specifically blocks Akt as a substrate without affecting the other mTORC2 substrates. Future biochemical and structural studies should prove informative for the dissection of the exact mechanism by which XPLN inhibits mTORC2 phosphorylation of Akt.

Removal of XPLN inhibition alone is not sufficient to induce Akt phosphorylation in the absence of upstream stimuli when the basal activity of Akt is low. This is not surprising, as presumably activation of the kinase (mTORC2) requires positive inputs in addition to removal of XPLN suppression. Although very little is known about such inputs, PI3K activity and TSC1/2 have been reported to mediate mitogenic stimulation of mTORC2 kinase activity (Gan et al., 2011; Huang et al., 2008). It is presently not known how or whether XPLN itself is regulated. Growth factor stimulation activates Akt in cells, but it does not affect XPLN levels (Fig. 2.9A) or the interaction between XPLN and mTORC2 (Fig. 2.9B&C). DEPTOR is degraded by the proteasome in an mTOR-dependent fashion in response to serum stimulation, which forms a positive feedback loop to maximize mTOR activation (Duan et al., 2011; Gao et al., 2011; Zhao et al., 2011). However, the slow kinetics of DEPTOR degradation (Peterson et al., 2009) does not explain the well-known rapid activation of mTORC1 and mTORC2 substrates upon growth factor stimulation. It is possible that the inhibitors – DEPTOR and XPLN alike – may be overcome by a conformational change or modification of the kinase (mTORC2) without physical removal. In the case of XPLN in myoblast differentiation, there may be a simple mechanism of de-repression: the level of

XPLN does not change (Fig. 2.10), but mTOR levels increase drastically in the course of differentiation, which may allow mTORC2 to overcome XPLN stoichiometrically.

Akt regulates many physiological processes in addition to cell survival and myogenic differentiation, including cell proliferation, glucose metabolism, and other types of cellular differentiation. Regulation of Akt by XPLN in those processes warrants future investigation. A proto-oncogene, Akt is involved in tumorigenesis by promoting proliferation, survival, and motility of cancer cells (Vivanco and Sawyers, 2002). Evidence supports a direct role of mTORC2, at least partly through Akt, in driving tumorigenesis (Zoncu et al., 2011). Future examination of a role of XPLN in tumor suppression, especially in the context of hyperactive Akt, may prove informative for the understanding of and therapeutic strategy against cancer.

2.5. Figures

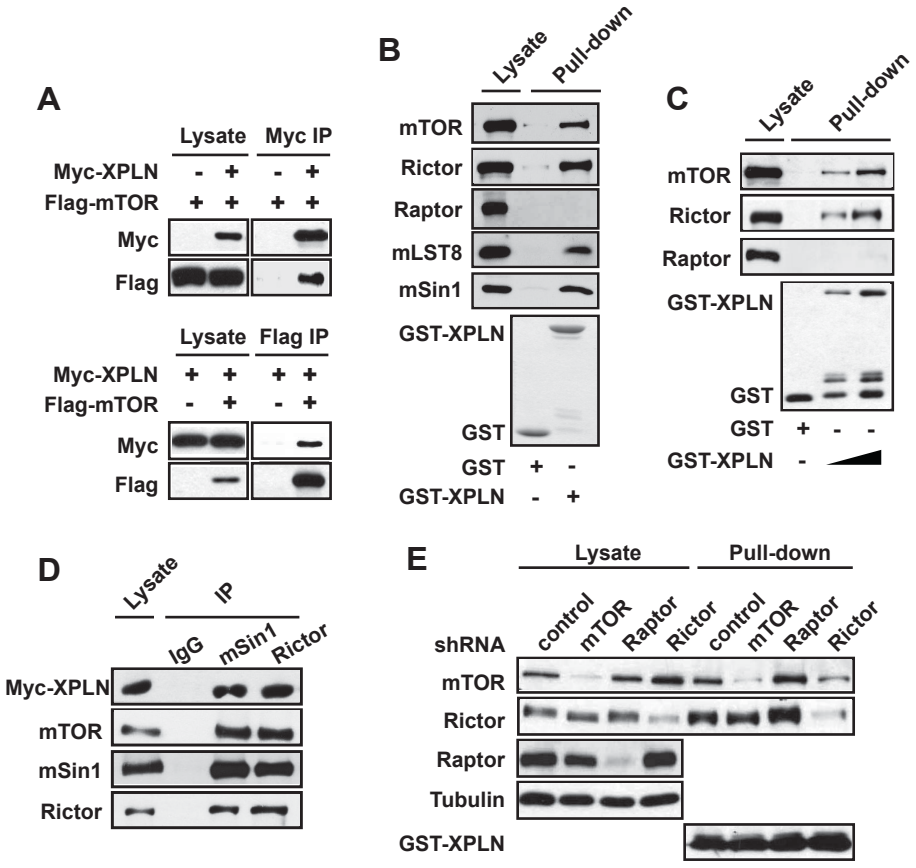

Fig. 2.1. XPLN interacts with mTORC2. **(A)** HEK293 cells stably expressing Flag-mTOR were transfected with Myc-XPLN. Anti-Myc or anti-Flag immunoprecipitation (IP) was followed by Western analysis. **(B-C)** GST pull-down assays were performed using purified GST-XPLN with GST as a negative control with HEK293 (B) or C2C12 (C) cell lysates, and analyzed by Western blotting. Some degradation fragments were present in the GST-XPLN protein preparation. **(D)** Endogenous rictor and mSin1 were IPed from HEK293 cells stably expressing Myc-XPLN, followed by Western analysis. **(E)** C2C12 cells were infected with lentiviruses expressing shRNAs for mTOR, raptor, rictor, or a scrambled sequence as control, and then subjected to GST-XPLN pull-down assays.

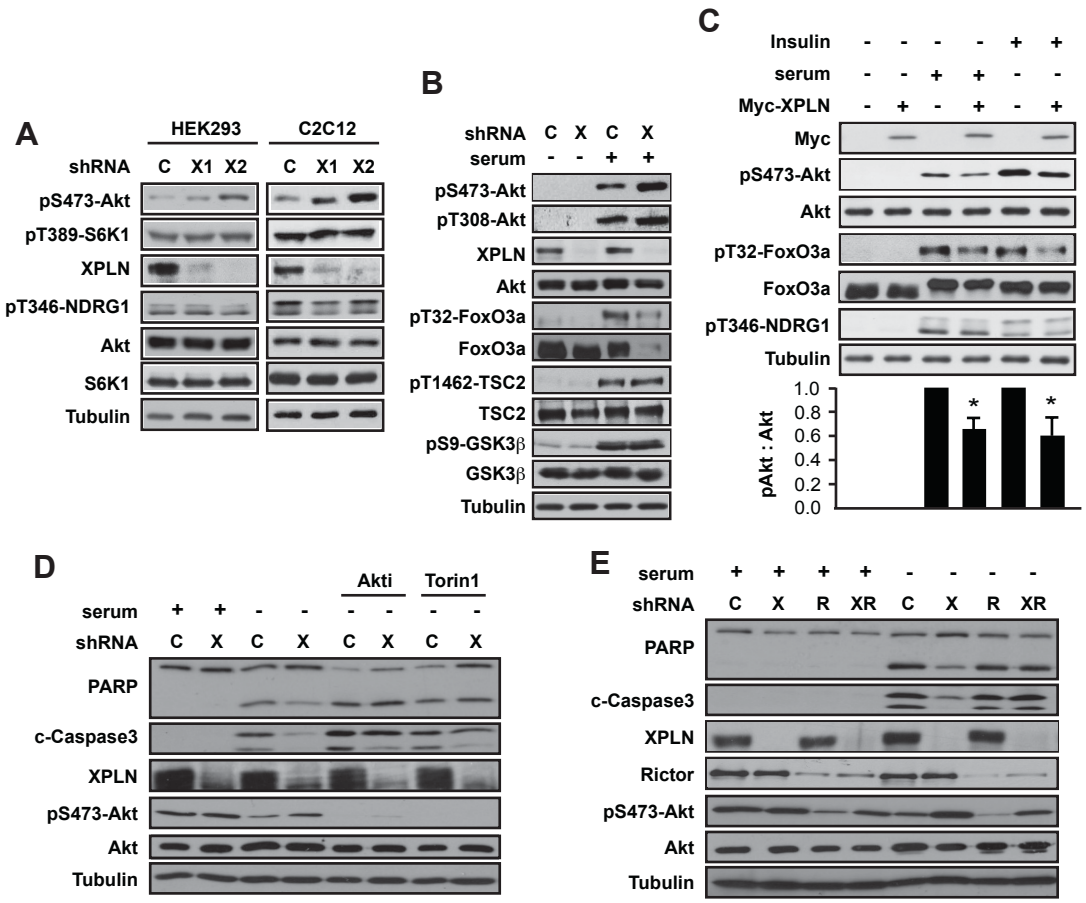

Fig. 2.2. XPLN negatively regulates Akt phosphorylation and cell survival. (A) HEK293 or C2C12 cells were infected with lentiviruses expressing two independent XPLN shRNA ("X1", "X2"), or a scrambled hairpin sequence as control ("C"), followed by Western analysis. Due to its lower abundance in HEK293 cells, XPLN was enriched by immunoprecipitation before Western blotting. **(B)** HEK293 cells were treated as in A and then serum starved overnight, followed by stimulation with 10% FBS for 30 min before Western analysis. **(C)** C2C12 cells were transfected with Myc-XPLN. After serum starvation overnight, the cells were stimulated with 10% FBS or 100 nM insulin for 30 min followed by Western analysis. pS473-Akt and Akt bands were quantified by densitometry, and the relative ratios of pS473 *versus* total Akt were calculated with empty vector-transfected and stimulated samples designated as 1. One-sample *t* test was performed to compare each data point to its respective control. **P*<0.05. **(D)** HeLa cells were infected with XPLN shRNA1 ("X") or control, serum starved for 48 hrs, followed by Western analysis. Some cells were treated with 1 μM Akti or 250 nM Torin1 for 3 hrs prior to cell lysis. **(E)** HeLa cells were infected with XPLN or rictor ("R") shRNA, or both, serum starved for 48 hrs, followed by Western analysis.

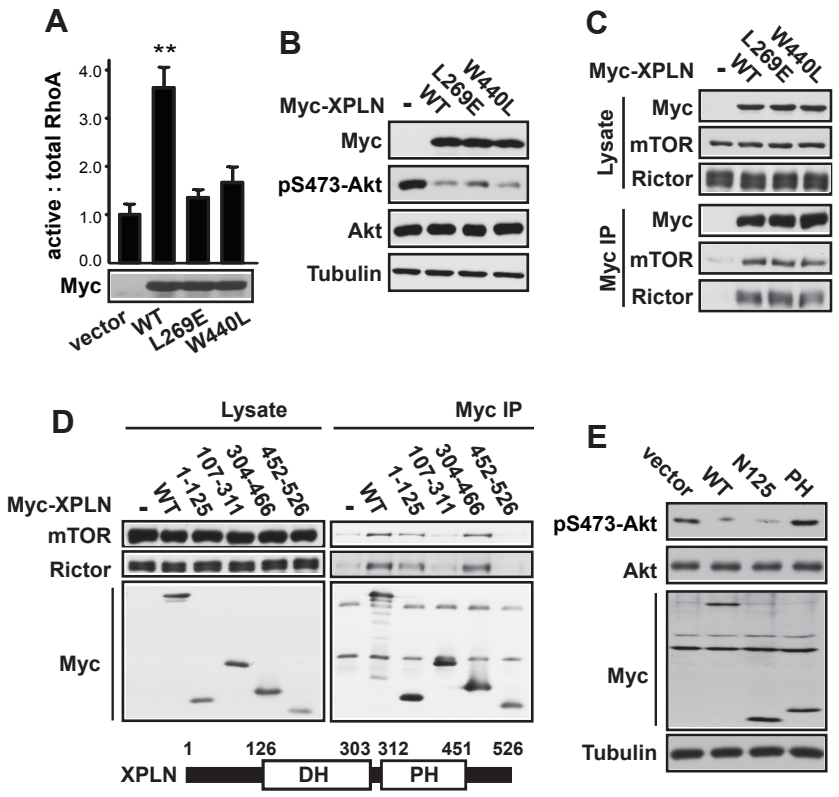

Fig. 2.3. XPLN regulation of Akt is independent of its GEF activity and dependent on its N-terminus. (A) HEK293 cells were transfected with wild type, L269E, or W440L Myc-XPLN, followed by GST-RBD pull-down assays. The active RhoA (RhoA pulled down with GST-RBD), and total RhoA (RhoA in cell lysates) were quantified by densitometry. The ratios of active RhoA *versus* total RhoA were calculated and normalized against the control (empty vector). Paired *t* tests were performed to compare each data point to vector control. $^{**}P<0.005$. **(B)** C2C12 cells were transfected with various Myc-XPLN as indicated, followed by Western analysis. **(C)** HEK293 cells were transfected with various Myc-XPLN, followed by anti-Myc IP and then Western analysis. **(D)** HEK293 cells were transfected with fragments of Myc-XPLN as indicated, followed by anti-Myc IP and then Western analysis. **(E)** C2C12 cells were transfected with various Myc-XPLN fragments, followed by Western analysis.

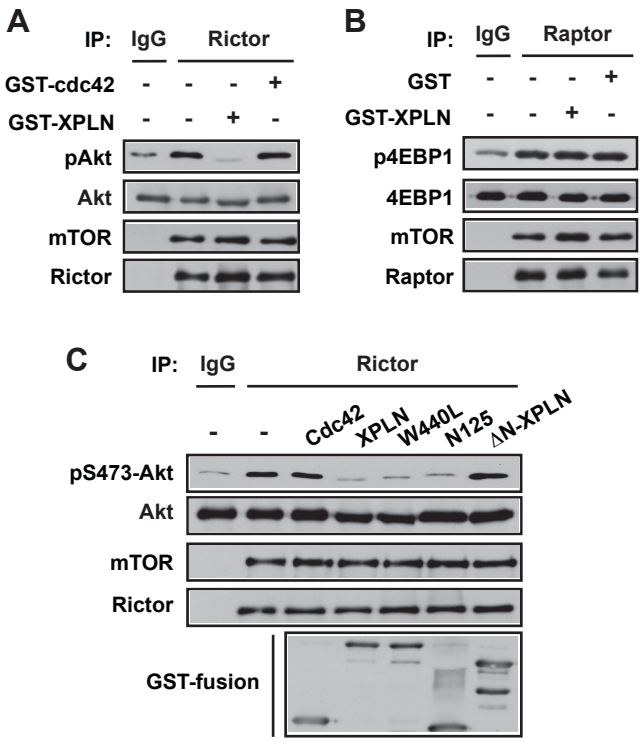

Fig. 2.4. XPLN inhibits mTORC2 phosphorylation of Akt *in vitro*. **(A)** Endogenous rictor was immunoprecipitated (IP) from HEK293 cells, and subjected to *in vitro* kinase assays using His-Akt as the substrate and anti-pSer473 as the readout. Bacterially purified GST-XPLN or GST-Cdc42 (1 μg each) was added prior to kinase assays in the indicated samples. **(B)** Endogenous raptor was immunoprecipitated, and subjected to *in vitro* kinase assays using GST-4EBP1 as the substrate and anti-pThr37/46 as the readout. GST-XPLN or GST (1 μg each) was added prior to kinase assays in the indicated samples. **(C)** Endogenous rictor immunoprecipitation and *in vitro* kinase assay were performed as described in A. Bacterially purified GST fusion protein of XPLN, W440L-XPLN, N125-XPLN, or DN-XPLN (1 μg each) was added prior to kinase assays.

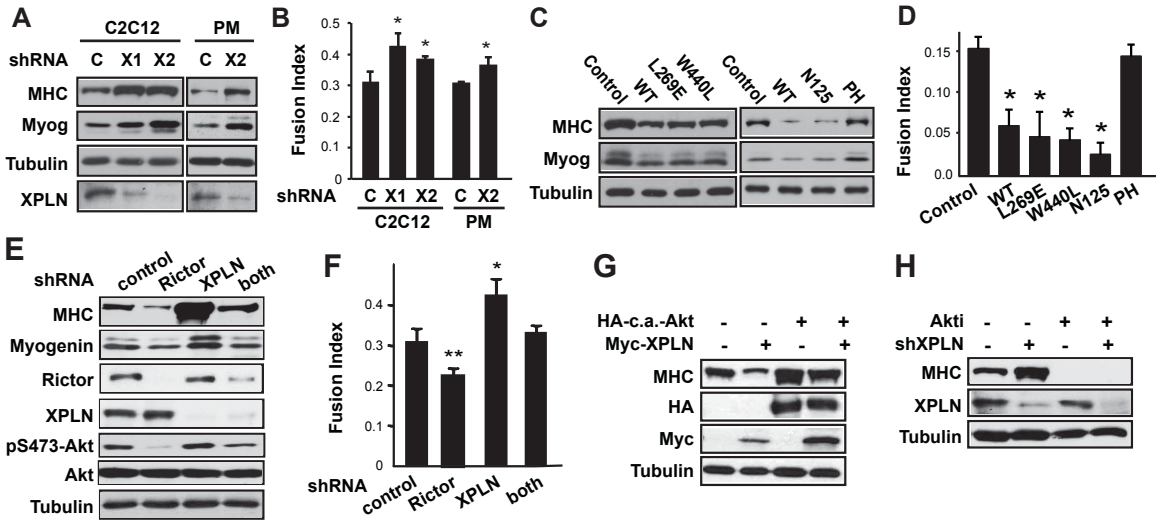

Fig. 2.5. XPLN negatively regulates myoblast differentiation through mTORC2 and Akt. (A) C2C12 myoblasts and mouse primary myoblasts (PM) were infected with lentiviruses expressing XPLN shRNA ("X1", "X2"), or the control hairpin ("C"). After differentiation for 3 days (C2C12) or 2 days (PM), the cells were subjected to Western analysis. **(B)** Cells as described in A were fixed and stained for MHC and DAPI, and quantified for fusion index. **(C)** C2C12 cells were transfected with WT, mutants, or fragments of XPLN as indicated. After differentiation, the cells were subjected to Western analysis. **(D)** Cells as described in C were stained for MHC and DAPI, and quantified for fusion index. **(E)** C2C12 cells were infected with lentiviruses expressing shRNA for XPLN, rictor, or both. After differentiation, the cells were subjected to Western analysis. **(F)** Cells as described in E were stained for MHC and DAPI, and quantified for fusion index. **(G)** Cells were transfected with Myc-XPLN, c.a.-Akt, or both, followed by differentiation and then Western analysis. **(H)** Cells were infected with XPLN shRNA lentivirus, differentiated in 1 μM Akti or DMSO, followed by Western analysis. Paired *t* test was performed to compare each data point to control. **P*<0.05. ***P*<0.01.

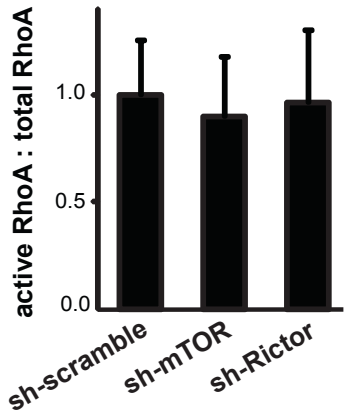

Fig. 2.6. Knockdown of mTORC2 does not affect RhoA-GTP loading. HEK293 cells were infected with lentiviruses expressing shRNAs for mTOR, rictor, or a scrambled sequence as control. Cell lysates were subjected to GST-RBD pull-down assays followed by Western analysis. Active RhoA (RhoA pulled down with GST-RBD), and total RhoA (RhoA in cell lysates) were quantified by densitometry. The ratios of active RhoA *versus* total RhoA were calculated and normalized against the control (scramble). Each data point is compared with the control by paired *t* test, and no significant difference was found.

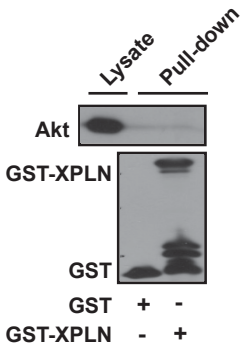

Fig. 2.7. There is no detectable interaction between XPLN and Akt. HEK293 cell lysates were subjected to pulldown assay with GST-XPLN or GST, and endogenous Akt was detected by Western.

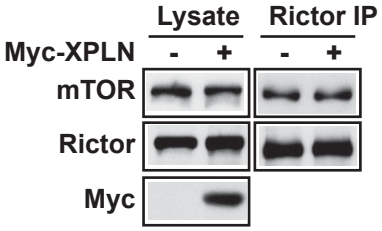

Fig. 2.8. Overexpression of XPLN does not affect mTOR-rictor interaction. HEK293 cells were transfected with Myc-XPLN. Cell lysates were subjected to endogenous rictor IP followed by Western analysis.

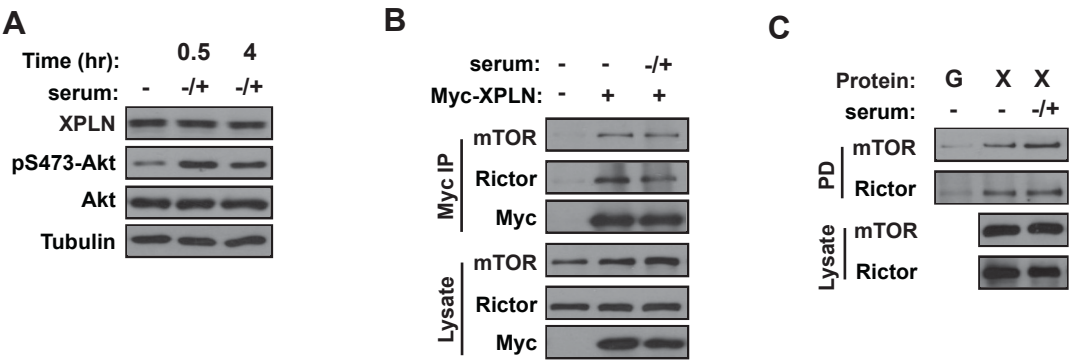

Fig. 2.9. Serum stimulation does not affect XPLN protein level or its interaction with mTORC2. (A) HEK293 cells were serum-starved overnight and then stimulated with 10% FBS for 30 min or 4 hrs, followed by Western analysis. **(B)** HEK293 cells were transfected with Myc-XPLN, serum-starved overnight followed by stimulation with 10% FBS for 30 min. IP was performed with anti-Myc antibody. **(C)** HEK293 cells were serum-starved and then stimulated with 10% FBS for 30 min, followed by GST pulldown assays.

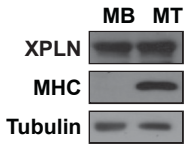

Fig. 2.10. XPLN protein level does not change during myoblast differentiation. C2C12 cells were lysed before (myoblast – "MB") or after (myotube – "MT") 3-day differentiation, and subjected to Western analysis.

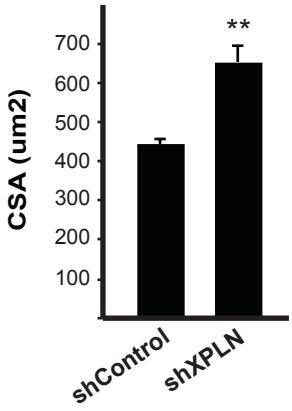

Fig. 2.11. XPLN depletion promotes muscle regeneration. Control or XPLN shRNA expressing lentiviruses were co-injected with $BaCl_2$ into TA muscles. Regenerating muscles after 5 days of injection were cryosectioned and subjected to H&E staining. These sections were quantified for regenerating myofiber cross-section area (CSA). Data is plotted as mean ± S.D (n=5). A paired t-test was performed to compare each value with that of the control. **p<0.01

2.6. References

Alberts, A.S., and Treisman, R. (1998). Activation of RhoA and SAPK/JNK signalling pathways by the RhoA-specific exchange factor mNET1. Embo J *17*, 4075-4085.

Arthur, W.T., Ellerbroek, S.M., Der, C.J., Burridge, K., and Wennerberg, K. (2002). XPLN, a guanine nucleotide exchange factor for RhoA and RhoB, but not RhoC. J Biol Chem *277*, 42964-42972.

Duan, S., Skaar, J.R., Kuchay, S., Toschi, A., Kanarek, N., Ben-Neriah, Y., and Pagano, M. (2011). mTOR Generates an Auto-Amplification Loop by Triggering the betaTrCP- and CK1alpha-Dependent Degradation of DEPTOR. Mol Cell *44*, 317-324.

Erbay, E., Park, I.H., Nuzzi, P.D., Schoenherr, C.J., and Chen, J. (2003). IGF-II transcription in skeletal myogenesis is controlled by mTOR and nutrients. J Cell Biol *163*, 931-936.

Facchinetti, V., Ouyang, W., Wei, H., Soto, N., Lazorchak, A., Gould, C., Lowry, C., Newton, A.C., Mao, Y., Miao, R.Q., *et al*. (2008). The mammalian target of rapamycin complex 2 controls folding and stability of Akt and protein kinase C. The EMBO Journal *27*, 1932-1943.

Foster, K.G., and Fingar, D.C. (2010). Mammalian target of rapamycin (mTOR): conducting the cellular signaling symphony. J Biol Chem *285*, 14071-14077. doi: 14010.11074/jbc.R14109.094003. Epub 092010 Mar 094015.

Frias, M.A., Thoreen, C.C., Jaffe, J.D., Schroder, W., Sculley, T., Carr, S.A., and Sabatini, D.M. (2006). mSin1 Is Necessary for Akt/PKB Phosphorylation, and Its Isoforms Define Three Distinct mTORC2s. Current Biology *16*, 1865-1870.

Gan, X., Wang, J., Su, B., and Wu, D. (2011). Evidence for direct activation of mTORC2 kinase activity by phosphatidylinositol 3,4,5-trisphosphate. J Biol Chem *286*, 10998-11002. doi: 10910.11074/jbc.M10110.195016. Epub 192011 Feb 195010.

Gao, D., Inuzuka, H., Tan, M.K., Fukushima, H., Locasale, J.W., Liu, P., Wan, L., Zhai, B., Chin, Y.R., Shaik, S., *et al*. (2011). mTOR Drives Its Own Activation via SCF(betaTrCP)-Dependent Degradation of the mTOR Inhibitor DEPTOR. Mol Cell *44*, 290-303.

Garcia-Martinez, J.M., and Alessi, D.R. (2008). mTOR complex 2 (mTORC2) controls hydrophobic motif phosphorylation and activation of serum- and glucocorticoid-induced protein kinase 1 (SGK1). Biochem J *416*, 375-385.

Ge, Y., and Chen, J. (2012). Mammalian target of rapamycin (mTOR) signaling network in skeletal myogenesis. J Biol Chem *31*, 31.

Ge, Y., Sun, Y., and Chen, J. (2011a). IGF-II is regulated by microRNA-125b in skeletal myogenesis. J Cell Biol *192*, 69-81. doi: 10.1083/jcb.201007165. Epub 201002011 Jan 201007163.

Ge, Y., Yoon, M.S., and Chen, J. (2011b). Raptor and Rheb negatively regulate skeletal myogenesis through suppression of insulin receptor substrate 1 (IRS1). J Biol Chem *286*, 35675-35682. doi: 35610.31074/jbc.M35111.262881. Epub 262011 Aug 262818.

Greer, E.L., and Brunet, A. (2005). FOXO transcription factors at the interface between longevity and tumor suppression. Oncogene *24*, 7410-7425.

Guertin, D.A., Stevens, D.M., Thoreen, C.C., Burds, A.A., Kalaany, N.Y., Moffat, J., Brown, M., Fitzgerald, K.J., and Sabatini, D.M. (2006). Ablation in mice of the mTORC components raptor, rictor, or mLST8 reveals that mTORC2 is required for signaling to Akt-FOXO and PKCalpha, but not S6K1. Dev Cell *11*, 859-871.

Huang, J., Dibble, C.C., Matsuzaki, M., and Manning, B.D. (2008). The TSC1-TSC2 complex is required for proper activation of mTOR complex 2. Mol Cell Biol *28*, 4104-4115.

Ikenoue, T., Hong, S., and Inoki, K. (2009). Monitoring mammalian target of rapamycin (mTOR) activity. Methods Enzymol *452*, 165-180.

Ikenoue, T., Inoki, K., Yang, Q., Zhou, X., and Guan, K.-L. (2008). Essential function of TORC2 in PKC and Akt turn motif phosphorylation, maturation and signalling. The EMBO Journal *27*, 1919-1931.

Jacinto, E., Facchinetti, V., Liu, D., Soto, N., Wei, S., Jung, S.Y., Huang, Q., Qin, J., and Su, B. (2006). SIN1/MIP1 maintains rictor-mTOR complex integrity and regulates Akt phosphorylation and substrate specificity. Cell *127*, 125-137. Epub 2006 Sep 2007.

Jacinto, E., Loewith, R., Schmidt, A., Lin, S., Ruegg, M.A., Hall, A., and Hall, M.N. (2004). Mammalian TOR complex 2 controls the actin cytoskeleton and is rapamycin insensitive. Nature cell biology *6*, 1122-1128.

Jiang, B.H., Aoki, M., Zheng, J.Z., Li, J., and Vogt, P.K. (1999). Myogenic signaling of phosphatidylinositol 3-kinase requires the serine-threonine kinase Akt/protein kinase B. Proc Natl Acad Sci U S A *96*, 2077-2081.

Joha, S., Nugues, A.L., Hetuin, D., Berthon, C., Dezitter, X., Dauphin, V., Mahon, F.X., Roche-Lestienne, C., Preudhomme, C., Quesnel, B.*, et al*. (2012). GILZ inhibits the mTORC2/AKT pathway in BCR-ABL(+) cells. Oncogene *31*, 1419-1430. doi: 1410.1038/onc.2011.1328. Epub 2011 Aug 1411.

Kuhne, M.R., Ku, G., and Weiss, A. (2000). A guanine nucleotide exchange factor-independent function of Vav1 in transcriptional activation. J Biol Chem *275*, 2185-2190.

Lawlor, M.A., and Alessi, D.R. (2001). PKB/Akt: a key mediator of cell proliferation, survival and insulin responses? J Cell Sci *114*, 2903-2910.

Ma, X.M., and Blenis, J. (2009). Molecular mechanisms of mTOR-mediated translational control. Nature Reviews Molecular Cell Biology *10*, 307-318.

Manning, B.D., and Cantley, L.C. (2007). AKT/PKB signaling: navigating downstream. Cell *129*, 1261-1274.

Oh, W.J., and Jacinto, E. (2011). mTOR complex 2 signaling and functions. Cell Cycle *10*, 2305-2316.

Oh, W.J., Wu, C.C., Kim, S.J., Facchinetti, V., Julien, L.A., Finlan, M., Roux, P.P., Su, B., and Jacinto, E. (2010). mTORC2 can associate with ribosomes to promote cotranslational phosphorylation and stability of nascent Akt polypeptide. Embo J *29*, 3939-3951.

Panasyuk, G., Nemazanyy, I., Zhyvoloup, A., Filonenko, V., Davies, D., Robson, M., Pedley, R.B., Waterfield, M., and Gout, I. (2009). mTOR Splicing Isoform Promotes Cell Proliferation and Tumorigenesis. Journal of Biological Chemistry *284*, 30807-30814.

Peng, X.D., Xu, P.Z., Chen, M.L., Hahn-Windgassen, A., Skeen, J., Jacobs, J., Sundararajan, D., Chen, W.S., Crawford, S.E., Coleman, K.G., *et al*. (2003). Dwarfism, impaired skin development, skeletal muscle atrophy, delayed bone development, and impeded adipogenesis in mice lacking Akt1 and Akt2. Genes Dev *17*, 1352-1365.

Peterson, T.R., Laplante, M., Thoreen, C.C., Sancak, Y., Kang, S.A., Kuehl, W.M., Gray, N.S., and Sabatini, D.M. (2009). DEPTOR is an mTOR inhibitor frequently overexpressed in multiple myeloma cells and required for their survival. Cell *137*, 873-886. Epub 2009 May 2014.

Plas, D.R., and Thompson, C.B. (2003). Akt activation promotes degradation of tuberin and FOXO3a via the proteasome. J Biol Chem *278*, 12361-12366. Epub 12003 Jan 12366.

Ren, X.D., and Schwartz, M.A. (2000). Determination of GTP loading on Rho. Methods Enzymol *325*, 264-272.

Rossman, K.L., Der, C.J., and Sondek, J. (2005). GEF means go: turning on RHO GTPases with guanine nucleotide-exchange factors. Nat Rev Mol Cell Biol *6*, 167-180.

Sarbassov, D., D., Ali, S.M., Kim, D.H., Guertin, D.A., Latek, R.R., Erdjument-Bromage, H., Tempst, P., and Sabatini, D.M. (2004). Rictor, a novel binding partner of mTOR, defines a rapamycin-insensitive and raptor-independent pathway that regulates the cytoskeleton. Curr Biol *14*, 1296-1302.

Sarbassov, D.D., Guertin, D.A., Ali, S.M., and Sabatini, D.M. (2005). Phosphorylation and regulation of Akt/PKB by the rictor-mTOR complex. Science *307*, 1098-1101.

Schmidt, A., Bickle, M., Beck, T., and Hall, M.N. (1997). The yeast phosphatidylinositol kinase homolog TOR2 activates RHO1 and RHO2 via the exchange factor ROM2. Cell *88*, 531-542.

Vanni, C., Parodi, A., Mancini, P., Visco, V., Ottaviano, C., Torrisi, M.R., and Eva, A. (2004). Phosphorylation-independent membrane relocalization of ezrin following association with Dbl in vivo. Oncogene *23*, 4098-4106.

Vivanco, I., and Sawyers, C.L. (2002). The phosphatidylinositol 3-Kinase AKT pathway in human cancer. Nat Rev Cancer *2*, 489-501.

Wullschleger, S., Loewith, R., Oppliger, W., and Hall, M.N. (2005). Molecular organization of target of rapamycin complex 2. J Biol Chem *280*, 30697-30704. Epub 32005 Jul 30697.

Yoon, M.S., and Chen, J. (2008). PLD regulates myoblast differentiation through the mTOR-IGF2 pathway. J Cell Sci *121*, 282-289. Epub 2008 Jan 2015.

Zhao, Y., Xiong, X., and Sun, Y. (2011). DEPTOR, an mTOR Inhibitor, Is a Physiological Substrate of SCF(betaTrCP) E3 Ubiquitin Ligase and Regulates Survival and Autophagy. Mol Cell *44*, 304-316.

Zinzalla, V., Stracka, D., Oppliger, W., and Hall, M.N. (2011). Activation of mTORC2 by Association with the Ribosome. Cell *144*, 757-768.

Zoncu, R., Efeyan, A., and Sabatini, D.M. (2011). mTOR: from growth signal integration to cancer, diabetes and ageing. Nat Rev Mol Cell Biol *12*, 21-35. doi: 10.1038/nrm3025. Epub 2010 Dec 1015.

CHAPTER 3. CHARACTERIZATION OF XPLN LOCALIZATION AND FUNCTION

3.1. Introduction

Once XPLN was established as an endogenous inhibitor of mTORC2 and Akt (Chapter 2), we wanted to probe into the mechanisms by which XPLN may be regulated in cells. Stimuli that are capable of activating mTORC2 activity towards Akt should somehow remove XPLN to allow Akt activation. Although, the exact stimuli that activate mTORC2 are ill defined, serum and growth factors are frequently used to stimulate mTORC2 activity.

First possible mechanism examined was regulation of XPLN protein itself or regulation of the interaction between XPLN and mTORC2 by serum. Surprisingly, neither the XPLN protein levels changed nor did the interaction between XPLN and mTORC2 after serum stimulation (Fig. 2.9). Although, there wasn't a dramatic change in the interaction between the two, one can never rule out a small but significant change in the interaction that can possibly be detected by more sensitive methods. Future biochemical and structural studies will further probe into this possibility.

Here we investigate possible ways by which XPLN could be regulated in cells in order to allow Akt activation following growth factor stimulation. To probe potential regulation of XPLN function in the cell, I investigated the subcellular localization of XPLN, as well as the function and localization of alternative isoforms of XPLN.

3.2. Materials and Methods

3.2.1. Antibodies and other reagents. Anti-GFP was from Roche, anti-tubulin antibody was from Abcam, and all other primary antibodies were from Cell Signaling Technology. All secondary antibodies were from Jackson ImmunoResearch Laboratories, Inc.

3.2.2. Plasmids. For NLS, oligonucleotides: ATTGAAGAAGAAGCGGAAGGTGGA GG and AATTCCTCCACCTTCCGCTTCTTCTTC and for NES, oligonucleotides: AATTGCTGCAGCTGCCTCCTCTGGAGCGGCTGACCCTGG and AATTCCAGGGTCAGCCGCTCCAGAGGAGGCAGCTGCAGC were used. Oligonucleotides were annealed and ligated into the EcoR1 site of the original vector encoding XPLN-YFP in pEYFP-N1. Positive colonies containing directional inserts were screened by PCR using CMV+ primer and NLS- or NES- primer. To generate transcript #1 and transcript #2 encoding XPLN-YFP plasmids, gene block fragments consisting of the first 750 nucleotides were bought from IDT. They were then ligated into PshA1/EcoR1 digested parental XPLN-YFP-transcript #3 vector. GFP-Akt in the vector backbone pEGFP-C1 was bought from Addgene (plasmid # 39531).

3.2.3. Cell culture. C2C12 myoblasts and HeLa cells were maintained in DME containing 10% fetal bovine serum (FBS) at 37 °C with 7% and 5% CO_2 respectively. IGROV-1 cells were maintained in RPMI containing 10% fetal bovine serum (FBS) at 37 °C with 5% CO_2. Transfections were performed using Lipofectamine-2000 following the manufacturer's recommendations.

Following transfection, cells on coverslips were fixed, and stained for DAPI. The stained cells were examined with a Leica DMI 4000B fluorescence microscope, and the

fluorescent images were captured using a RETIGA EXi camera and analyzed with Q-capture Pro51 software (Q-Imaging™).

3.2.4. Western blotting. Cells were lysed in ice-cold lysis buffer (40 mM HEPES, pH7.2, 120 mM NaCl, 10 mM pyrophosphate, 50 mM NaF, 10 mM b-glycerophosphate, 2 mM EDTA, 1x Sigma protease inhibitor cocktail, and 0.3% CHAPS). The supernatant after microcentrifugation at 13,000 rpm for 10 min was collected and then boiled in SDS sample buffer. Proteins were resolved on SDS-PAGE and transferred onto PVDF membrane (Millipore), followed by incubation with various antibodies according to the manufacturers' recommendations. Detection of horseradish peroxidase-conjugated secondary antibodies was performed with Western Lightning™ Chemiluminescence Reagent Plus (Perkin Elmer, Inc.).

3.3. Results

3.3.1. Nuclear-cytoplasmic localization of XPLN. To examine the localization of XPLN, I transfected cells with a plasmid expressing XPLN-YFP followed by immunofluorescence studies. As shown in Fig. 3.1A, although the protein is diffused across the entire cell, the majority of the protein is concentrated in the nucleus. This pattern of localization is consistent among a variety of cell lines tested such as HeLa, IGROV-1, C2C12, HEK-293, MCF-7, MDA-MB-231, PC-3, HepG2, Hep-3b, TD-47, H661, H292, and U2OS (Fig. 3.1A).

Next, I wanted to examine the localization of the endogenous protein. Since no XPLN antibody is available to specifically detect the endogenous protein by immunostaining, we performed subcellular fractionation experiments. HeLa cells were

processed to generate two distinct fractions, nuclear and cytoplasmic, the latter consisting of everything except nucleus. To investigate a potential regulation of the localization, fractionation was performed under serum starvation and serum stimulation conditions. Comparing lanes 1,2 vs 3,4 in Fig. 3.1B, PARP is present exclusively in the nuclear fraction, as one would expect for a nuclear marker. On the other hand, MEK and tubulin are limited to the cytoplasmic fraction, as should be the case for cytoplasmic markers (Fig. 3.1B). Interestingly, XPLN is present predominantly in the nuclear fraction (comparing lane 1 vs 3 of Fig. 3.1B) in comparison to the cytoplasmic fraction under serum starvation conditions. Surprisingly, the majority of the XPLN protein disappears after serum stimulation from both cytoplasmic and nuclear fractions (lanes 2, 4 of Fig. 3.1B). This disappearance of XPLN protein cannot be accounted for by the loss of total protein following serum stimulation since MEK, tubulin, and PARP showed no change in the levels before or after serum starvation. This is especially interesting considering the fact that total amount of XPLN protein did not change following serum starvation and stimulation (Fig. 2.9A). Although, I do not have explanation for this observation, it is possible that when stimulated with serum, the XPLN protein might have undergone some conformational change and become more susceptible to the proteases in the lysates.

3.3.2. Manipulation of XPLN localization and the effect on Akt phosphorylation.

Once the XPLN localization was confirmed to be mostly nuclear by both fractionation and immunofluorescence studies, I wanted to perturb this localization and analyze its effect on Akt phosphorylation. To this end, I tagged XPLN-YFP construct separately with a nuclear localization signal (NLS) and a nuclear export signal (NES). As shown in

Fig. 3.2A, NLS-XPLN-YFP was almost exclusively nuclear, whereas NES tagged XPLN-YFP was less concentrated in the nucleus than the wildtype XPLN-YFP, and rather diffusely present throughout the cell.

Next, I co-expressed GFP-Akt along with various XPLN-YFP proteins in cells and analyzed the effect of NLS-, NES- tagged XPLN-YFP on Akt phosphorylation. GFP tag allowed easy separation of GFP-Akt from endogenous Akt during western blotting making distinct analysis of exogenous Akt phosphorylation plausible. Surprisingly, when over-expressed both exclusively nuclear and more cytoplasmic versions of XPLN were capable of inhibiting the Akt phosphorylation to a similar extent as wild-type XPLN-YFP (Fig. 3.2B).

3.3.3. Localization of alternative transcripts of XPLN. In mammals, XPLN coding sequence is alternatively spliced to generate different transcript isoforms that differ in the N terminal exons (Fig. 3.3A). These splice isoforms differ in the first ~ 60 amino acid residues at the N terminus of the protein (Fig. 3.3B). This is extremely interesting considering the fact that the N terminal fragment of XPLN consisting of 125 amino acids is necessary and sufficient to inhibit Akt phosphorylation by mTORC2 (Fig. 2.4C).

I first examined the localization of the protein products of these alternate transcripts by immunofluorescence experiments. Construct encoding transcript #3 was used for all the experiments in Chapter 2. As shown in Fig. 3.4A, transcript #1 is almost exclusively nuclear, in contrast to the transcript #3 and transcript #2. This is consistent with the fact that transcript#1 contains a predicted 6-amino acid nuclear localization signal (Fig. 3.3B).

3.3.4. Effect of over-expression of alternative transcripts of XPLN on Akt phosphorylation. Next, I examined how each of these XPLN transcripts individually affects Akt phosphorylation. YFP-fusion of the 3 transcripts were co-expressed with GFP-Akt in IGROV-1 cells. As shown in Fig. 3.4B, over-expression of transcript isoforms #1 and #2 was capable of reducing GFP-Akt phosphorylation to a similar extent as the transcript #3. Similar effect of XPLN transcripts on Akt phosphorylation was also seen in C2C12 cells (data not shown).

3.4. Discussion

In this chapter, I examined various possible ways by which XPLN could be regulated. XPLN protein was predominantly present in the nucleus. Serum starvation and stimulation did not change the localization of XPLN (data not shown). Furthermore, constitutively nuclear and cytoplasmic XPLN inhibited Akt phosphorylation to the same extent as the WT-XPLN (Fig. 3.2B) raising doubts over any role-played by XPLN localization towards regulating its inhibitory activity towards Akt. Although, the results may be complicated by the fact that the NLS and NES tagged XPLN proteins were over-expressed on top of the endogenous XPLN protein. Same is true for the effect of over-expression of various XPLN proteins differing in the first 60 amino acids on Akt phosphorylation. Only conclusion that can be obtained from the experiment is that each protein is equally capable of inhibiting Akt phosphorylation when over-expressed. A cleaner system would be to knock out XPLN gene altogether to eliminate all endogenous protein isoforms and then introducing one transcript at a time in a physiological amount to examine its effect on Akt phosphorylation. I am currently in the process of knocking

out XPLN gene in mouse (Appendix B). Mouse embryonic fibroblasts derived from the knockout mouse will then be utilized as an excellent system to address these questions.

Presence of XPLN in the nucleus was a surprising finding for an mTORC2 regulator since there is little mTORC2 activity in the nucleus (Rosner and Hengstschlager, 2008; Staus et al., 2014). Future experiments will examine the possibility of nuclear sequestration of XPLN. In fact, it was earlier believed that Net1 is sequestered in the nucleus (Schmidt and Hall, 2002) and Rac1 activation allows translocation of Net1 to plasma membrane (Carr et al., 2013). Additionally, Rac1 has been proposed to localize mTORC2 and regulate its activation (Saci et al., 2011). To examine if XPLN could be regulated by Rac1, I coexpressed constitutively active Rac1 along with XPLN-YFP. Presence of c.a. Rac1 had no effect on the localization of XPLN (data not shown). In contrast, some recent evidence points to the existence of RhoA in nucleus (Dubash et al., 2011; Rajakyla and Vartiainen, 2014). Future experiments will further probe into a potential role of nuclear XPLN as a GEF for RhoA in nucleus.

XPLN adds to the growing list of RhoGEF proteins that are known to have GEF activity-independent functions (Rossman et al., 2005). The exact mechanism by which such non-canonical functions are exerted by these GEFs is not clear, although protein-protein interactions mediated by modular domains outside of the catalytic region are proposed to play a role. DH-associated PH (pleckstrin homology) domains are the most well-characterized domains for this purpose. For many of the Dbl family members, PH domains allow membrane targeting by binding lipids (Rossman et al., 2003). More recently, PH domains gained acceptance as protein docking sites besides acting as lipid binding modules (Bellanger et al., 2000; Bellanger et al., 2003). An interesting example

is the binding of PH domain of Dbl with Ezrin, linking plasma membrane with actin cytoskeleton (Vanni et al., 2004). In fact, the PH domain of XPLN is capable of binding mTORC2 when expressed alone, though is not sufficient to elicit an effect on mTORC2 kinase activity (Chapter 2). It is highly likely that the PH domain plays a role in conferring the localization to XPLN. Besides PH domains, PDZ domains are also proposed to play a crucial role in localization of GEFs (Garcia-Mata and Burridge, 2007; Garcia-Mata et al., 2007).

Outside the DH-PH domains, Dbl family proteins show considerable sequence diversity and typically contain domains that underlie the unique functions of the protein (Rossman et al., 2005). In fact, XPLN binds and inhibits mTORC2 via an N-terminal region that lacks sequence homology to any known modular domain (Chapter 2). This is particularly interesting considering the fact that the XPLN gene is alternately spliced in mammals to generate transcript isoforms that differ in their N terminal sequences.

An intriguing possibility is the regulation of XPLN through phosphorylation. In fact, XPLN is predicted to contain several phosphorylatable amino acid residues by the online softwares (such as netphos2.1) that search for consensus sequences of various kinases. Although, XPLN is not part of the published HeLa phosphoproteomic database, this data cannot completely exclude a phosphorylation event, specifically if the phosphorylation takes place under specific cell conditions or is rapidly turned over. Hence, it is worth taking a candidate approach with a list of potential kinases in future.

3.5. Figures

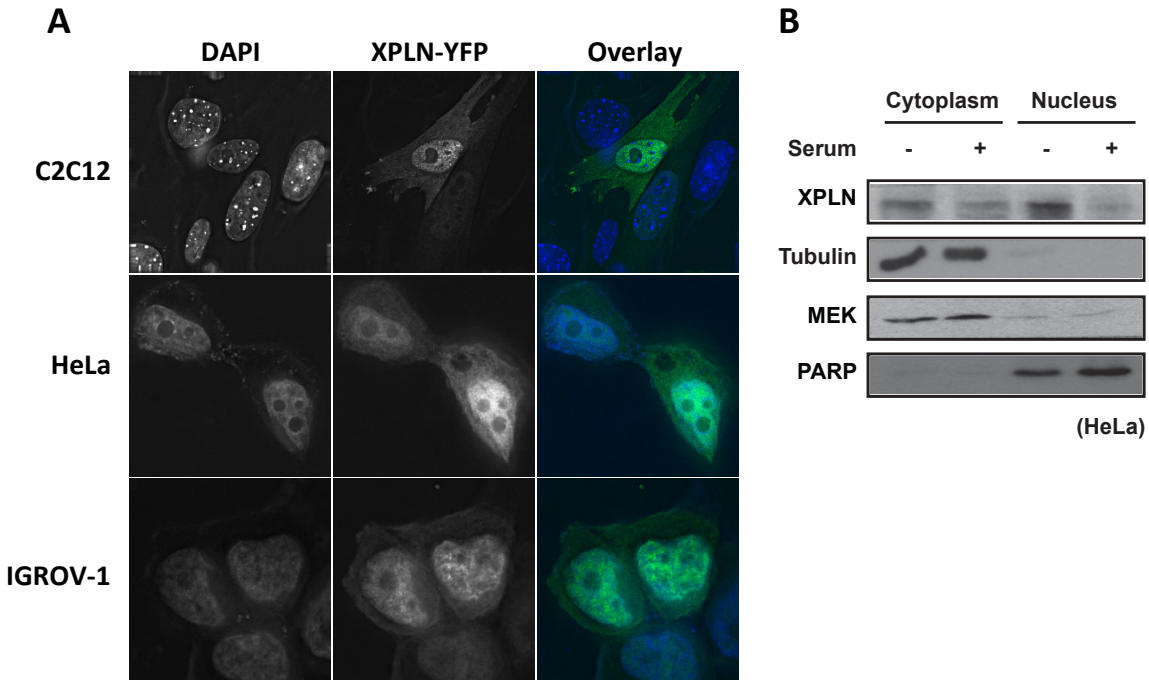

Fig. 3.1. XPLN is predominantly localized in the nucleus. (A) C2C12, HeLa and IGROV-1 cells were transfected with XPLN-YFP. After 24 hours, cells were fixed and stained with DAPI. **(B)** HeLa cells were starved of serum overnight followed by stimulation with 10% FBS for 30'. Cells were then fractionated to generate nuclear and cytoplasmic fractions (Performed by Dr. MeeSup Yoon). Images and blots are representatives of at least 3 independent experiments.

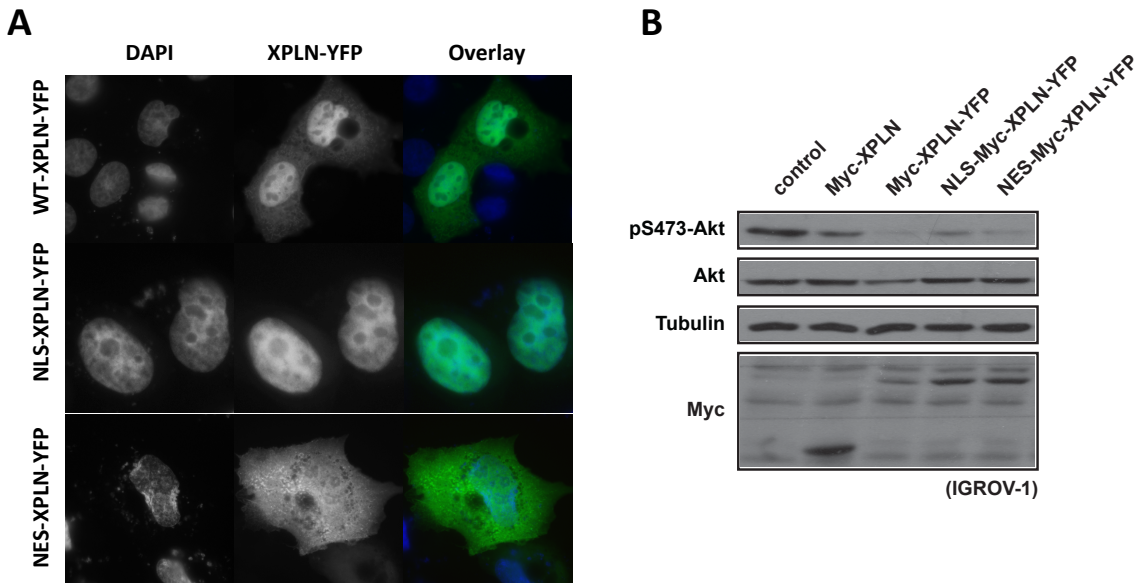

Fig. 3.2. Manipulation of XPLN localization and the effect on Akt phosphorylation. **(A)** IGROV-1 cells were transfected with WT- or NLS- or NES-XPLN-YFP. After 24 hours, cells were fixed and stained with DAPI. **(B)** IGROV-1 cells were transfected with Myc-XPLN or WT- or NLS- or NES-XPLN-YFP along with GFP-Akt. After 24 hours of transfection, cells were lysed for western blotting. Images and blots are representatives of at least 3 independent experiments.

A

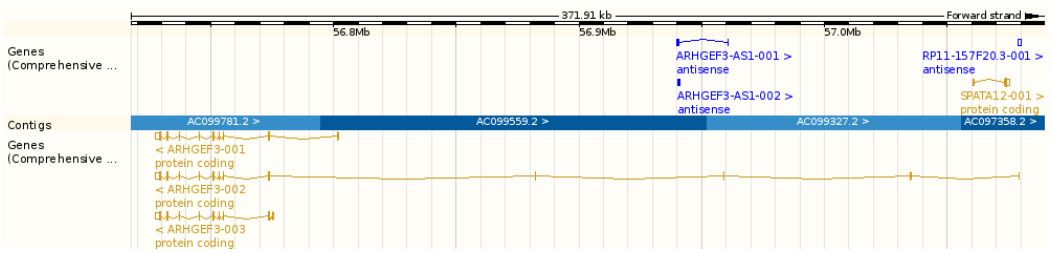

B

Unique amino acids at N terminus of Human XPLN transcripts:

#1 (002)-MDSSTAMNQCSCRGMEENKERPKRQRQNNFPMFPSPKAWNFR**GRKRK**QSTQDEDAVSLCSLDIS (64AA)
#2 (003)-MIEVCHHNWLLWLCPSKFGIFMCCLASTTGQMELRRTR (38AA)
#3 (001)-MVAKDYPFYLTVKRANCSLELPPASGPAKDAE (32AA)

GRKRK bioinformatically predicted NLS in Transcript#1.

Fig. 3.3. Alternative splice isoforms of XPLN. (A) Image from ENSEMBL showing the exons in various isoforms. **(B)** Unique amino acids present at the N terminus of these transcripts.

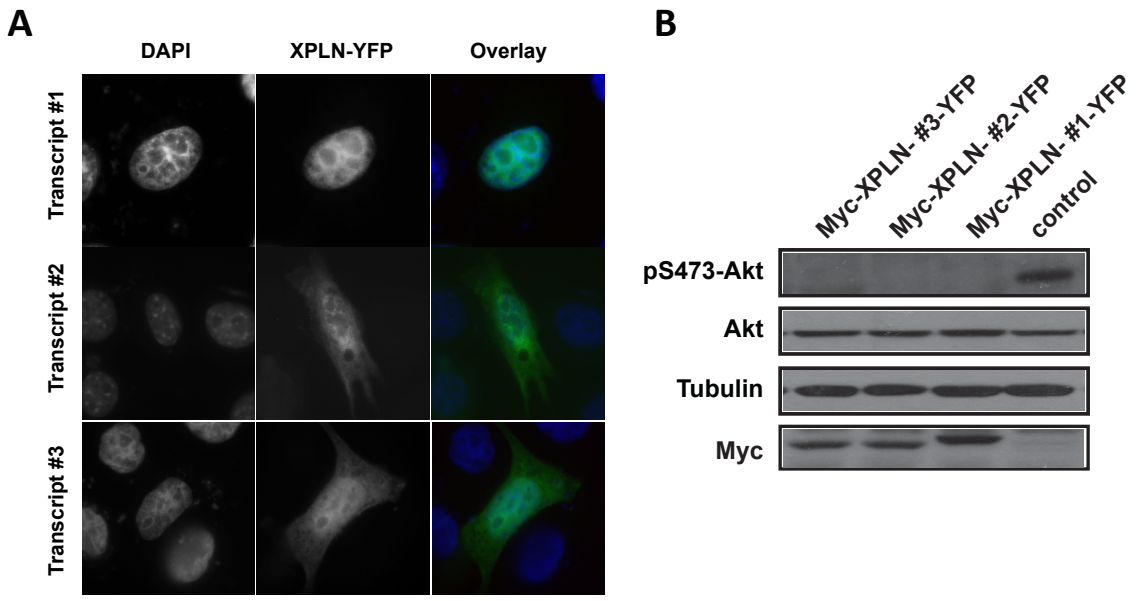

Fig. 3.4. Localization and function of various XPLN transcripts. (A) IGROV-1 cells were transfected with various XPLN transcripts tagged with YFP. After 24 hours, cells were fixed and stained with DAPI. **(B)** IGROV-1 cells were transfected with various XPLN transcripts-YFP along with GFP-Akt. After 24 hours of transfection, cells were lysed for western blotting. Images and blots are representatives of at least 3 independent experiments.

3.6. References

Bellanger, J.M., Astier, C., Sardet, C., Ohta, Y., Stossel, T.P., and Debant, A. (2000). The Rac1- and RhoG-specific GEF domain of Trio targets filamin to remodel cytoskeletal actin. Nature cell biology *2*, 888-892.

Bellanger, J.M., Estrach, S., Schmidt, S., Briancon-Marjollet, A., Zugasti, O., Fromont, S., and Debant, A. (2003). Different regulation of the Trio Dbl-Homology domains by their associated PH domains. Biology of the cell / under the auspices of the European Cell Biology Organization *95*, 625-634.

Carr, H.S., Morris, C.A., Menon, S., Song, E.H., and Frost, J.A. (2013). Rac1 controls the subcellular localization of the Rho guanine nucleotide exchange factor Net1A to regulate focal adhesion formation and cell spreading. Mol Cell Biol *33*, 622-634.

Dubash, A.D., Guilluy, C., Srougi, M.C., Boulter, E., Burridge, K., and Garcia-Mata, R. (2011). The small GTPase RhoA localizes to the nucleus and is activated by Net1 and DNA damage signals. PloS one *6*, e17380.

Garcia-Mata, R., and Burridge, K. (2007). Catching a GEF by its tail. Trends in cell biology *17*, 36-43.

Garcia-Mata, R., Dubash, A.D., Sharek, L., Carr, H.S., Frost, J.A., and Burridge, K. (2007). The nuclear RhoA exchange factor Net1 interacts with proteins of the Dlg family, affects their localization, and influences their tumor suppressor activity. Mol Cell Biol *27*, 8683-8697.

Rajakyla, E.K., and Vartiainen, M.K. (2014). Rho, nuclear actin, and actin-binding proteins in the regulation of transcription and gene expression. Small GTPases *5*, e27539.

Rosner, M., and Hengstschlager, M. (2008). Cytoplasmic and nuclear distribution of the protein complexes mTORC1 and mTORC2: rapamycin triggers dephosphorylation and delocalization of the mTORC2 components rictor and sin1. Human molecular genetics *17*, 2934-2948.

Rossman, K.L., Cheng, L., Mahon, G.M., Rojas, R.J., Snyder, J.T., Whitehead, I.P., and Sondek, J. (2003). Multifunctional roles for the PH domain of Dbs in regulating Rho GTPase activation. J Biol Chem *278*, 18393-18400.

Rossman, K.L., Der, C.J., and Sondek, J. (2005). GEF means go: turning on RHO GTPases with guanine nucleotide-exchange factors. Nat Rev Mol Cell Biol *6*, 167-180.

Saci, A., Cantley, L.C., and Carpenter, C.L. (2011). Rac1 regulates the activity of mTORC1 and mTORC2 and controls cellular size. Molecular cell *42*, 50-61.

Schmidt, A., and Hall, A. (2002). The Rho exchange factor Net1 is regulated by nuclear sequestration. J Biol Chem *277*, 14581-14588.

Staus, D.P., Weise-Cross, L., Mangum, K.D., Medlin, M.D., Mangiante, L., Taylor, J.M., and Mack, C.P. (2014). Nuclear RhoA signaling regulates MRTF-dependent SMC-specific transcription. American journal of physiology Heart and circulatory physiology *307*, H379-390.

Vanni, C., Parodi, A., Mancini, P., Visco, V., Ottaviano, C., Torrisi, M.R., and Eva, A. (2004). Phosphorylation-independent membrane relocalization of ezrin following association with Dbl in vivo. Oncogene *23*, 4098-4106.

CHAPTER 4. miRNA-146b PROMOTES MYOGENIC DIFFERENTIATION AND MODULATES MULTIPLE GENE TARGETS IN MUSCLE CELLS [2]

4.1. Introduction

Skeletal myogenesis is a highly coordinated process involving myogenic lineage commitment, myoblast proliferation, differentiation and fusion. Myoblasts must undergo a complex series of molecular and morphological changes during this process, the exact mechanism of which is not completely understood. The life-long action of skeletal muscle relies on maintenance and regeneration of myofibers. Muscle repair is carried out by adult stem cells such as satellite cells present between plasma membrane and surrounding basal lamina of mature muscle fibers (Wagers and Conboy, 2005). Following injury, mitotically quiescent satellite cells re-enter cell cycle, divide and ultimately fuse with existing myofibers or with each other to promote repair and regeneration (Sabourin and Rudnicki, 2000).

MicroRNAs (MiRNAs) are a class of small non-coding RNAs that have emerged as important modulators of gene expression (Bartel, 2009). There are more than 2500 miRNAs in humans (miRBase.org) and they are predicted to target ~30-40% genes of the human genome. MiRNAs are involved in the regulation of many cellular and developmental processes as diverse as cell proliferation, cell survival, embryonic

[2] This chapter appeared in its entirety as:
Khanna N., et al, 2014. MicroRNA-146b promotes myogenic differentiation and modulates multiple gene targets in muscle cells. PLoS One. 2014 Jun 23;9(6):e100657. It is available from http://www.plosone.org/article/info%3Adoi%2F10.1371%2Fjournal.pone.0100657 and using doi: 10.1371/journal.pone.0100657.

development and tissue differentiation (Felekkis et al., 2010; Stefani and Slack, 2008). Every aspect of skeletal myogenesis has been shown to be regulated by miRNAs (Ge and Chen, 2011). The activity of the miRNA processing enzyme, Dicer, is essential for normal muscle development during embryogenesis. Muscle-specific Dicer knockout mice have severely reduced muscle mass along with abnormal myofiber morphology leading to death within minutes of birth (O'Rourke et al., 2007). Various miRNAs have been shown to regulate key steps of skeletal myogenesis, of which the best-characterized myogenic miRNAs are miR-1, 206 and 133 (Chen et al., 2006; Chen et al., 2010; Kim et al., 2006). To date, 20 or so miRNAs have been reported to regulate myogenesis (Novak et al., 2013). Considering the prevalence of miRNA regulation in all aspects of biology, it is likely that additional myogenic miRNAs are to be identified. Indeed, expression profiling has revealed many miRNAs with differential expression patterns during myogenic differentiation (Sun et al., 2010), and they are likely candidates for novel myogenic regulators.

MiR-146b is conserved among most vertebrates, and its expression increases during mouse prenatal development from E9.5 to E11.5 (Mineno et al., 2006). The function of miR-146b has been implicated in breast cancer metastasis (Hurst et al., 2009), innate immunity (Perry et al., 2009; Taganov et al., 2006), inflammation (Nakasa et al., 2008), senescence (Bhaumik et al., 2009), and glioma cell migration and invasion (Xia et al., 2009). MiR-146b is also among the miRNAs identified in microarray studies to be up-regulated during satellite cell activation (Cheung et al., 2012) and myoblast differentiation (Sun et al., 2010), but a role of miR-146b in skeletal myogenesis has never

been reported. In the current study, we examined the potential function of miR-146b in myoblast differentiation.

4.2. Materials and Methods

4.2.1. Ethics statement. All animal experiments in this study were performed following protocols approved by the Animal Care and Use Committee at the University of Illinois at Urbana-Champaign, and conforming to the National Institutes of Health standards.

4.2.2. Antibodies and other reagents. Anti-MHC (MF20) and anti-myogenin (F5D) were obtained from the Developmental Studies Hybridoma Bank developed under the auspices of the NICHD, National Institutes of Health and maintained by The University of Iowa, Department of Biological Sciences. Anti-tubulin was from Abcam. Antibodies against Hmga2, Smad4 and Notch1 were from Cell Signaling Technology. All secondary antibodies were obtained from Jackson ImmunoResearch Laboratories, Inc. All reagents were from Sigma-Aldrich.

4.2.3. Cell culture and transfection. C2C12 myoblasts were maintained in Dulbecco's modified Eagle's medium (DMEM) containing 1 g/L glucose with 10% fetal bovine serum at 37°C with 7.5% CO_2. Primary myoblasts were maintained in F-10 medium supplemented with 25 ng/ml bFGF and 20% fetal bovine serum at 37°C with 7.5% CO_2. To induce differentiation, cells were plated on tissue culture plates coated with 0.2% gelatin and grown to 100% confluence for C2C12 and 60-70% confluence for primary myoblasts, changed into differentiation medium (DMEM containing 2% horse serum), and replenished with fresh medium daily for 3 days for C2C12 cells and 2 days for primary myoblasts. HEK293 cells were maintained in DMEM containing 4.5 g/L glucose

with 10% fetal bovine serum at 37°C with 5.5% CO_2. Transfections were performed using Lipofectamine 2000 (Invitrogen).

4.2.4. Mouse primary myoblast isolation. Primary myoblast isolation was performed as described previously (Ge et al., 2011). Briefly, hind limb muscles from 5 to 7-day-old FVB mice were isolated and minced in HBSS, digested in dispase II (2.4 U/mL, Roche) and collagenase D (1.5 U/mL, Roche) solution containing 2.5 mM $CaCl_2$ at 37°C for 2hr. Upon sequential filtering through 70 μm and 40 μm cell strainers (BD biosciences), the cells were collected by centrifugation at 350 g, and resuspended in F-10 culture medium. Serial plating was performed to enrich for myoblasts and eliminate fibroblasts.

4.2.5. Mouse muscle injury and regeneration. Eight to 10-week-old male FVB mice were used in all the regeneration experiments. Muscle injury was induced by injection of barium chloride ($BaCl_2$, 50 μL of 1.2% w/v in saline) into TA muscles as previously described (Ge et al., 2009). On various days after injury, the mice were euthanized and the TA muscles were collected, followed by RNA isolation.

4.2.6. Plasmids and oligonucleotides. All the reporters were generated by inserting synthetic oligonucleotide DNA linkers of MRE sequences or their mutants into the pMIR-REPORTER vector (Applied Biosystems) downstream of luciferase gene through Hind III and Spe I sites. Native RNA duplexes for miR-146b and siEGFP (siRNA against EGFP) were custom-synthesized by Integrated DNA Technology. miRIDIAN miR-146b mimic and a negative control (cel-miR-67, which has no sequence identity with miRNAs in human, mouse and rat) were purchased from Dharmacon. Locked nucleic acid (LNA) anti-sense oligonucleotides were purchased from Exiqon, Inc.

4.2.7. Western blotting. Cells were lysed in a buffer containing 50 mM Tris-HCl, pH 7.2, 150 mM NaCl, 1% NP-40, and 1% protease inhibitor cocktail (Sigma). The lysates were cleared by micro-centrifugation at 13000 rpm, and then mixed with SDS sample buffer. Proteins were resolved on SDS-PAGE and transferred onto PVDF membrane (Millipore), and incubated with various antibodies following the manufacturer's recommendations. Detection of horseradish peroxidase-conjugated secondary antibodies was performed with Western Lightning™ Chemiluminescence Reagent Plus (Perkin Elmer Life Sciences, Inc.), and images were developed on x-ray films.

4.2.8. Immunofluorescence microscopy and quantitative analysis of myocytes. C2C12 cells differentiated in 12-well plates were fixed and stained for MHC and DAPI as previously described (Ge et al., 2011). The stained cells were examined under a Leica DMI 4000B microscope with a 10x dry objective (Leica Fluotar, numerical aperture 0.4), and the fluorescent images were captured at 8-bit at room temperature using a RETIGA EXi camera equipped with Qcapture Pro51 software (QImaging™). The images were then pseudo-colored in Adobe Photoshop CS5, where brightness and contrast were adjusted. Fusion index was calculated as the percentage of nuclei in MHC-positive myotubes with ≥2 nuclei. Each data point was generated from randomly chosen microscopic fields containing in total 200 or more nuclei.

4.2.9. Quantitative reverse transcription PCR (qRT-PCR). Mouse TA muscles were isolated, ground into powder in liquid nitrogen, and lysed in Trizol (Invitrogen). C2C12 cells or mouse primary myoblasts were lysed directly in Trizol. RNA was isolated following the manufacturer's protocol. Real-time PCR reactions were performed for Smad4, Notch1 and Hmga2 using Syber mix on a StepOnePlus system (Applied

Biosystems). β-Actin was used as a reference to obtain the relative fold change for target samples using the comparative CT method. The sequences of PCR primers are as follows. Smad4 forward: AGCCATAGTGAAGGACTGTTGCAG, Smad4 reverse: TACTTCCAGTCCAGGTGGTAGTGC; Notch1 forward: CACCTGTGACCTGCTCA CTC, Notch 1 reverse: ATTGGCACAGGGGTTGG A; Hmga2 forward: GTGCCACAGAAGC GAGGAC, Hmga2 reverse: GCTGCTTTAGAGGGGCTCTT. Mature miR-146b levels were quantified using a qPCR-based Taqman assay kit (Applied Biosystems). SnoRNA-202 was used as the internal control for normalization.

4.2.10. Luciferase reporter assays. HEK293 or C2C12 cells transfected with the luciferase reporters were lysed in Passive Lysis Buffer (Promega), and luciferase assays were performed using the Luciferase Assay Systems kit (Promega) following the manufacturer's protocol.

4.2.11. Statistical analysis. All quantitative data are presented as mean ± standard deviation (SD). Whenever necessary, statistical significance of the data was analyzed by performing one-sample or paired t-tests. The specific types of tests and the *P* values, when applicable, are indicated in figure legends.

4.3. Results

4.3.1. MiR-146b expression is up-regulated during myogenesis. Our previous microarray profiling of miRNA expression revealed multiple miRNAs that were differentially expressed in differentiated versus undifferentiated mouse C2C12 myoblasts, and miR-146b-5p was among those up-regulated upon differentiation (Sun et al., 2010). Dicing of pre-miR-146b stem loop gives rise to two distinct mature miRNA

species, with miR-146-5p being the major and miR-146b-3p being the minor one (miRBase.org). For simplicity, we refer to miR-146b-5p as miR-146b from here on. Of note, all reagents used in this study were specific for miR-146b-5p. To validate the microarray data and further examine miR-146b expression, we performed qRT-PCR experiments with RNAs isolated from C2C12 cells over the course of differentiation induced by serum withdrawal. As shown in Fig. 4.1A, miR-146b levels increased steadily during differentiation and reached ~3.5-fold by day 3. This expression pattern was also observed during primary myoblast differentiation, albeit to a more modest degree (Fig. 4.1B).

We also examined miR-146b expression in vivo during muscle regeneration in a mouse model. $BaCl_2$ was injected into tibialis anterior (TA) muscle to induce degeneration, followed by myofiber regeneration (Ge et al., 2009). As shown in Fig. 4.1C, expression of miR-146b increased during day 3-5 after injury, a period of satellite cell activation and new myofiber formation, and returned to basal level after that. Taken together, these observations imply that miR-146b may have a positive role in myogenesis.

4.3.2. MiR-146b positively regulates myoblast differentiation. To examine a possible role of miR-146b in myoblast differentiation, we inhibited miR-146b function in cells by delivering an anti-sense LNA-oligo by transfection, at an efficiency of ~75% as previously described (Ge et al., 2011). A scrambled LNA oligo with no sequence homology to any known miRNA was used as a control. As shown in Fig. 4.2A, transfection of LNA-anti-miR-146b into C2C12 cells led to inhibition of myotube

formation. Quantification of myotubes revealed significant reduction in fusion index (Fig. 4.2B). Anti-miR-146b also inhibited the expression of myosin heavy chain (MHC), a late marker of differentiation, with no significant effect on the early differentiation marker myogenin (Fig. 4.2C). We also examined the effect of miR-146b inhibition on primary myoblast differentiation, and found that anti-miR-146b suppressed differentiation as indicated by impaired myotube formation (Fig. 4.2D) and reduced fusion index (Fig. 4.2E). Thus, miR-146b appears to be necessary for optimal myoblast differentiation.

To further validate this positive function of miR-146b in myoblast differentiation, we introduced a chemically stabilized RNA duplex (miRIDIAN) of miR-146b into C2C12 myoblasts by transfection at ~90% efficiency as previously reported (Ge et al., 2011). The *C elegans* miR-67 (cel-67), with no homology to any known mouse miRNA, was used as a control. Delivery of the stabilized miR-146b into myoblasts (equivalent of overexpressing miR-146b) led to enhanced myotube formation (Fig. 4.3A), elevated fusion index (Fig. 4.3B) as well as an increase in MHC expression, but no effect on myogenin expression (Fig. 4.3C). A native (unmodified) miR-146b duplex also increased fusion index (Fig. 4.3B), albeit to a lesser degree compared to the stabilized mimic. It is important to note that the passenger strand in the miR-146b miRIDIAN mimic, which was similar (but not identical) to miR-146b*, was chemically modified to prevent its incorporation into the RNA-induced silencing complex (RISC). The fact that the native duplex was less effective than the mimic further confirmed that the passenger strand (miR-146b*-like) was not responsible for the observed phenotype. Taken together, these data strongly suggest that miR-146b is a positive regulator of myoblast differentiation.

4.3.3. Smad4, Hmga2 and Notch1 are targets of miR-146b during myoblast differentiation. MiRNAs modulate gene expression by targeting mRNAs for translational repression and mRNA degradation. In most cases, miRNAs bind to their target mRNAs in the 3'UTR by imperfect base pairing. Perfect and contiguous base pairing of mature miRNA nucleotides 2 to 8 (seed region) to its target mRNA has been found to be critical for the majority of mRNA targeting (Bartel, 2009), although seedless targeting is also reported (Juan et al., 2009; Lal et al., 2009; Shin et al., 2010). Computational target prediction by miRanda, TargetScan and Pictar altogether yielded hundreds of putative targets for miR-146b. Because miRNAs almost always trigger the decay of their mRNA targets (Baek et al., 2008; Guo et al., 2010), within the predicted miR-146b target list we looked for genes that were reported to be down-regulated at the mRNA levels during differentiation of C2C12 cells as well as implied in myogenesis. We then examined the effect of miR-146b overexpression on the expression of each of those genes in C2C12 cells. Smad4, Hmga2 (high-mobility-group proteins containing AT-hook DNA binding domains), and Notch1 emerged as strong candidates for miR-146b targets because the expression of each was dampened by miR-146b overexpression (Fig. 4.4A). The modest degree of reduction (20-30%) in the mRNA levels is commonly observed for target genes in response to the overexpression of a single miRNA. Examples of genes not suppressed by miR-146b overexpression are also shown in Fig. 4.4A, including Ccna2, Suv39h1, Id1, and Hells. The increase of Ccna2 levels is likely an indirect effect of miR-146b overexpression. Importantly, the protein levels of Smad4, Hmga2, and Notch1 were also reduced by the overexpression of miR-146b in myoblasts (Fig. 4.4B).

Protein levels for each of the putative targets of miR-146b have been reported to be down-regulated during myoblast differentiation (Conboy and Rando, 2002; Dey et al., 2012; Li et al., 2012) (also see Fig. 4.5D), inversely correlating with the increased expression of endogenous miR-146b during myoblast differentiation (Fig. 4.1A&B). Of the three genes, Smad4 had previously been reported to be a miR-146b target in immune cells (Geraldo et al., 2012; Taganov et al., 2006), but its regulation in myoblasts by miR-146b has never been examined. To gain further insight into the regulation of Smad4, Hmga2, and Notch1 during myoblast differentiation, we measured mRNA levels for each of these genes throughout the course of differentiation. As shown in Fig. 4.5A, a significant reduction in mRNA expression levels was observed for all three genes upon differentiation. Next, we examined the expression of these genes during muscle regeneration. We reasoned that the targets of miR-146b in regenerating muscles would be down-regulated upon miR-146b up-regulation. Indeed, we found that the mRNA levels of Smad4, Notch1 and Hmga2 were all reduced by 30-60% on day 3 and day 5 after injury (Fig. 4.5B). These expression patterns are perfectly in line with the possibility that miR-146b targets these genes both in vitro and in vivo to impact skeletal myogenesis. Importantly, inhibition of endogenous miR-146b by the antisense LNA oligo almost completely prevented the decline in both mRNA and protein expression of Smad4, Hmga2, and Notch1 during myoblast differentiation (Fig. 4.5C&D), further supporting a critical role of miR-146b in suppressing those genes.

4.3.4. MiR-146b directly targets the MREs in 3'UTRs of Smad4, Notch1, and Hmga2. 3'UTRs of Smad4 and Notch1 are each predicted to have a single miRNA

recognition element (MRE) for miR-146b, which is broadly conserved in vertebrates. Hmga2, on the other hand, contains 3 predicted MREs for miR-146b in its 3'UTR (Fig. 4.6A). To assess whether miR-146b directly regulates one or more of these 3'UTRs, we constructed reporters containing one copy of each putative MRE downstream of the luciferase gene. These reporters were then transfected in HEK293 cells, a non-myogenic cell line with little endogenous miR-146b (data not shown), along with the miR-146b duplex. As shown in Fig. 4.6B, miR-146b targeted the Smad4 and Notch1 MREs, as indicated by the repression of reporter activities to a similar degree as its suppression of a positive control reporter containing sequences perfectly complementary to miR-146b. For Hmga2, miR-146b targeting was limited to only one of the three predicted MREs (Fig. 4.6B). To further validate the specificity of the targeting, we constructed reporters with the seed regions mutated in the MREs (Fig. 4.6A). These mutant reporters were completely resistant to the presence of miR-146b duplex (Fig. 4.6B), confirming the specificity of the miR-146b action. To examine this targeting in a more physiologically relevant context, we expressed the MRE reporters in C2C12 cells, and introduced LNA-anti-miR-146b. As shown in Fig. 6C, inhibition of endogenous miR-146b was sufficient to activate the reporters, suggesting that miR-146b normally suppresses those MREs in myocytes.

4.4. Discussion

Our results have identified miR-146b as a novel regulator of myoblast differentiation. In addition, we provide evidence to establish Smad4, Notch1 and Hmga2 as direct targets of miR-146b during myoblast differentiation. Expression of miR-146b is

up-regulated during myoblast differentiation and muscle regeneration, accompanied by down-regulation of the target genes. Our previous miRNA profiling results indicated that miR-146b was the fourth most up-regulated miRNA after miR-1, miR-206, and miR-133 upon differentiation of C2C12 cells (Sun et al., 2010). While the myogenic roles of the other three miRNAs have been well documented (Chen et al., 2006; Chen et al., 2010; Kim et al., 2006), this is the first report of miR-146b as a myogenic regulator, which also attests to the power of expression profiling in predicting function. New myogenic miRNAs may continue to be discovered by this approach.

Major myogenic miRNAs, miR-1, miR-133, and miR-206, are expressed in muscles under the control of the myogenic transcription factors SRF, MyoD, and MEF2 (Liu et al., 2007; Rao et al., 2006; Rosenberg et al., 2006; Zhao et al., 2005). One or more of those transcription factors may also regulate the expression of miR-146b. Another potential regulator is NF-κB, which has been reported to regulate miR-146b biogenesis in immune cells (Taganov et al., 2006). Future investigations will probe the mechanisms of miR-146b biogenesis in myogenesis.

Transforming growth factor β (TGFβ)/bone morphogenetic protein (BMP) signaling pathways regulate satellite cell activation and proliferation during muscle development (Wang et al., 2010). TGFβ and BMP signal through specific Smad proteins, which on activation form a complex with the common regulator Smad4 to regulate gene expression. Similarly, Notch signaling is known to control satellite cell quiescence and activation (Bjornson et al., 2012; Conboy and Rando, 2002; Mourikis et al., 2012; Wilson-Rawls et al., 1999). In addition to regulating myoblast proliferation, these signaling pathways inhibit the transcriptional activity of myogenic regulatory factors

(MRFs) and prevent myoblast differentiation, maintaining muscle stem cell self-renewal (Kopan et al., 1994; Martin et al., 1992; Wilson-Rawls et al., 1999). Hmga2 is also a key regulator of satellite cell activation and proliferation both in vivo and in vitro (Li et al., 2012). As cell cycle withdrawal is a prerequisite for myogenic differentiation, these regulators of myoblast proliferation need to be down regulated upon entering myogenic differentiation. In fact, forced expression of either Hmga2 or Smad4, or constitutive activation of Notch, is sufficient to prevent myoblast differentiation (Dey et al., 2012; Li et al., 2012; Wen et al., 2012). Here we provide compelling evidence for miR-146b regulation of these inhibitors of myogenesis. We propose that the increased level of miR-146b during myogenesis serves to posttranscriptionally suppress Smad4, Notch1, and Hmga2 (and potentially other genes) in order to allow the activation of myogenic differentiation program.

Smad4 has been shown to be targeted by miR-146b in human papillary thyroid cells on the same MRE as that on the mouse gene discovered in our study (Geraldo et al., 2012), suggesting that this regulation may exist in multiple cell/tissue types. There are four mammalian Notch receptors, Notch1-4, of which Notch1 and 3 are known to be anti-myogenic (Gagan et al., 2012; Shawber et al., 1996). Regulation of Notch3 by myogenic miRNAs, miR-1 and 206, has been reported (Gagan et al., 2012), and now our findings reveal targeting of Notch1 by miR-146b. Hence, a concerted suppression of Notch 1 and Notch 3 can be achieved, as miR-1, miR-206, and miR-146b are all up-regulated upon differentiation (Sun et al., 2010).

It is now commonly accepted that the regulation of any gene is rarely controlled by a single miRNA. Rather, multiple miRNAs often coordinate to modulate the

expression of a gene (Tsang et al., 2010). It is unlikely that miR-146b is solely responsible for suppressing the target genes we have identified during myogenic differentiation. In fact, miR-26a has been reported to target Smad4 during myogenesis (Dey et al., 2012) and it is conceivable that miR-26a and miR-146b act together to regulate Smad4. Similarly, Hmga2 has been reported to be targeted by let-7 (Lee and Dutta, 2007) and miR-98 (Hebert et al., 2007) in cancer cells, both of which are up-regulated during myoblast differentiation (Dmitriev et al., 2013; Kallen et al., 2013). Hence, a concerted targeting of Hmga2 by let-7, miR-98 and miR-146b during myoblast differentiation is possible. Regardless of the potential coordination, however, the contribution of miR-146b may be indispensible in bringing the levels of those genes below a threshold for the activation of the myogenic program to occur. This notion is supported by our observation that inhibition of miR-146b almost completely prevents down-regulation of Smad4, Notch1, and Hmga2 (Fig. 4.5C&D).

MicroRNAs hold the potential as therapeutic targets or tools in aging and dystrophic muscles. For instance, over-expression of miR-1/206 suppresses rhabdomyosarcoma development through c-met expression (Yan et al., 2009). Additionally, intramuscular injections of miR-1, miR-206, and miR-133 in rat skeletal muscle promote muscle regeneration (Nakasa et al., 2010), and so does intramuscular injection of anti-miR-125b, a negative regulator of myogenesis (Ge et al., 2011) The physiological significance and therapeutic potential of miR-146b as a myogenic regulator warrants future investigations.

4.5. Figures

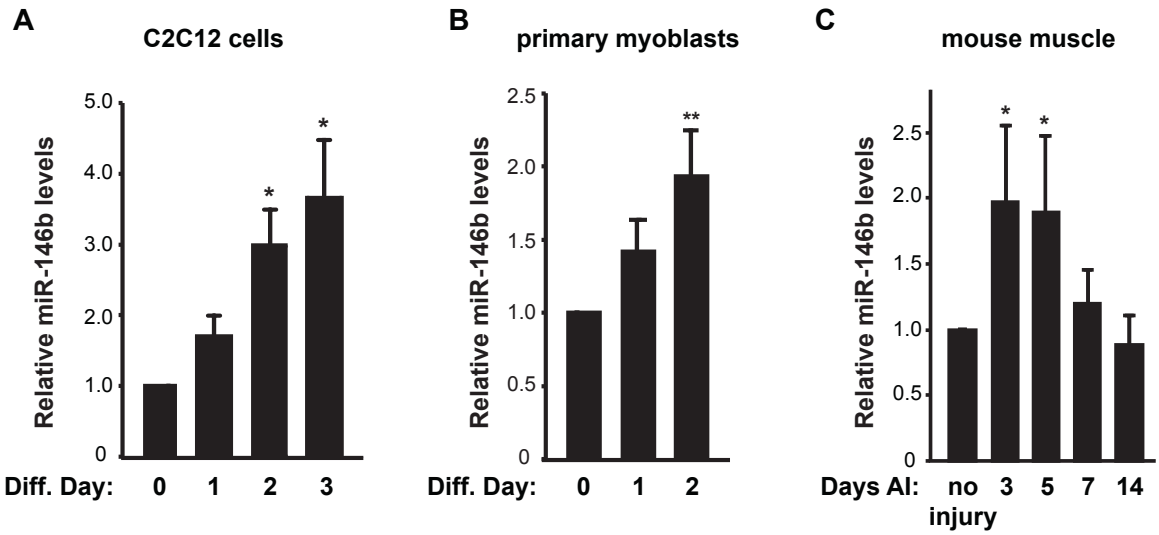

Fig. 4.1. miR-146b expression is up-regulated during myogenesis. (A, B) C2C12 myoblasts **(A)** and mouse primary myoblasts **(B)** were induced to differentiate. Total RNA was isolated from the differentiating cells on various days as indicated (diff. day) and subjected to analysis by qRT-PCR to determine the relative levels of mature miR-146b with that on day 0 as 1. Data shown are mean ± SD from three to four independent experiments. **(C)** Regeneration of mouse TA muscles was induced by $BaCl_2$ injury. On various days after injury (AI), total RNA was isolated from the TA muscles and subjected to analysis by qRT-PCR to determine the relative levels of mature miR-146b. Saline injection into contralateral TA muscles served as "no injury" control and was designated as 1. Data shown are mean ± SD with at least three mice per time point. One-sample *t* test was performed to analyze each data point. $*P < 0.05$; $**P < 0.01$.

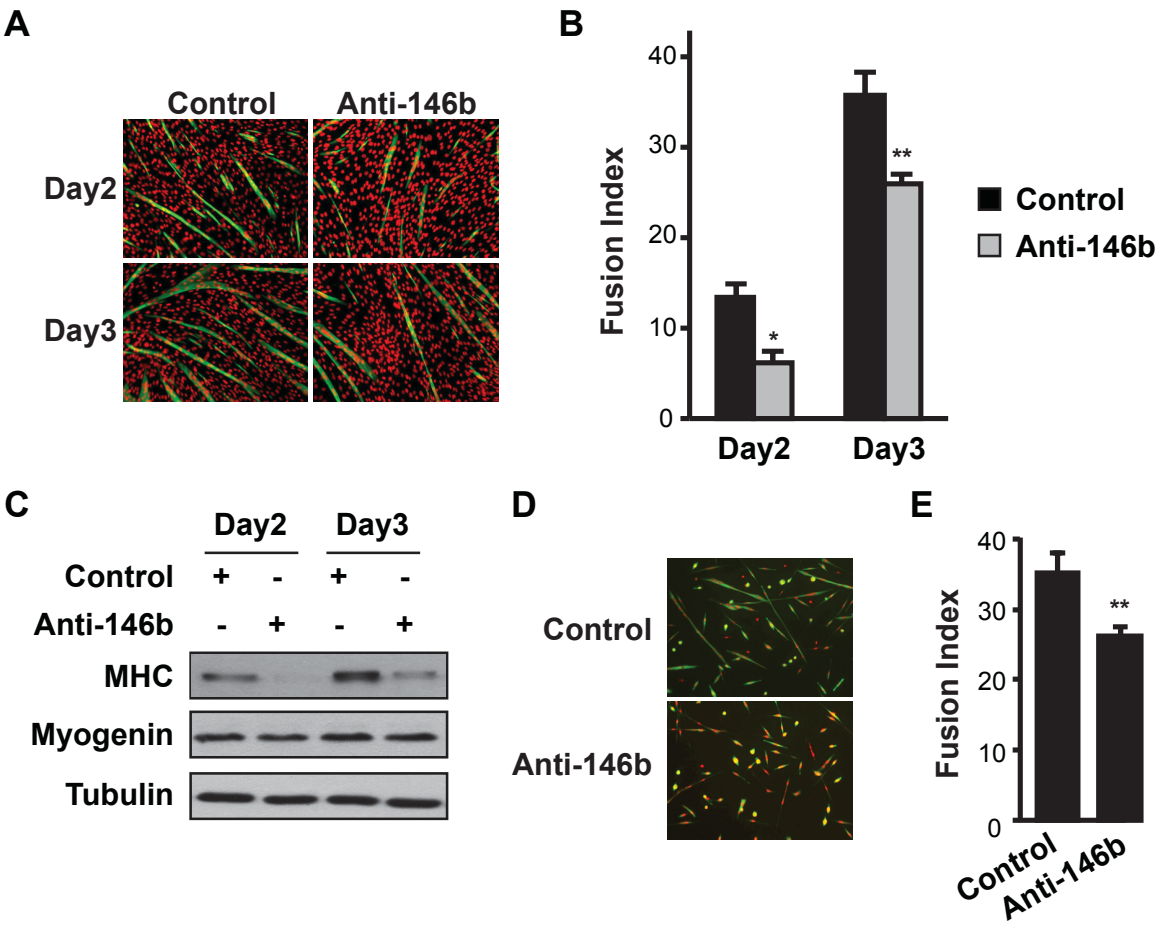

Fig. 4.2. Inhibition of miR-146b suppresses myoblast differentiation. C2C12 myoblasts **(A-C)** or primary myoblasts **(D-E)** were transfected with 50 nM LNA-anti-miR-146b for 1 day and then induced to differentiate for 3 or 2 days, respectively. An LNA oligonucleotide with scrambled sequence served as a negative control. **(A, D)** The differentiated cells were fixed and immunostained for MHC (green) and DAPI (red). **(B, E)** Fusion indexes were quantified. **(C)** Cell lysates were subjected to Western blot analysis. In A, C, and D representative results of at least three independent experiments are shown. Data in B & E are shown as mean ± SD from three to four independent experiments. Paired *t* tests were performed to compare the data. $*P < 0.05$; $**P < 0.01$.

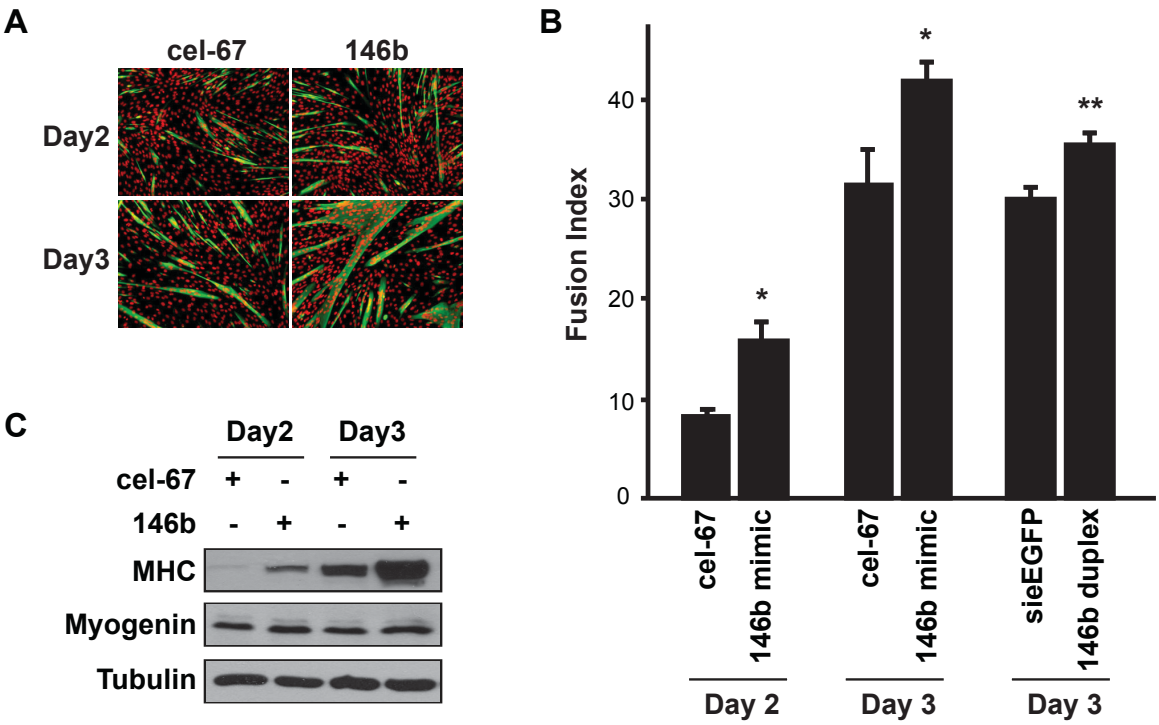

Fig. 4.3. Overexpression of miR-146b promotes myoblast differentiation. (A) C2C12 myoblasts were transfected with 50 nM miRIDIAN miR-146b mimic for 1 day and then induced to differentiate for 3 days. A *C elegans* miRNA (cel-67) mimic was used as negative control. The differentiated cells were fixed and immunostained for MHC (green) and DAPI (red). **(B)** Fusion indexes for the cells described in A were quantified. In addition, cells transfected with 50 nM native miR-146b duplex, with an siRNA against EGFP (siEGFP) as control, were differentiated and quantified for fusion index. **(C)** Cells described in A were lysed and subjected to Western blot analysis. In A and C, representative results of at least three independent experiments are shown. Data in B is the mean ± SD from three independent experiments. Paired *t* test was performed to compare the data. $*P < 0.05$

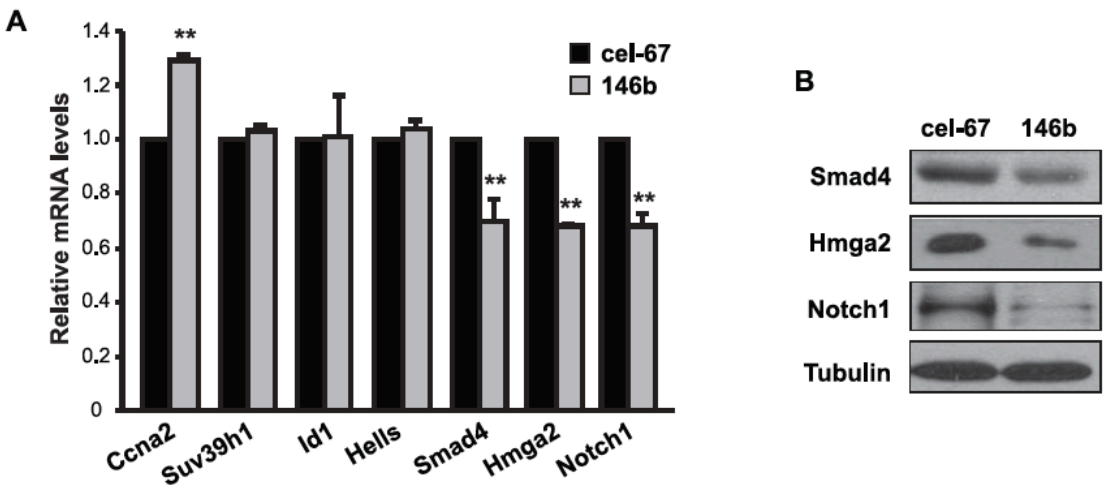

Fig. 4.4. Overexpression of miR-146b suppresses expression of Smad4, Hmga2 and Notch1 in myoblasts. (A) C2C12 myoblasts were transfected with 50 nM miRIDIAN miR-146b mimic or cel-miR-67 mimic as control. After 24 hours, cells were lysed for RNA isolation, followed by qRT-PCR to measure mRNA levels for the genes shown. Relative mRNA levels are shown with that of cel-miR-67 as 1. Data shown are the mean ± SD from three independent experiments. One-sample *t* test was performed. $^{**}P < 0.01$. **(B)** Cells as described in A were lysed after 48 hours of transfection and subjected to Western blotting analysis. Representative results of three independent experiments are shown.

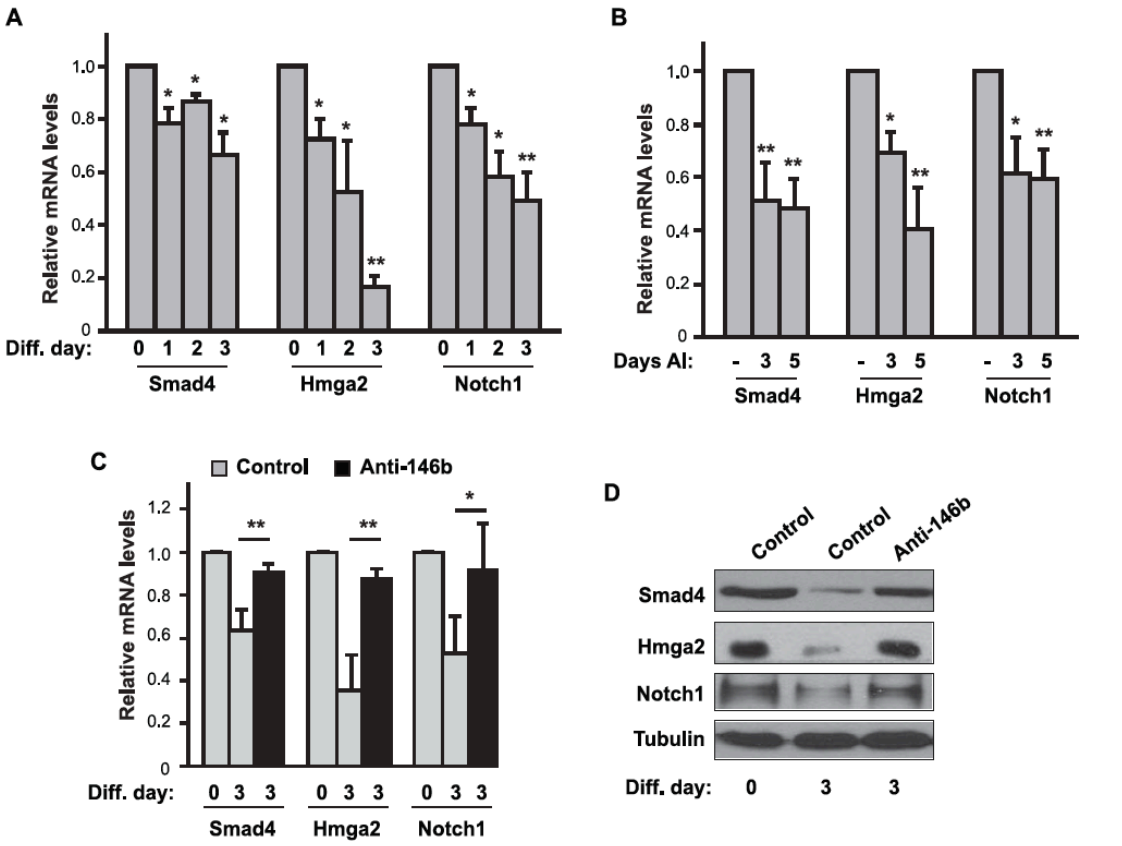

Fig. 4.5. Smad4, Hmga2 and Notch1 are targets of miR-146b during myoblast differentiation. (A) C2C12 cells were induced to differentiate, and total RNA was isolated from the differentiating cells on various days as indicated (Diff. day) and subjected to analysis by qRT-PCR to determine the relative levels of mRNA for each gene, with that at day 0 as 1. **(B)** Regeneration of mouse TA muscles was induced by $BaCl_2$ injury. On day 3 and day 5 AI, the TA muscles were isolated for RNA extraction, followed by qRT-PCR assays to measure relative mRNA levels. Saline injection into contralateral TA muscles served as control ("-") and was designated as 1. **(C)** C2C12 cells were transfected with 50 nM LNA-anti-miR-146b or LNA control for 1 day and then induced to differentiate for 3 days. Total RNA was isolated on day 0 and day 3 of differentiation and analyzed by qRT-PCR. **(D)** Cells as described in C were lysed and subjected to Western blotting analysis. Data shown are mean ± SD from three to four independent experiments **(A & C)** or at least three mice per time point **(B),** or representative results of three independent experiments **(D).** One-sample *t* test was performed to analyze data in A & B, and paired t test was performed for data in C. $*P < 0.05$; $**P < 0.01$.

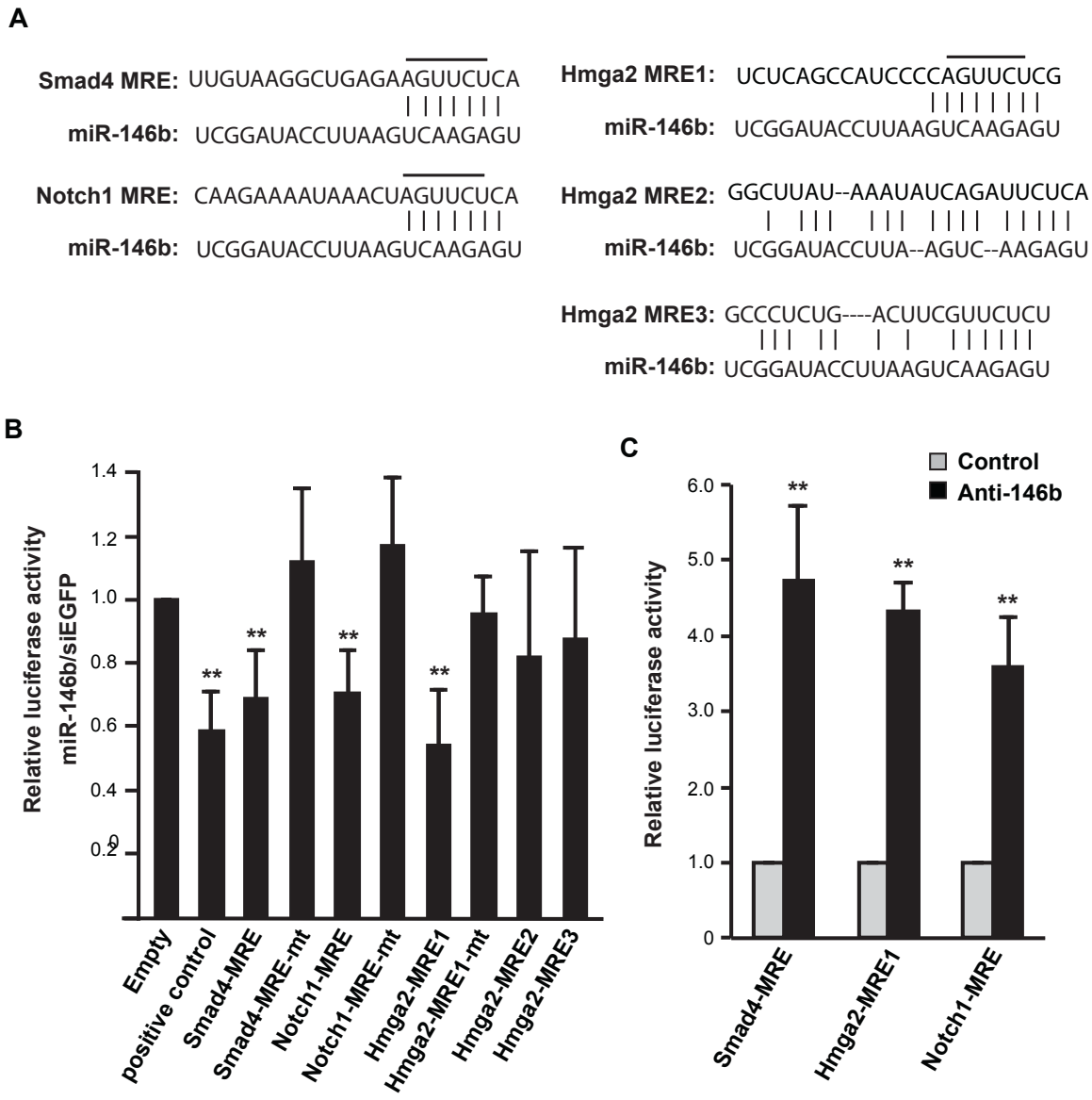

Fig. 4.6. miR-146b directly targets the MREs in 3'UTRs of Smad4, Hmga2 and Notch1. **(A)** Predicted miR-146b target sites in the 3'UTRs of mouse Smad4, Notch1 and Hmga2 are shown. The nucleotides in the seed region that were changed to complementary sequence in the mutant 3'UTR reporters are indicated by lines above them. **(B)** The MRE reporters or their mutant counterparts were cotransfected with miR-146b duplex into HEK293 cells, with siEGFP as a negative control. Twenty-four hours after transfection the cells were lysed and subjected to luciferase assays. A sequence perfectly complementary to the active strand of miR-146b was cloned into the reporter and used as a positive control. **(C)** The MRE reporters were transfected into C2C12 cells together with 50 nM LNA-anti-miR-146b or LNA control for 1 day, followed by cell lysis and luciferase assays. All data shown are mean ± SD from three independent experiments. One-sample *t* test was performed to analyze each data in B&C. $^{**}P < 0.01$.

4.6. References

Baek, D., Villen, J., Shin, C., Camargo, F.D., Gygi, S.P., and Bartel, D.P. (2008). The impact of microRNAs on protein output. Nature *455*, 64-71. Epub 2008 Jul 2030.

Bartel, D.P. (2009). MicroRNAs: target recognition and regulatory functions. Cell *136*, 215-233.

Bhaumik, D., Scott, G.K., Schokrpur, S., Patil, C.K., Orjalo, A.V., Rodier, F., Lithgow, G.J., and Campisi, J. (2009). MicroRNAs miR-146a/b negatively modulate the senescence-associated inflammatory mediators IL-6 and IL-8. Aging (Albany NY) *1*, 402-411.

Bjornson, C.R., Cheung, T.H., Liu, L., Tripathi, P.V., Steeper, K.M., and Rando, T.A. (2012). Notch signaling is necessary to maintain quiescence in adult muscle stem cells. Stem Cells *30*, 232-242. doi: 210.1002/stem.1773.

Chen, J.F., Mandel, E.M., Thomson, J.M., Wu, Q., Callis, T.E., Hammond, S.M., Conlon, F.L., and Wang, D.Z. (2006). The role of microRNA-1 and microRNA-133 in skeletal muscle proliferation and differentiation. Nat Genet *38*, 228-233. Epub 2005 Dec 2025.

Chen, J.F., Tao, Y., Li, J., Deng, Z., Yan, Z., Xiao, X., and Wang, D.Z. (2010). microRNA-1 and microRNA-206 regulate skeletal muscle satellite cell proliferation and differentiation by repressing Pax7. J Cell Biol *190*, 867-879. doi: 810.1083/jcb.200911036.

Cheung, T.H., Quach, N.L., Charville, G.W., Liu, L., Park, L., Edalati, A., Yoo, B., Hoang, P., and Rando, T.A. (2012). Maintenance of muscle stem-cell quiescence by microRNA-489. Nature *482*, 524-528. doi: 510.1038/nature10834.

Conboy, I.M., and Rando, T.A. (2002). The regulation of Notch signaling controls satellite cell activation and cell fate determination in postnatal myogenesis. Dev Cell *3*, 397-409.

Dey, B.K., Gagan, J., Yan, Z., and Dutta, A. (2012). miR-26a is required for skeletal muscle differentiation and regeneration in mice. Genes Dev *26*, 2180-2191. doi: 2110.1101/gad.198085.198112.

Dmitriev, P., Barat, A., Polesskaya, A., O'Connell, M.J., Robert, T., Dessen, P., Walsh, T.A., Lazar, V., Turki, A., Carnac, G., *et al*. (2013). Simultaneous miRNA and mRNA transcriptome profiling of human myoblasts reveals a novel set of myogenic differentiation-associated miRNAs and their target genes. BMC Genomics *14:265*., 10.1186/1471-2164-1114-1265.

Felekkis, K., Touvana, E., Stefanou, C., and Deltas, C. (2010). microRNAs: a newly described class of encoded molecules that play a role in health and disease. Hippokratia *14*, 236-240.

Gagan, J., Dey, B.K., Layer, R., Yan, Z., and Dutta, A. (2012). Notch3 and Mef2c proteins are mutually antagonistic via Mkp1 protein and miR-1/206 microRNAs in differentiating myoblasts. J Biol Chem *287*, 40360-40370. doi: 40310.41074/jbc.M40112.378414. Epub 372012 Oct 378410.

Ge, Y., and Chen, J. (2011). MicroRNAs in skeletal myogenesis. Cell Cycle *10*, 441-448. Epub 2011 Feb 2011.

Ge, Y., Sun, Y., and Chen, J. (2011). IGF-II is regulated by microRNA-125b in skeletal myogenesis. J Cell Biol *192*, 69-81. doi: 10.1083/jcb.201007165. Epub 201002011 Jan 201007163.

Ge, Y., Wu, A.L., Warnes, C., Liu, J., Zhang, C., Kawasome, H., Terada, N., Boppart, M.D., Schoenherr, C.J., and Chen, J. (2009). mTOR regulates skeletal muscle regeneration in vivo through kinase-dependent and kinase-independent mechanisms. Am J Physiol Cell Physiol *297*, C1434-1444. doi: 1410.1152/ajpcell.00248.02009. Epub 02009 Sep 00230.

Geraldo, M.V., Yamashita, A.S., and Kimura, E.T. (2012). MicroRNA miR-146b-5p regulates signal transduction of TGF-beta by repressing SMAD4 in thyroid cancer. Oncogene *31*, 1910-1922. doi: 1910.1038/onc.2011.1381. Epub 2011 Aug 1929.

Guo, H., Ingolia, N.T., Weissman, J.S., and Bartel, D.P. (2010). Mammalian microRNAs predominantly act to decrease target mRNA levels. Nature *466*, 835-840. doi: 810.1038/nature09267.

Hebert, C., Norris, K., Scheper, M.A., Nikitakis, N., and Sauk, J.J. (2007). High mobility group A2 is a target for miRNA-98 in head and neck squamous cell carcinoma. Mol Cancer *6*, 5.

Hurst, D.R., Edmonds, M.D., Scott, G.K., Benz, C.C., Vaidya, K.S., and Welch, D.R. (2009). Breast cancer metastasis suppressor 1 up-regulates miR-146, which suppresses breast cancer metastasis. Cancer Res *69*, 1279-1283. doi: 1210.1158/0008-5472.CAN-1208-3559. Epub 2009 Feb 1273.

Juan, A.H., Kumar, R.M., Marx, J.G., Young, R.A., and Sartorelli, V. (2009). Mir-214-dependent regulation of the polycomb protein Ezh2 in skeletal muscle and embryonic stem cells. Mol Cell *36*, 61-74.

Kallen, A.N., Zhou, X.B., Xu, J., Qiao, C., Ma, J., Yan, L., Lu, L., Liu, C., Yi, J.S., Zhang, H., *et al*. (2013). The imprinted H19 lncRNA antagonizes let-7 microRNAs. Mol Cell *52*, 101-112. doi: 110.1016/j.molcel.2013.1008.1027. Epub 2013 Sep 1019.

Kim, H.K., Lee, Y.S., Sivaprasad, U., Malhotra, A., and Dutta, A. (2006). Muscle-specific microRNA miR-206 promotes muscle differentiation. J Cell Biol *174*, 677-687. Epub 2006 Aug 2021.

Kopan, R., Nye, J.S., and Weintraub, H. (1994). The intracellular domain of mouse Notch: a constitutively activated repressor of myogenesis directed at the basic helix-loop-helix region of MyoD. Development *120*, 2385-2396.

Lal, A., Navarro, F., Maher, C.A., Maliszewski, L.E., Yan, N., O'Day, E., Chowdhury, D., Dykxhoorn, D.M., Tsai, P., Hofmann, O., *et al*. (2009). miR-24 Inhibits cell proliferation by targeting E2F2, MYC, and other cell-cycle genes via binding to "seedless" 3'UTR microRNA recognition elements. Mol Cell *35*, 610-625.

Lee, Y.S., and Dutta, A. (2007). The tumor suppressor microRNA let-7 represses the HMGA2 oncogene. Genes Dev *21*, 1025-1030. Epub 2007 Apr 1016.

Li, Z., Gilbert, J.A., Zhang, Y., Zhang, M., Qiu, Q., Ramanujan, K., Shavlakadze, T., Eash, J.K., Scaramozza, A., Goddeeris, M.M., *et al*. (2012). An HMGA2-IGF2BP2 axis regulates myoblast proliferation and myogenesis. Dev Cell *23*, 1176-1188. doi: 1110.1016/j.devcel.2012.1110.1019. Epub 2012 Nov 1121.

Liu, N., Williams, A.H., Kim, Y., McAnally, J., Bezprozvannaya, S., Sutherland, L.B., Richardson, J.A., Bassel-Duby, R., and Olson, E.N. (2007). An intragenic MEF2-dependent enhancer directs muscle-specific expression of microRNAs 1 and 133. Proc Natl Acad Sci U S A *104*, 20844-20849. Epub 22007 Dec 20819.

Martin, J.F., Li, L., and Olson, E.N. (1992). Repression of myogenin function by TGF-beta 1 is targeted at the basic helix-loop-helix motif and is independent of E2A products. J Biol Chem *267*, 10956-10960.

Mineno, J., Okamoto, S., Ando, T., Sato, M., Chono, H., Izu, H., Takayama, M., Asada, K., Mirochnitchenko, O., Inouye, M., *et al*. (2006). The expression profile of microRNAs in mouse embryos. Nucleic Acids Res *34*, 1765-1771. Print 2006.

Mourikis, P., Sambasivan, R., Castel, D., Rocheteau, P., Bizzarro, V., and Tajbakhsh, S. (2012). A critical requirement for notch signaling in maintenance of the quiescent skeletal muscle stem cell state. Stem Cells *30*, 243-252. doi: 210.1002/stem.1775.

Nakasa, T., Ishikawa, M., Shi, M., Shibuya, H., Adachi, N., and Ochi, M. (2010). Acceleration of muscle regeneration by local injection of muscle-specific microRNAs in rat skeletal muscle injury model. J Cell Mol Med *14*, 2495-2505. doi: 2410.1111/j.1582-4934.2009.00898.x.

Nakasa, T., Miyaki, S., Okubo, A., Hashimoto, M., Nishida, K., Ochi, M., and Asahara, H. (2008). Expression of microRNA-146 in rheumatoid arthritis synovial tissue. Arthritis Rheum *58*, 1284-1292. doi: 1210.1002/art.23429.

Novak, J., Vinklarek, J., Bienertova-Vasku, J., and Slaby, O. (2013). MicroRNAs involved in skeletal muscle development and their roles in rhabdomyosarcoma pathogenesis. Pediatr Blood Cancer *60*, 1739-1746. doi: 1710.1002/pbc.24664. Epub 22013 Jun 24627.

O'Rourke, J.R., Georges, S.A., Seay, H.R., Tapscott, S.J., McManus, M.T., Goldhamer, D.J., Swanson, M.S., and Harfe, B.D. (2007). Essential role for Dicer during skeletal muscle development. Dev Biol *311*, 359-368. Epub 2007 Aug 2025.

Perry, M.M., Williams, A.E., Tsitsiou, E., Larner-Svensson, H.M., and Lindsay, M.A. (2009). Divergent intracellular pathways regulate interleukin-1beta-induced miR-146a and miR-146b expression and chemokine release in human alveolar epithelial cells. FEBS Lett *583*, 3349-3355. doi: 3310.1016/j.febslet.2009.3309.3038. Epub 2009 Sep 3326.

Rao, P.K., Kumar, R.M., Farkhondeh, M., Baskerville, S., and Lodish, H.F. (2006). Myogenic factors that regulate expression of muscle-specific microRNAs. Proc Natl Acad Sci U S A *103*, 8721-8726. Epub 2006 May 8726.

Rosenberg, M.I., Georges, S.A., Asawachaicharn, A., Analau, E., and Tapscott, S.J. (2006). MyoD inhibits Fstl1 and Utrn expression by inducing transcription of miR-206. J Cell Biol *175*, 77-85.

Sabourin, L.A., and Rudnicki, M.A. (2000). The molecular regulation of myogenesis. Clin Genet *57*, 16-25.

Shawber, C., Nofziger, D., Hsieh, J.J., Lindsell, C., Bogler, O., Hayward, D., and Weinmaster, G. (1996). Notch signaling inhibits muscle cell differentiation through a CBF1-independent pathway. Development *122*, 3765-3773.

Shin, C., Nam, J.W., Farh, K.K., Chiang, H.R., Shkumatava, A., and Bartel, D.P. (2010). Expanding the microRNA targeting code: functional sites with centered pairing. Mol Cell *38*, 789-802. doi: 710.1016/j.molcel.2010.1006.1005.

Stefani, G., and Slack, F.J. (2008). Small non-coding RNAs in animal development. Nat Rev Mol Cell Biol *9*, 219-230. doi: 210.1038/nrm2347.

Sun, Y., Ge, Y., Drnevich, J., Zhao, Y., Band, M., and Chen, J. (2010). Mammalian target of rapamycin regulates miRNA-1 and follistatin in skeletal myogenesis. J Cell Biol *189*, 1157-1169. doi: 1110.1083/jcb.200912093. Epub 200912010 Jun 200912021.

Taganov, K.D., Boldin, M.P., Chang, K.J., and Baltimore, D. (2006). NF-kappaB-dependent induction of microRNA miR-146, an inhibitor targeted to signaling proteins of innate immune responses. Proc Natl Acad Sci U S A *103*, 12481-12486. Epub 12006 Aug 12482.

Tsang, J.S., Ebert, M.S., and van Oudenaarden, A. (2010). Genome-wide dissection of microRNA functions and cotargeting networks using gene set signatures. Mol Cell *38*, 140-153. doi: 110.1016/j.molcel.2010.1003.1007.

Wagers, A.J., and Conboy, I.M. (2005). Cellular and molecular signatures of muscle regeneration: current concepts and controversies in adult myogenesis. Cell *122*, 659-667.

Wang, H., Noulet, F., Edom-Vovard, F., Tozer, S., Le Grand, F., and Duprez, D. (2010). Bmp signaling at the tips of skeletal muscles regulates the number of fetal muscle progenitors and satellite cells during development. Dev Cell *18*, 643-654. doi: 610.1016/j.devcel.2010.1002.1008.

Wen, Y., Bi, P., Liu, W., Asakura, A., Keller, C., and Kuang, S. (2012). Constitutive Notch activation upregulates Pax7 and promotes the self-renewal of skeletal muscle satellite cells. Mol Cell Biol *32*, 2300-2311. doi: 2310.1128/MCB.06753-06711. Epub 02012 Apr 06759.

Wilson-Rawls, J., Molkentin, J.D., Black, B.L., and Olson, E.N. (1999). Activated notch inhibits myogenic activity of the MADS-Box transcription factor myocyte enhancer factor 2C. Mol Cell Biol *19*, 2853-2862.

Xia, H., Qi, Y., Ng, S.S., Chen, X., Li, D., Chen, S., Ge, R., Jiang, S., Li, G., Chen, Y., *et al*. (2009). microRNA-146b inhibits glioma cell migration and invasion by targeting MMPs. Brain Res *1269:158-65*., 10.1016/j.brainres.2009.1002.1037. Epub 2009 Mar 1013.

Yan, D., Dong Xda, E., Chen, X., Wang, L., Lu, C., Wang, J., Qu, J., and Tu, L. (2009). MicroRNA-1/206 targets c-Met and inhibits rhabdomyosarcoma development. J Biol Chem *284*, 29596-29604. Epub 22009 Aug 29526.

Zhao, Y., Samal, E., and Srivastava, D. (2005). Serum response factor regulates a muscle-specific microRNA that targets Hand2 during cardiogenesis. Nature *436*, 214-220.

CHAPTER 5. CONCLUSIONS AND PERSPECTIVES

The protein kinase mammalian target of rapamycin (mTOR) is a master regulator of cell growth, survival, differentiation, and metabolism. Two biochemically unique protein complexes of mTOR – mTORC1 and mTORC2 – have distinct kinase activities and assemble signaling pathways that differentially regulate those cellular and developmental processes. As hyper-activation of mTOR signaling underlies many human diseases including diabetes and cancer, Nature has most likely designed intrinsic breaks for these pathways. Here, I identify one such control mechanism for mTORC2. The guanine nucleotide exchange factor (GEF) for Rho small GTPases, XPLN, was first found to interact with mTOR in a yeast two-hybrid screen. Experiments in mammalian cells subsequently revealed that XPLN specifically interacts with mTORC2, not mTORC1. XPLN inhibits mTORC2 kinase activity in vitro and signaling in cells. The inhibitory function of XPLN is specific for one of the targets of mTORC2 – the protein kinase Akt. In line with the well-established functions of Akt, XPLN negatively regulates cell survival and skeletal muscle differentiation through its inhibitory effect on mTORC2 and Akt. Interestingly, this novel function of XPLN is independent of its GEF activity, but instead requires its N-terminal region, most likely via direct physical interaction with mTORC2.

Akt regulates many physiological processes in addition to cell survival and myogenic differentiation, including cell proliferation, glucose metabolism, and other types of cellular differentiation. Regulation of Akt by XPLN in those processes warrants future investigation. A proto-oncogene, Akt is involved in tumorigenesis by promoting

proliferation, survival, and motility of cancer cells. Evidence supports a direct role of mTORC2, at least partly through Akt, in driving tumorigenesis. Future examination of a role of XPLN in tumor suppression, especially in the context of hyperactive Akt, may prove informative for the understanding of and therapeutic strategy against cancer.

In search for novel miRNAs that regulate skeletal myogenesis, I identified miR-146b as a regulator of myoblast differentiation and established Smad4, Notch1 and Hmga2 as direct targets of miR-146b. Expression of miR-146b is up-regulated during myoblast differentiation and muscle regeneration, accompanied by down-regulation of the target genes. MicroRNAs hold the potential as therapeutic targets or tools in aging and dystrophic muscles. For instance, over-expression of miR-1/206 suppresses rhabdomyo-sarcoma development through c-met expression (Yan et al., 2009). The physiological significance and therapeutic potential of miR-146b as a myogenic regulator warrants future investigations.

APPENDIX A. EXPLORATION OF THE ROLE OF XPLN IN CANCER

A.1. Materials and Methods

A.1.1. Antibodies and other reagents. Anti-XPLN antibody was as described in Chapter II, anti-tubulin antibody from Abcam. All other primary antibodies were from Cell Signaling Technology. All secondary antibodies were from Jackson ImmunoResearch Laboratories, Inc.

A.1.2. Cell culture. HeLa, U2OS, MCF-7, TD47, MDA-MB-231, H661, Calu-6, H292, and A549 cells were maintained in DME containing 10% fetal bovine serum (FBS) at 37 °C with 5% CO_2. IGROV-1 and PC-3 cells were maintained in RPMI containing 10% fetal bovine serum (FBS) at 37 °C with 5% CO_2. Transfections were performed using Lipofectamine-2000 following the manufacturer's recommendations. Viral transductions were performed as described earlier in Chapter II.

A.1.3. Western blotting. Cells were lysed in ice-cold lysis buffer (40 mM HEPES, pH7.2, 120 mM NaCl, 10 mM pyrophosphate, 50 mM NaF, 10 mM b-glycerophosphate, 2 mM EDTA, 1x Sigma protease inhibitor cocktail, and 0.3% CHAPS). The supernatant after microcentrifugation at 13,000 rpm for 10 min was collected and then boiled in SDS sample buffer. Proteins were resolved on SDS-PAGE and transferred onto PVDF membrane (Millipore), followed by incubation with various antibodies according to the manufacturers' recommendations. Detection of horseradish peroxidase-conjugated secondary antibodies was performed with Western Lightning™ Chemiluminescence Reagent Plus (Perkin Elmer, Inc.).

A.2. Results and Discussion

A.2.1. Examination of XPLN copy number in various cancer databases. Hyperactive Akt signaling is frequently seen in cancer and we established XPLN to be an endogenous inhibitor of Akt activation. So, we next wanted to examine if XPLN gene was lost in tumor samples potentially contributing to Akt hyperactivation. To this end, I checked XPLN copy number in human tumor samples profiled by various databases. Interestingly, I found loss of XPLN DNA in a small number of tumor samples along with a small number of somatic mutations at a low frequency (Fig. A.1). Although, XPLN gene was amplified in some tumor samples, the amplification frequency was less than the deletion and mutation combined together. XPLN deletion can potentially nicely correlate with the Akt hyperactivation in these tumor samples.

A.2.2. XPLN protein expression in different cancer cell lines. To directly examine XPLN level during different types of cancer, we decided to check the level of XPLN protein in various available cancer cell lines established from tumor tissues. Contrary to the expectations, XPLN protein level was comparable between cancer cell lines and corresponding epithelial normal cell lines (Fig. A.2A). Additionally, knockdown of XPLN in cancer cells had no effect on phospho Akt levels much in contrast to the enhanced pAkt seen after XPLN depletion in normal cells (Fig A.2B). So, we wondered if XPLN was somehow dysregulated in cancer cells allowing the cells to achieve hyperactivated Akt signaling without the need to physically remove XPLN.

A.2.3. Effect of XPLN over-expression on Akt phosphorylation in cancer cell lines. **T**o examine this possible oncogenic mechanism of endogenous XPLN being dysregulated, I over-expressed recombinant XPLN in various cancer cell lines to check its effect on co-expressed GFP-Akt. We hypothesized that by over-expression of XPLN, we may overburden the machinery that normally regulates its function and hence allow over-expressed protein to elicit an effect on phospho Akt. In fact, this is exactly what we observed in IGROV-1 cells (first panel, Fig. A.3). I further extended this experiment to other cancer cell lines and noticed that there were two separate groups. First group, which showed inhibition of pAkt following XPLN over-expression, consisted of cell lines IGROV-1, PC-3, Calu-6, HeLa, U2OS, and Hep3B (Fig. A.3). In contrast, second group of cell lines were resistant to XPLN over-expression and showed no effect on pAkt levels following XPLN over-expression. This group of cell lines consisted of H-661, MDA-MB-231, MCF-7, and A549 (Fig. A.3).

A.2.4. Exploration of potential link between CDKN2A and XPLN. Next, I wanted to figure out why are some of the cancer cell lines resistant to XPLN overexpression. To probe this, I asked what is a common element for these resistant cell lines or how do they differ from the first set of cell lines that show sensitivity towards XPLN overexpression.

Since PTEN is an inhibitor of Akt signaling and a well-established tumor suppressor that is lost in a variety of tumor cell lines, we first looked at PTEN. IGROV-1 and PC-3 are the only two PTEN null cell lines among all the cancer cell lines tested for the effect of XPLN overexpression on Akt phosphorylation. Since, both PTEN null and PTEN WT cell lines belong to the XPLN over-expression sensitive group cell lines, it

suggested that PTEN might not be the factor that regulates effect of XPLN over-expression on Akt phosphorylation.

Next, I looked at other well-established tumor suppressors or oncogenes and found that all the cancer cell lines that were resistant to XPLN over-expression were CDKN2A null (Oncomine). The CDKN2A (INK4a, MTS1, CDKN2) gene locus is a unique gene locus in mammals that codes for 2 different proteins through splicing and alternate reading frames (Quelle, Zindy et al. 1995). It encodes p16INK4a, an inhibitor of the cyclin D-dependent kinases CDK4/CDK6 and hence inhibiting them from phosphorylating the retinoblastoma protein (pRB) and ultimately preventing exit from the G1 phase of the cell cycle (Quelle, Zindy et al. 1995). Second protein, p19ARF, arises from an alternative reading frame of the INK4a gene, and its ectopic expression induces both G1 and G2 phase arrest (Quelle, Zindy et al. 1995). ARF physically interacts with MDM2 to block MDM2 mediated degradation and transcriptional inactivation of p53 and hence activating p53 (Pomerantz, Schreiber-Agus et al. 1998).

To examine a potential role of p16INK4 in regulating Akt inhibition by XPLN, I knocked down INK4a in a CDKN2A WT cell line to check if it loses its sensitivity towards XPLN over-expression. As shown in Fig. A.4, knockdown of INK4a enhanced basal level of Akt phosphorylation, but XPLN over-expression was still capable of reducing pAkt levels even in INK4a depleted cells. This suggested that while INK4a itself may have a role in regulating Akt phosphorylation directly or indirectly through its effect on cell cycle (see below), it probably doesn't regulate XPLN function towards Akt inhibition.

Recently, a direct link between cell cycle and Akt phosphorylation was established (Liu, Begley et al. 2014). Specifically, it was shown that Akt activity mirrored cyclin A2 expression level during cell cycle and Cdk2/cyclin A2 was established as a physiological kinase to phosphorylate Akt1 at both S477 and T479 both in vivo and in vitro. Additionally, they showed that pS477/pT479 might prime Akt for mTORC2-mediated phosphorylation of S473. So, it is likely that INK4a depletion enhanced Akt phosphorylation through an indirect effect on cell cycle progression.

A.3. Figures

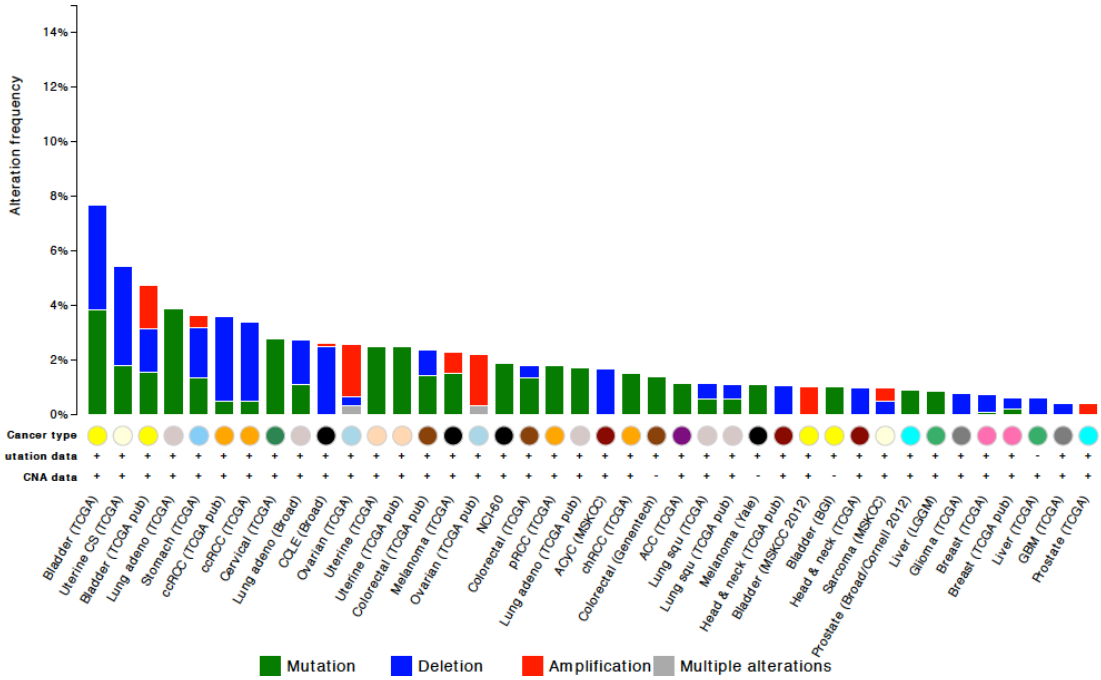

Fig. A.1. Analysis of XPLN copy number in human tumor samples (Oncomine).

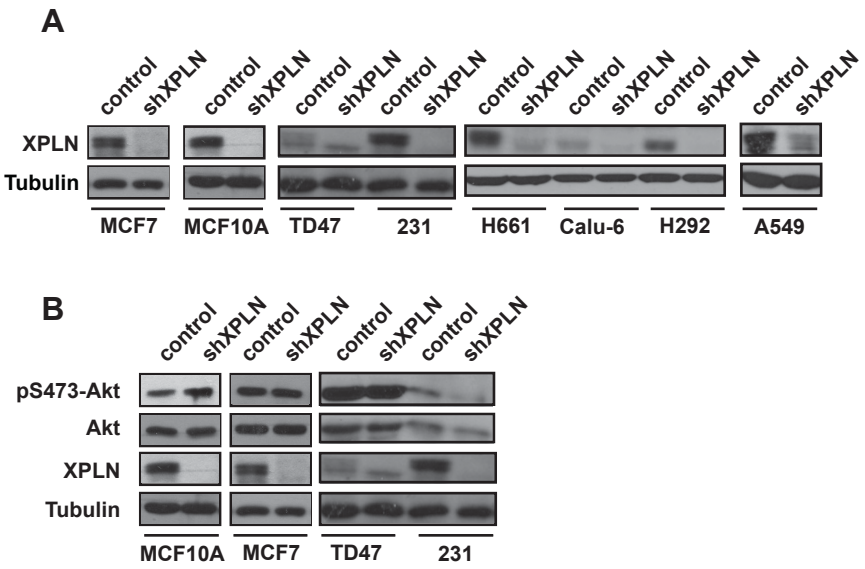

Fig. A.2. XPLN expression and effect of XPLN knockdown on phospho Akt levels in cancer cells. (A) Various cancer cells were transduced with XPLN virus followed by puromycin selection for 2-3 days. Cells were then lysed and lysates analyzed by western blotting. **(B)** Different cell lines were transduced with XPLN virus followed by puromycin selection for 2-3 days. Cells were then lysed and lysates analyzed by western blotting. Blots are representatives of at least 3 individual experiments.

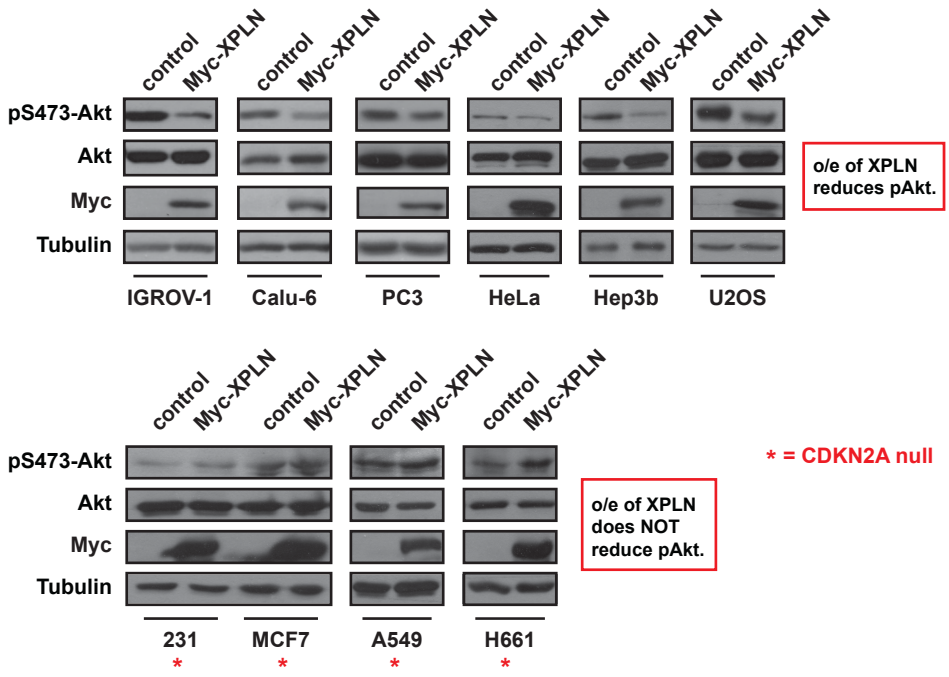

Fig. A.3. Effect of XPLN over-expression on Akt phosphorylation in cancer cell lines. Various cancer cells were co-transfected with Myc-XPLN, GFP-Akt. Following 24 hours of transfection, cells were lysed for western blotting. Images and blots are representatives of at least 3 individual experiments.

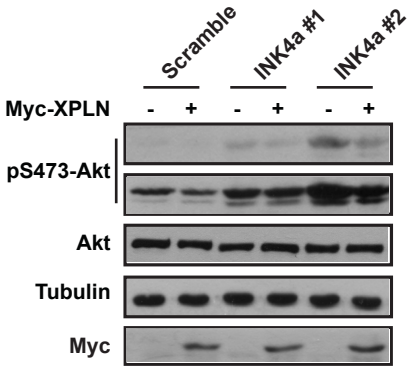

Fig. A.4. Effect of INK4a knockdown on XPLN mediated Akt inhibition. IGROV-1 cells were transduced with lentiviruses followed by puromycin selection for 2 days. Cells were then transfected with Myc-XPLN and GFP-Akt. Following 24 hours of transfection, cells were lysed for western blotting. Images and blots are representatives of at least 3 individual experiments.

A.4. References

Liu, P., M. Begley, et al. (2014). "Cell-cycle-regulated activation of Akt kinase by phosphorylation at its carboxyl terminus." Nature **508**(7497): 541-545.

Pomerantz, J., N. Schreiber-Agus, et al. (1998). "The Ink4a tumor suppressor gene product, p19Arf, interacts with MDM2 and neutralizes MDM2's inhibition of p53." Cell **92**(6): 713-723.

Quelle, D. E., F. Zindy, et al. (1995). "Alternative reading frames of the INK4a tumor suppressor gene encode two unrelated proteins capable of inducing cell cycle arrest." Cell **83**(6): 993-1000.

APPENDIX B. CONSTRUCTION OF XPLN KO MOUSE USING TALEN TECHNOLOGY

B.1. Materials and Methods

B.1.1. C2C12 Transfection. pCS2+TALEN plasmids were constructed in collaboration with Zehua Bao in Huimin Zhao lab. C2C12 cells were transfected with 1.5 ug of each plasmid of the TALEN pair with Lipofectamine following manufacturer's recommendations. Following 3 days of transfection, cells were lysed to isolate genomic DNA.

B.1.2. TALEN mRNA production and embryo microinjection. 10 μg of pCS2+-TALE plasmid was digested with 50 U of ApaI in a total reaction volume of 100 μl. Linearised plasmid was then gel purified and the DNA concentration was determined. For in vitro transcription, 20-μl transcription reaction was set up by using the reagents from the mMESSAGE mMACHINE SP6 Kit as follows: 10 μl of 2× NTP/CAP reagent, 2 μl of 10× reaction buffer, 1 μg of template DNA, 2 μl Sp6 enzyme mix. Reaction was mixed by pipetting and incubated for 2 h at 37 °C. Following the incubation, 1ul Turbo DNase was added for 15' at 37°C. RNA was purified by adding 350 μl of binding buffer from the MegaClear kit and 250 μl of ethanol. Sample was applied to a MegaClear spin column followed by performing RNA purification according to the manufacturer's directions. To 100 μl of the eluted sample, 10 μl of 5 M ammonium acetate and 275 μl of ethanol were added for RNA precipitation and buffer exchange. Mixture was incubated overnight at −20 °C and centrifuged at 13krpm for 15 min at RT. Pellet was washed with 500 μl of 70% ethanol (prepared with embryo-tested water) followed by air-drying the

pellet for 5 min. RNA pellet was then resuspended in 20 µl of $T_{10}E_{0.1}$ microinjection buffer (prepared with embryo tested water) followed by checking concentration using nanodrop and integrity of RNA by running on an agarose gel. Purified RNA from the TALEN pair plasmids was then microinjected by mouse facility in to one cell embryo. Animal housing and handling followed all relevant regulations and institutional animal care committee's guidelines.

B.1.3. Genomic DNA isolation and PCR amplification. Genomic DNA was isolated using proteinase K method. Briefly, tail tips were digested in 0.6 ml of genomic DNA isolation buffer (20mM Tris, pH-7.5, 50mM EDTA, 100mM NaCl, 0.5% SDS, freshly added 500ug/ml proteinase K) at 42 degrees overnight. After incubation, added 240ul tail salts (4.21 M NaCl, 0.63M KCl, 10mM Tris, pH-8.0), vortexed, incubated at 4 degrees for 30 minutes. Tubes were centrifuged at 13krmp for 10 minutes and supernatant removed into a different tube, followed by adding 1X 100% ethanol. DNA was then pelleted at maximum speed for 2 minutes, washed with 80% ethanol, followed by suspension in 100ul TE buffer. 50 ng genomic DNA was used as a template for PCR amplification using primer sequences indicated in Fig. B.1. PCR conditions used were 98°C 5', followed by 25 cycles of 98°C 15'', 62°C 15'', 72°C 15''.

B.1.4. Surveyor Assay. Procedure was performed following the manufacturer's protocol. Briefly, 400ng PCR amplicons in a 7.5 µl reaction were denatured and reannealed using PCR program as described in manual. After hybridization reaction was over, added 0.25 µl nuclease and 1 µl enhancer followed by incubation at 37°C 60'. Reaction products were then run on a 2% agarose gel.

B.2. Results and Discussion

B.2.1. Screening for best TALEN pair. Five different TALEN pairs were designed to target exon 3 of the murine XPLN gene. Exon 3 was selected for targeting since it is the earliest exon in the XPLN coding sequence that was shared by all alternate transcripts of XPLN, except transcript 1 and 10 that lack the functional part (first 125 amino acids) of the XPLN protein altogether. Their sequences and binding sites in XPLN gene are depicted in Fig. B.1.

As shown in Fig. B.2, Surveyor enzyme consistently showed cutting for genomic DNA isolated from TALEN pair 2 transfected C2C12 cells. Hence, TALEN pair 2 was chosen for in vitro transcription and embryo injection.

B.2.2. Identification of F0 mutant founder mice. 10 founder females gave birth to a total of 44 pups. Genomic DNA was isolated from the tail tips of these pups upon weaning followed by PCR amplification and surveyor assay. As shown in Fig. B.3, DNA from 9 pups generated cleavage bands following surveyor assay, as indicated by star. These pups could be potentially heterozygous for XPLN mutated DNA.

Additionally, genomic DNA from pup #5, #36, #37 showed strong PCR products of size ~310bp, 250bp, and 290bp, besides the normal 400bp WT parental band, as indicated by arrowheads. These bands were gel purified followed by sequencing. Results from sequencing confirmed deletion of varying number of nucleotides ranging from 8-9 nucleotides (Fig. B.4).

Pups #5, 36: deletion of 8 nucleotides from 242-249 (AAGCGCTT)

Pup #37: deletion of 9 nucleotides from 238-245 (ATTAAAGCG)

B.3. Figures

GGGGGGTGGGGAAGGGGGGGTAGGATCCCTACCTTTCTGTCACCCACTGCTTCAGTGTGC
CTCCTCCGTCTTTTCTCTTTCATGGCTCCCCAGCCAGATCACCTGTGCAGATCCTGGGGC
ACCGTTCACGGGTCTACAGATCACCCTGTCGCCTGCAAGTCTCAGAGCAGGATGGATGTG
ATGTTGTGGCAGACATCTGTAAGATTGGTCTTGACACTGTCCTCTTTTTTTTTTTTTTTT
CTTTTATACAG**GAACCTAGTAACAAAAGGGTCAAACCCCTTTCCAGAGTCACATCGCTAG**
CAAACCTCATTCCACCTGTGAAGACCACACCATTAAAGCGCTTCAGCCAGACCTTGCAGG
TAAGGGAACGTGGGCTTGGGCTTGGGCTTGCAGAGAGCCATGCTGTGCTCATGCACCTAG
CATCTCTGTGGGTCTCCGGTGGAGCTGAATCACCACTTGCTACTGTAGAAGAGTGCACAG
GTGAAGGGGAATAAAAGGACGAGAAATGTGTGCACGCCACAACCCCGGGTCAGGCAGGGT
CAGGGCCACTTCTGATAGTTCATAGTTGTATGTCTATGTCATAGGTCCTATCCGAGTGTA

ARHGEF3 Exon 3 sequence
Primer Pair used for amplification

GGGGGGTGGGGAAGGGGGGGTAGGATCCCTACCTTTCTGTCACCCACTGCTTCAGTGTGC
CTCCTCCGTCTTTTCTCTTTCATGGCTCCCCAGCCAGATCACCTGTGCAGATCCTGGGGC
ACCGTTCACGGGTCTACAGATCACCCTGTCGCCTGCAAGTCTCAGAGCAGGATGGATGTG
ATGTTGTGGCAGACATCTGTAAGATTGGTCTTGACACTGTCCTCTTTTTTTTTTTTTTTT
CTTTTATACAG**GAACCTAGTAACAAAAGGGTCAAACCCCTTTCCAGAGTCACATCGCTAG**
CAAACCTCATTCCACCTGTGAAGACCACACCATTAAAGCGCTTCAGCCAGACCTTGCAGG
TAAGGGAACGTGGGCTTGGGCTTGGGCTTGCAGAGAGCCATGCTGTGCTCATGCACCTAG
CATCTCTGTGGGTCTCCGGTGGAGCTGAATCACCACTTGCTACTGTAGAAGAGTGCACAG
GTGAAGGGGAATAAAAGGACGAGAAATGTGTGCACGCCACAACCCCGGGTCAGGCAGGGT
CAGGGCCACTTCTGATAGTTCATAGTTGTATGTCTATGTCATAGGTCCTATCCGAGTGTA

ARHGEF3 Exon 3 sequence
TALEN 1 LEFT SEQUENCE: T-TTCCAGAGTCACATCGCTAG
TALEN 1 RIGHT SEQUENCE: T- CTGGCTGAAGCGCTTTAAT

GGGGGGTGGGGAAGGGGGGGTAGGATCCCTACCTTTCTGTCACCCACTGCTTCAGTGTGC
CTCCTCCGTCTTTTCTCTTTCATGGCTCCCCAGCCAGATCACCTGTGCAGATCCTGGGGC
ACCGTTCACGGGTCTACAGATCACCCTGTCGCCTGCAAGTCTCAGAGCAGGATGGATGTG
ATGTTGTGGCAGACATCTGTAAGATTGGTCTTGACACTGTCCTCTTTTTTTTTTTTTTTT
CTTTTATACAG**GAACCTAGTAACAAAAGGGTCAAACCCCTTTCCAGAGTCACATCGCTAG**
CAAACCTCATTCCACCTGTGAAGACCACACCATTAAAGCGCTTCAGCCAGACCTTGCAGG
TAAGGGAACGTGGGCTTGGGCTTGGGCTTGCAGAGAGCCATGCTGTGCTCATGCACCTAG
CATCTCTGTGGGTCTCCGGTGGAGCTGAATCACCACTTGCTACTGTAGAAGAGTGCACAG
GTGAAGGGGAATAAAAGGACGAGAAATGTGTGCACGCCACAACCCCGGGTCAGGCAGGGT
CAGGGCCACTTCTGATAGTTCATAGTTGTATGTCTATGTCATAGGTCCTATCCGAGTGTA

ARHGEF3 Exon 3 sequence
TALEN 2 LEFT SEQUENCE: T-CCACCTGTGAAGACCACAC
TALEN 2 RIGHT SEQUENCE: T-CCCTTACCTGCAAGGTCT

GGGGGGTGGGGAAGGGGGGGTAGGATCCCTACCTTTCTGTCACCCACTGCTTCAGTGTGC
CTCCTCCGTCTTTTCTCTTTCATGGCTCCCCAGCCAGATCACCTGTGCAGATCCTGGGGC
ACCGTTCACGGGTCTACAGATCACCCTGTCGCCTGCAAGTCTCAGAGCAGGATGGATGTG
ATGTTGTGGCAGACATCTGTAAGATTGGTCTTGACACTGTCCTCTTTTTTTTTTTTTTTT
CTTTTATACAG**GAACCTAGTAACAAAAGGGTCAAACCCCTTTCCAGAGTCACATCGCTAG**
CAAACCTCATTCCACCTGTGAAGACCACACCATTAAAGCGCTTCAGCCAGACCTTGCAGG
TAAGGGAACGTGGGCTTGGGCTTGGGCTTGCAGAGAGCCATGCTGTGCTCATGCACCTAG
CATCTCTGTGGGTCTCCGGTGGAGCTGAATCACCACTTGCTACTGTAGAAGAGTGCACAG
GTGAAGGGGAATAAAAGGACGAGAAATGTGTGCACGCCACAACCCCGGGTCAGGCAGGGT
CAGGGCCACTTCTGATAGTTCATAGTTGTATGTCTATGTCATAGGTCCTATCCGAGTGTA

ARHGEF3 Exon 3 sequence
TALEN 3 LEFT SEQUENCE: T-CAAACCCCTTTCCAGAG
TALEN 3 RIGHT SEQUENCE: T-GTGGTCTTCACAGGTG

Fig. B.1. Sequences of 5 TALEN pairs and their binding sites in XPLN gene.

Fig. B.1. (Continued)

GGGGGGTGGGGAAGGGGGGGTAGGATCCCTACCTTTCTGTCACCCACTGCTTCAGTGTGC
CTCCTCCGTCTTTTCTCTTTCATGGCTCCCCAGCCAGATCACCTGTGCAGATCCTGGGGC
ACCGTTCACGGGTCTACAGATCACCCTGTCGCCTGCAAGTCTCAGAGCAGGATGGATGTG
ATGTTGTGGCAGACATCTGTAAGATTGGTCTTGACACTGTCCTCTTTTTTTTTTTTTTTT
CTTTTATACAG**GAACCTAGTAACAAAAGGGTCAAACCCCTTTCCAGAGTCACATCGCTAG**
CAAACCTCATTCCACCTGTGAAGACCACACCATTAAAGCGCTTCAGCC**AGACCTTGCAGG**
TAAGGGAACGTGGGCTTGGGCTTGGGCTTGCAGAGAGCCATGCTGTGCTCATGCACCTAG
CATCTCTGTGGGTCTCCGGTGGAGCTGAATCACCACTTGCTACTGTAGAAGAGTGCACAG
GTGAAGGGGAATAAAAGGACGAGAAATGTGTGCACGCCACAACCCCGGGTCAGGCAGGGT
CAGGGCCACTTCTGATAGTTCATAGTTGTATGTCTATGTCATAGGTCCTATCCGAGTGTA

ARHGEF3 Exon 3 sequence
TALEN 4 LEFT SEQUENCE: T-CATTCCACCTGTGAAGAC
TALEN 4 RIGHT SEQUENCE: T-CCCTTACCTGCAAGGTCT

GGGGGGTGGGGAAGGGGGGGTAGGATCCCTACCTTTCTGTCACCCACTGCTTCAGTGTGC
CTCCTCCGTCTTTTCTCTTTCATGGCTCCCCAGCCAGATCACCTGTGCAGATCCTGGGGC
ACCGTTCACGGGTCTACAGATCACCCTGTCGCCTGCAAGTCTCAGAGCAGGATGGATGTG
ATGTTGTGGCAGACATCTGTAAGATTGGTCTTGACACTGTCCTCTTTTTTTTTTTTTTTT
CTTTT**ATACAGGAACCTAGTAACAA**AAGGGTCAAACCCCTTTCC**AGAGTCACATCGCTAG**
CAAACCTCATTCCACCTGTGAAGACCACACCATTAAAGCGCTTCAGCCAGACCTTGCAGG
TAAGGGAACGTGGGCTTGGGCTTGGGCTTGCAGAGAGCCATGCTGTGCTCATGCACCTAG
CATCTCTGTGGGTCTCCGGTGGAGCTGAATCACCACTTGCTACTGTAGAAGAGTGCACAG
GTGAAGGGGAATAAAAGGACGAGAAATGTGTGCACGCCACAACCCCGGGTCAGGCAGGGT
CAGGGCCACTTCTGATAGTTCATAGTTGTATGTCTATGTCATAGGTCCTATCCGAGTGTA

ARHGEF3 Exon 3 sequence
TALEN 5 LEFT SEQUENCE: T-ATACAGGAACCTAGTAACAA
TALEN 5 RIGHT SEQUENCE: T-TTGCTAGCGATGTGACTCT

Fig. B.1. Sequences of 5 TALEN pairs and their binding sites in XPLN gene.

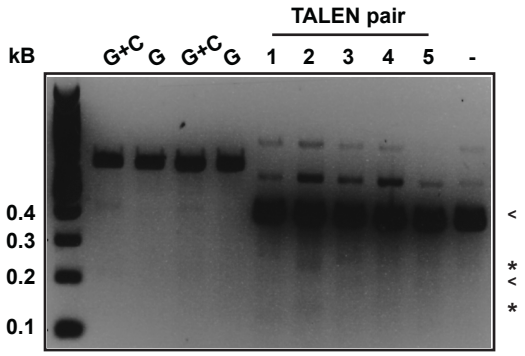

Fig. B.2. Gel showing the Surveyor nuclease result from five XPLN TALEN pairs. Lane 1: DNA ladder. Lanes 2,4: positive control for surveyor assay. Lane 3,5: negative control for surveyor assay. Lane 6-10: cells transfected with a plasmid carrying XPLN TALEN pair (number as indicated) Lane 11: control from un-transfected cells The two lower bands as indicated by stars are Surveyor-cleaved DNA products. The arrowheads indicate bands generated from positive control.

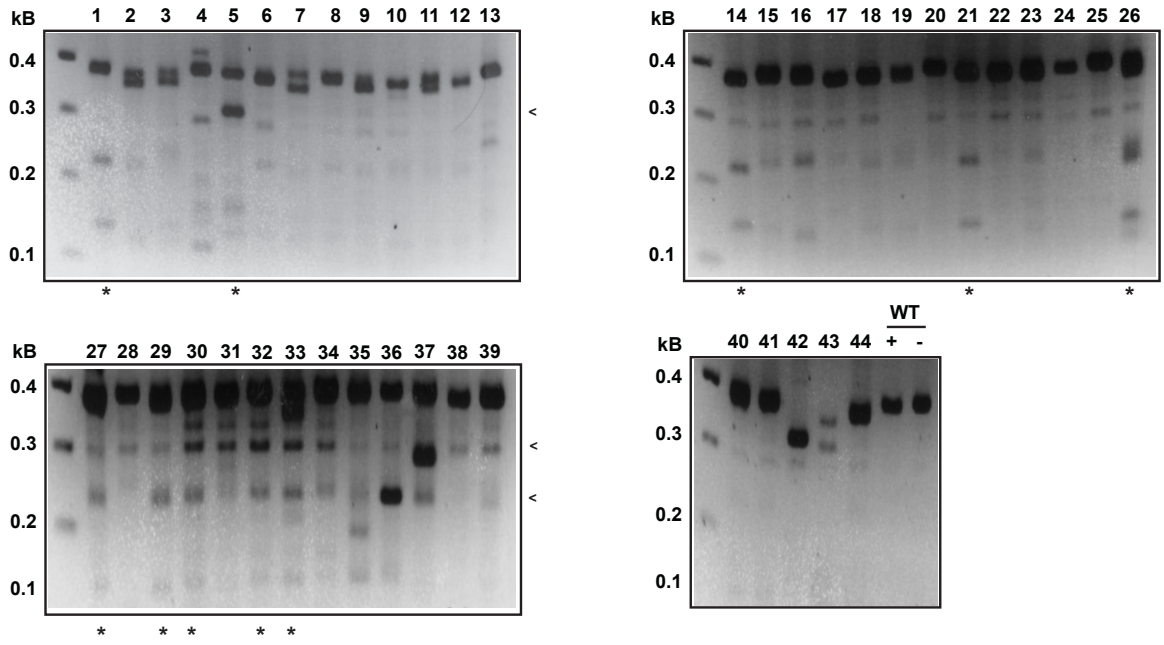

Fig. B.3. Gels showing the Surveyor nuclease result from 44 F0 pups. Each gel has lane 1 as marker followed by surveyor nuclease result from the pups (numbers as indicated above). Last gel contains WT DNA with (+) or without surveyor enzyme (-) as control. The arrowheads indicate strong PCR amplicons generated by pups #5, #36, and #37 that were sent for sequencing. Pups whose genomic DNA reliably generate cleavage products following surveyor assay are indicated by stars underneath.